

**COASTAL UPWELLING OF THE SOUTH
EASTERN ARABIAN SEA – AN
INTEGRATED APPROACH**

Thesis submitted to the

COCHIN UNIVERSITY OF SCIENCE AND TECHNOLOGY

*In partial fulfilment of the Requirements for
the Award of the Degree of*

DOCTOR OF PHILOSOPHY

In

PHYSICAL OCEANOGRAPHY

UNDER THE FACULTY OF MARINE SCIENCES

by

SMITHA B. R.



**DEPARTMENT OF PHYSICAL OCEANOGRAPHY
SCHOOL OF MARINE SCIENCES
COCHIN UNIVERSITY OF SCIENCE AND TECHNOLOGY
KOCHI-682 016, KERALA, INDIA.**

NOVEMBER 2010

Declaration

I hereby declare that the thesis entitled “**Coastal Upwelling of the South Eastern Arabian Sea – An Integrated Approach**” is an authentic record of the research carried out by me, under the supervision of Dr. R. Sajeev, Associate Professor, Department of Physical Oceanography, School of Marine Sciences, Cochin University of Science and Technology, Kochi-16., in partial fulfilment of the requirement for the Ph.D degree of the Cochin University of Science and Technology in the faculty of Marine Sciences and that no part of this has been presented before for any other degree, diploma or associateship in any university.

*Kochi-16,
15th November 2010.*

(Smitha B. R.)

Certificate

I hereby certify that the thesis entitled “**Coastal Upwelling of the South Eastern Arabian Sea – An Integrated Approach**” submitted by **Mrs. Smitha B. R.**, Part-time Research Scholar (Reg. No. **3287**) of this Department, is an authentic record of research carried out by her under my supervision, in partial fulfilment of the requirement for the Ph.D degree of Cochin University of Science and Technology in the faculty of Marine Sciences and that no part thereof has previously formed the basis for the award of any degree, diploma or associateship in any university.

Dr. R. Sajeev,

(Supervising Guide),

Associate Professor,

Dept. of Physical Oceanography,

School of Marine Sciences,

Cochin University of Science & Technology,

*Kochi-16,
15th November 2010.*

Kochi – 682 016.

Acknowledgement

I gladly express my immense gratitude to my supervising guide Dr. R. Sajeev, Associate Professor, Department of Physical Oceanography, School of Marine Sciences, CUSAT, for giving me an opportunity to work in the Department to obtain my doctoral degree. His patient support and encouragement throughout the period of my work were valuable for the fruitful and timely submission of the work. I should say, he is great to accommodate even my divergent thoughts and approach to the problem through various angles, which helped me to make an integrated view on coastal ocean processes.

My research in upwelling started while working in Centre for Marine Living Resources and Ecology, Ministry of Earth Sciences, Kochi, and it was Dr. V.N. Sanjeevan, the present Director of the centre who introduced me to the world of upwelling of the SEAS. My experience at the centre and the team work with him moulded my career and provided me a comprehensive outlook on oceanic processes and its physico-chemical and biological responses. The facilities onboard FORV Sagar Sampada helped me in availing the in situ evidences of my work which are worth full and I believe, are an added advantage to the quality of the work. I am extremely thankful to Sir for the immense support I received from him.

Also, I would like to thank Dr. A. N. Balchand, Head of the department of Physical Oceanography, for giving me the opportunity to work in the department as a scholar. The support and suggestions provided by him during the semester presentations were extremely helpful in moulding the content of the thesis.

Gratitude to Prof V Ravindranath, Advisor (Retired), MoES, also is expressed for permitting me to start my doctoral work while working in CMLRE. This extends to Dr. T. Shunmugaraj for the selfless support and facilities provided in the Centre.

Also I would like to mention the name of Dr. R. Damodaran (Retd. Professor & Dean, Faculty of marine Sciences, CUSAT), who has directed me to CMLRE immediately after the tenure of my work with his team after my post graduation. Heartfelt thanks to Dr. R. Revichandran (Scientist F, National Institute of Oceanography, Regional Centre, Kochi, for the support and suggestions to successfully carry out my studies in the earlier stages of the work.

Other personalities whom I would like to thank in this occasion is Dr. S. Prasannakumar of NIO Goa, who was always there with kind patience to listen, discuss and guide in different stages of my work. I extend my thanks to Dr. K.K. Balachandran of NIO Regional Centre, Kochi, for the valuable suggestions/corrections pointed out.

I have used enormous amount of in situ data collected onboard FORV

Sagar Sampada during the rough weather of southwest monsoon. I would like to express my heartfelt thanks to all the fellow participants, technical hands and fishing hands for their kind hearted selfless support provided during the cruises. The support which I received from each and every staff of CMLRE is very precious and is also remembered with gratitude. Similarly, the support from research scholars and staff of the Physical Oceanography Department (CUSAT) is also counted here.

Friends are always precious for me in all phase of my studies and research life. They are there in different Oceanographic institutes in India and abroad, CUSAT and CMLRE. Of course the gratitude and love to them cannot be expressed through words. Still my deepest sense of gratitude to all...

My strength is the unconditional support and encouragement from my family... and they are the ones who encouraged me the most and energised me during the busy schedules and hectic sea days. Aniyettan and Achu stood with me with constant inspiration along with my parents and all the family members and I believe that without their support the thesis would not have materialized.

Last, I would like to dedicate this work to those who are not with me to share the moment...our Pathithu, Valiachan and my dearest friend Prabha...

- Smitha B R

*"One who loves practice without theory is like the sailor who boards ship
without a rudder and compass and never knows where he may cast."*

-- Leonardo da Vinci

Contents

List of Figures

List of Tables

Acronyms

Preamble

1 Introduction	1
1.1 Types of Upwelling	3
1.1.1 Coastal Upwelling	3
1.1.2 Open Ocean Upwelling.	5
1.1.3 Equatorial Upwelling.	6
1.1.4 Southern Ocean Upwelling.	7
1.1.5 Other types of Upwelling.	7
1.2 Variations in Upwelling	8
1.3 Chemical and Biological Response to Upwelling.	10
1.4 Description of the Study Region.	11
1.5 Earlier Studies	15
1.6 Objectives of the Present Study.	24

2	Upwelling Mechanism	27
2.1	Introduction	27
2.2	Materials and Methods	29
2.2.1	Upwelling Index (UI) from SST	29
2.2.2	Upwelling Index (UI) from Wind	31
2.2.3	In Situ Observations	34
2.2.4	Observations from Satellite	36
2.3	Results and Discussion	36
2.3.1	Upwelling Off Southern Tip (Cape)	36
2.3.2	Upwelling Off Southwest Coast	37
2.3.3	Surface Salinity Distribution	41
2.3.4	Surface Chlorophyll <i>a</i> Distribution	46
2.4	Conclusion	48
3	Theoretical Formulation of the Process of Upwelling	51
3.1	Introduction	51
3.2	Data and Methodology	54
3.2.1	Upwelling Index from SST and Wind	54
3.2.2	SSHA from Satellite Altimetry	54
3.2.3	Bottom Topography	55
3.3	Theoretical Formulation	56
3.3.1	Southern Tip (Cape)	58
3.3.2	Cape-Kollam Stretch (Shadow Zone)	60
3.3.3	Kollam- Mangalore Stretch	61
3.3.4	Mangalore-Goa Stretch	62
3.4	Validity and limitations of the Theory	63
4	Differential Response of the Upwelling on Biological Production	65
4.1	Introduction	65

4.2	Data and Methods	68
4.2.1	In Situ Observations	68
4.2.2	Satellite Observations	72
4.3	Results and Discussion	73
4.3.1	Spatial Variation	73
4.3.1.1	Physical Forcing and Hydrography During SM 2004	73
4.3.1.2	Dissolved Inorganic Nutrients	76
4.3.1.3	Biological Responses	77
4.3.1.4	Sea Surface Height Anomaly During the Season	84
4.3.1.5	Upwelling Front	86
4.3.2	Temporal Variation	92
4.3.2.1	Upwelling off Kollam and Tvpm - A comparison	95
4.4	Conclusion	101
5	Primary Production Associated with Upwelling	105
5.1	Introduction	105
5.2	Data and Methodology	108
5.2.1	Upwelling Index from SST	108
5.2.2	Model Description	110
5.2.2.1	Vertically Generalised Production Model (VGPM)	110
5.2.2.2	Validation Against the In Situ Data	112
5.3	Results and Discussion	114
5.3.1	Upwelling- Inter Annual Variation	114
5.3.2	Primary Production - Inter Annual Variation	117
5.4	Conclusion	124
6	Summary and Conclusion	125
6.1	Concluding Remarks	130
6.2	Scope for Future Work	131

Bibliography 133

Publications 147

List of Figures

1.1 Ekman transport moves surface waters away from the coast, surface waters are replaced by water that wells up from below (NH)	4
1.2 Ekman spiral showing the direction of wind, current and net transport.	5
1.3 Surface circulation in the NIO	12
1.4 Trajectory of the Kelvin wave (blue thick arrow), Coastal Kelvin wave (violet thin arrow) and westward propagating Rossby waves (red arrows) along the west coast of India. . .	22
2.1 Location map and the 1°X 1° squares used to derive upwelling indices.	31
2.2 Wind pattern during July 2005 (from Quikscat Scatterometer) showing the tangential winds at the southern tip. . . .	32
2.3 Variation of (a) LTA and (b) Ekman mass transport ($kg/m/s$) as a function of time (month) and space (longitude) at Cape. Shaded part indicates negative values.	37

2.4	Variation of (a) LTA and (b) Ekman mass transport (kg/m/s) as a function of time (month) and space (latitude) along the south-west coast of India. Shaded part indicates negative values	39
2.5	Sea surface salinity for (a) May, (b) June, and (c) September show the southwards propagation of the ASHSW.	42
2.6	Schematic representation of different upwelling zones classified according to the formation mechanism, as well as intensity. Arrows along the coast represent coastal Kelvin waves. Westwards-directed black arrows depict Rossby waves, the phase velocity of which decreases moving from the equator; upwelling at area 1 is strongly wind driven; area 2 is a shadow zone with weak wind-driven upwelling; upwelling at area 3 is the result of remote forcing, as well as wind stress.	44
2.7	SST (<i>C</i>) variation along the 15°N transect during September 2003, showing the limited offshore extension of upwelling.	46
2.8	Four-year climatology (2003–2006) of monthly composite surface Chlorophyll from MODIS AQUA for June–September.	47
3.1	Bottom topography for the SEAS from etopo2v2	56
3.2	Eleven year Average UI derived from Wind stress (Red line) and SST (Green line)	57
3.3	Latitudinal variation of Ekman drift (<i>cm/sec</i>) and direction for differnt SM months (red line represents observation during June, blue for July and green for September)	59
4.1	Station location during SS227 and SS246	70

4.2	SST distribution	74
4.3	Variation in the Mixed Layer Depth	75
4.4	Distribution of Surface Salinity	76
4.5	Distribution of Nitrate (NO_3 in μM) at 10 m.	78
4.6	phosphate (PO_4 in μM) at 10 m	79
4.7	$DO(ml/l)$ at 10 m	80
4.8	Distribution of Surface Chlorophyll (mg/m^3)	81
4.9	Surface PP $mgC/m^3/day$	82
4.10	Latitudinal variations of different parameters 20 m (A) and 200 m (B) isobath.	83
4.11	Ten day average SSH (cm) during May to September 2004 along the selected grids shown in the left	85
4.12	Monthly composite of surface Chlorophyll from MODIS Aqua for July 2004	88
4.13	10 day composite of SSH for the period 20 th – 30 th July 2004	90
4.14	Weekly scatterometer data from QuikSCAT July 16 th -23 rd (a) and July 23 rd to 30 th (b). In situ data on wind along the cruise track of SS227 (c).	91
4.15	Variation in different parameters off Tvpm (during 25 th June to 5 th July 2006)..	96
4.16	Variations in temperature in the TSS off Tvpm during the 12 th day study period	97
4.17	Variation in different parameters off Kollam (during 26 th June to 6 th July 2006)	99
5.1	Relation between In-situ and satellite PP	113
5.2	LTA (UI) for each sub region	115

5.3	Distribution of monthly averaged PP in $mgC/m^2/d$ for SM	
	months in each sector during 2003-2009	123
5.4	Relation between UI and PP for 2003-2009.	123

List of Tables

4.1 Offshore spreading of 26C isotherm along different transects	87
4.2 Calculated Rossby Radius of deformation (RRD).	89
5.1 Upwelling Indices (<i>LTA</i>)-Average for the SEAS	117
5.2 Year wise/sub region wise and total PP for the SEAS .	118
5.3 Region wise - month wise long term averaged PP ($mgC/m^2/d$)	120

Acronyms

ADCP	Acoustic Doppler Current Profiler
AS	Arabian Sea
ASHSW	Arabian Sea High Salinity Water mass
AWS	Automated Weather Station
BoB	Bay of Bengal
CTD	Conductivity - Temperature - Depth
DO	Dissolved Oxygen
E	East
EEZ	Exclusive Economic Zone
EICC	East India Coastal Current
ERSS	European Remote Sensing Satellite
<i>et. al.</i>	et alii (Latin word meaning 'and others')
etc.	et cetera (Latin word meaning 'and other similar things; and so on')

Fig.	Figure
FIM	Fall Inter Monsoon
FORV SS	Fishery & Oceanographic Research Vessel Sagar Sampada
GW	Great Whirl
IDAS	Integrated Data Acquisition System
ILD	Isothermal Layer Depth
IO	Indian Ocean
Lat	Latitude
LL	Lakshadweep Low
Long	Longitude
LTA	Local Temperature Anomaly
MICOM	Miami Isopycnic Coordinate Ocean model
MLD	Mixed Layer Depth
MODIS	Moderate Resolution Imaging Spectroradiometer
mtC	Million ton Carbon
N	North
NASA	National Aeronautics and Space Administration
NE	North East
NH	Northern Hemisphere
NIO	North Indian Ocean

NNW	North-North West
NO ₂	Nitrite
NO ₃	Nitrate
NW	North West
OEW	Optimum Environment Window
PAR	Photosynthetically Active Radiation
PGW	Persian Gulf Water
PO ₄	Phosphate
POM	Princeton Ocean Model
PP	Primary Productivity
psu	Practical Salinity Unit
RHJ	Razz al Hadd jet
RRD	Rossby Radius of Deformation
RSW	Red Sea Water
SD	Sri Lankan Dome
SE	Succotra Eddy
SeaDAS	SeaWiFS Data Analysis System
SEAS	South Eastern Arabian Sea
SeaWiFS	Sea-viewing Wide Field-of-view Sensor
SIM	Spring Inter Monsoon

SiO ₄	Silicate
SM	Summer Monsoon
SMC	Summer Monsoon Current
SS	Sagar Sampada
SSHA	Sea Surface Height Anomaly
SST	Sea Surface Temperature
SW	South West
T/P	TOPEX/Poseidon
TSS	Time Series station
Tvpm	Thiruvananthapuram
UI	Upwelling Index
UNESCO	United Nations Education, Scientific and Cultural Organisation
VGPM	Vertically Generalised Production Model
viz	videlicet (Latin word meaning 'namely')
WICC	West India Coastal Current
WM	Winter Monsoon
μM	Micro Mole

Preamble

Upwelling regions occupies only a small portion of the global ocean surface. However it accounts for a large fraction of the oceanic primary production as well as fishery. Therefore understanding and quantifying the upwelling is of great importance for the marine resources management. Most of the coastal upwelling zones in the Arabian Sea are wind driven uniform systems. Mesoscale studies along the southwest coast of India have shown high spatial and temporal variability in the forcing mechanism and intensity of upwelling. There exists an equatorward component of wind stress as similar to the most upwelling zones along the eastern oceanic boundaries. Therefore an offshore component of surface Ekman transport is expected throughout the year. But several studies supported with in situ evidences have revealed that the process is purely recurring on seasonal basis. The explanation merely based on local wind forcing alone is not sufficient to support the observations. So, it is assumed that upwelling along the South Eastern Arabian Sea is an effect of basin wide wind forcing rather than local wind forcing. In the present study an integrated approach has been made

to understand the process of upwelling of the South Eastern Arabian Sea. The latitudinal and seasonal variations (based on Sea Surface Temperature, wind forcing, Chlorophyll a and primary production), forcing mechanisms (local wind and remote forcing) and the factors influencing the system (Arabian Sea High Saline Water, Bay of Bengal water, runoff, coastal geomorphology) are addressed herewith.

The thesis is organised in six chapters. Subsequent to the introduction chapter, the second chapter explains the analysis pertaining to the upwelling pattern, upwelling indices from Sea Surface Temperature & wind fields for 1990-2000, vertical velocities due to Ekman pumping and the isothermal shifts due to upwelling. The surface salinity as well as chlorophyll a distributions are also used to explain the spatial variations in the process. With this, the preliminary understanding of the process of upwelling of the South Eastern Arabian Sea was done and different upwelling zones were delineated based on the intensity and forcing mechanisms.

A theoretical formulation of upwelling in the region is proposed in the third chapter. Based on the results from the second chapter, and other earlier studies from this area, an attempt has been made to derive a new relation to quantify the process. Seven years of monthly averaged data (1993-2000) on wind field from QuickSCAT Scatterometer, satellite Sea Surface Temperature and altimeter derived Sea Surface Height Anomaly has been used for the analysis.

Fourth chapter narrates the in situ as well as satellite evidences of upwelling and associated characteristics during active upwelling. Spatial variation in the process of upwelling, influence of fresh water runoff, nutrients, alongshore currents, the offshore extension of upwelling fronts are addressed in this chapter. The biological response to the physical forcing and the time lag for the response are also discussed here.

Total primary production associated with the coastal upwelling process is explained in the fifth chapter. Primary Production for the region was derived from satellite chlorophyll a images using the temperature dependent Vertically Generalised Production Model (VGPM) after validation and applying of proper correction factors and is used to study the physico-biological relationship due to the process of upwelling in the region. The data collected for seven years (2003 to 2009) were used to study the inter-annual variation of the process and the associated primary production.

The sixth and the last chapter summaries the entire work. The literature used for the present study is incorporated under references and the list of publication is also attached at the end.

Chapter 1

Introduction

“Science is the belief in the ignorance of experts.”

– Richard Feynman

UPWELLING is an ascending motion for minimum duration, extend by which, water from subsurface layer is brought into the surface, removing the prevalent waters by horizontal flow. Vertical motions are integral part of ocean circulation, but they are quite insignificant when comparing to horizontal currents. As the temperature decreases and the density increases with depth more energy is required to displace water vertically upwards. Hence, vertical motions are normally inhibited by the density stratification of the ocean. The ocean is also stratified with other properties; for example, nutrient concentration generally increases with depth. Thus, even a weak vertical flow may cause significant effect on biological production due to the advecting nutrients.

There are two important upwelling processes in the ocean. The first one is the slow upwelling of cold abyssal water, occurring over large areas of the ocean to compensate the sinking of the surface water in limited Polar Regions. The second one is the upwelling of subsurface waters into the euphotic zone to balance for the horizontal divergence occurring in the surface, usually caused by winds. Coastal upwelling systems are highly dynamic and exhibit wide variations in the hydrographic, nutrient and phytoplankton characteristics controlled by local meteorology on short time scales and remote forcing on longer time scales. Deep waters are rich in nutrients, such as nitrate, phosphate and silicate, due to the decomposition of sinking organic matter and lack biological uptake. When brought to the surface, these nutrients are utilised immediately for the production of phytoplankton along with CO_2 and solar irradiation, through the process known as photosynthesis. Upwelling regions are therefore, significant for very high levels of primary production in comparison to other areas of the ocean. This high primary production propagates through the food chain, as phytoplankton is at the base of the oceanic food chain. Approximately 25% of the total global marine fish catches are reported to come from five upwelling systems that occupy only 5% of the total ocean area. Upwelling driven by coastal currents or diverging open ocean currents has the greatest impact on the nutrient

enrichment and global fishery yields (¹²⁷Wiggert et al., 2005).

1.1 Types of Upwelling

The major upwelling systems in the ocean are associated with the divergence of currents that bring deep, cold and nutrient rich waters to the surface. There are at least seven types of upwelling systems such as, coastal upwelling, open ocean upwelling, equatorial upwelling, southern ocean upwelling, upwelling associated with eddies/meanders, topographically-associated upwelling, and broad-diffusive upwelling along the ocean interior. Some of these processes are discussed below.

1.1.1 Coastal Upwelling

Coastal upwelling is the most known type of upwelling, which is closely related to mankind as it sustains one of the richest fisheries in the world. Wind-driven currents get deflected to the right of the winds in the Northern Hemisphere (Fig.1.1) and to the left in the Southern Hemisphere due to the Coriolis effect. The result is a net movement of surface water at right angles to the direction of the wind (45° at surface to total shift of 90° for the water column), which is known as the Ekman transport (Fig. 1.2)(²³Ekman). When Ekman transport occurs along the coast, the surface wa-

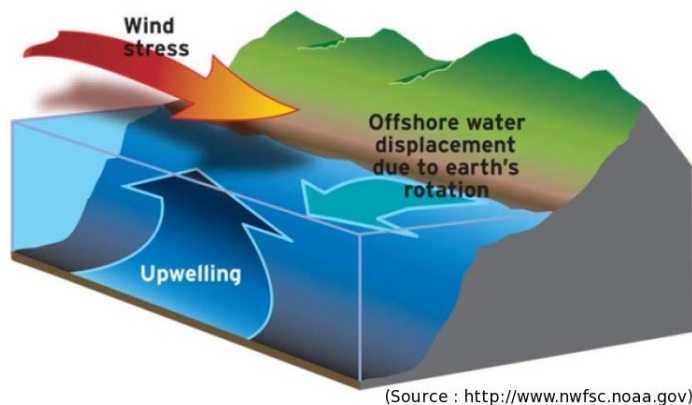


Figure 1.1: Ekman transport moves surface waters away from the coast, surface waters are replaced by water that wells up from below (NH)

ters are replaced by nutrient rich deep, cold, and denser waters, indicating coastal upwelling.

When the Ekman transport carries the surface waters toward the coast, the water piles up and then sinks, initiating the process known as coastal downwelling. Thus Upwelling and downwelling illustrate a mass continuity in the ocean; that is, a change in the water level in one area is compensated by an opposite change in water level in another area.

Worldwide, there are five major coastal upwelling areas associated with different coastal currents: the Canary Current off Northwest Africa, the Benguela Current off southern Africa, the California Current off California and Oregon, the Humboldt Current off Peru and Chile and the Somali Current along Western Ara-

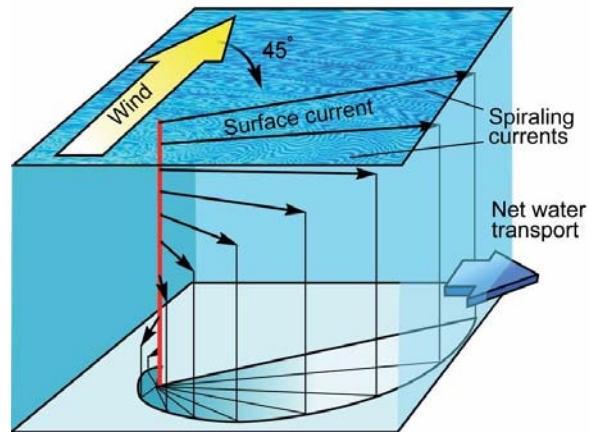


Figure 1.2: Ekman spiral showing the direction of wind, current and net transport.

bian Sea. All these upwelling systems are well known, as they support major fisheries (²³ Ekman 1905).

1.1.2 Open Ocean Upwelling

In the open ocean, the wind induces divergence (move away) of surface waters causing upwelling followed by convergence adjacent to this region causing downwelling, which are the characteristics of the open ocean upwelling systems. Upwelling observed in the open ocean, normally induced by wind stress curl, falls under this category. The best known example of Open Ocean upwelling system is that along the central Arabian Sea associated with Findlater jet during SM (⁷⁵ Prasannakumar et al., 2001 and ⁴⁹ Madhuprathap, et al., 2001). The wind maximum around 17°N

and 64°E indicates the axis of the Findlater jet.

The shoaling and deepening of isotherms on either sides of the axis are the signatures of the upwelling and downwelling associated with the jet. The MLD and SST in the central AS are, to a large extent, regulated by these wind forcing and incoming solar radiation. However, the Ekman dynamics associated with the Findlater jet controls the mixed layer depth during SM (⁷⁵Prasannakumar et al., 2001).

1.1.3 Equatorial Upwelling

Upwelling along the equator is associated with the Intertropical Convergence Zone (ITCZ), which actually moves and is consequently, located to the north or south of the equator. Easterly (westward) winds blowing along the ITCZ in both the Pacific and Atlantic basins, drive the surface waters to the right (northwards) in the Northern Hemisphere and to the left (southwards) in the Southern Hemisphere (¹²⁶Weisberg and Weiyarate, 1991).

If the ITCZ gets displaced above the equator, the wind south of it becomes southwesterly and drives water to its right (southeasterly), away from the ITCZ. Irrespective of the location, this results in a divergence, with dense, nutrient-rich waters being upwelled from the below, leading to an enhanced phytoplankton biomass.

1.1.4 Southern Ocean Upwelling

Large-scale upwelling is observed in the Southern Ocean. Here, strong westerly (eastward) winds blow around Antarctica, inducing a significant northward water flow. This is actually a type of coastal upwelling. Since there are no continents in between South America and the Antarctic Peninsula, some of this upwelled water is drawn up from great depths. In many numerical models and observational syntheses, the Southern Ocean upwelling represents a primary means by which, deep and dense waters are brought to the surface.

1.1.5 Other Types of Upwelling

- Local and intermittent upwelling may occur when offshore islands, ridges, or seamounts cause a deflection of deep ocean currents, providing a nutrient enrichment to an area, in otherwise low productivity areas. Examples include upwelling around the Galapagos Islands and the Seychelles Islands, which sustain major pelagic fisheries.
- Presence of internal waves and the intensification thereby in the coastal currents also can cause upwelling as observed off Ivory Coast and off Ghana. Study from these areas suggests the nutrient enrichment and enhanced biological production,

with minimal influence due to alongshore windstress.

- Upwelling can also occur in link with eddies (cold core), meanders and filaments normally observed in association with coastal currents. The cyclonic circulation pattern associated with these features causes the isotherm to move upwards, and this in turn replenish the nutrient rich less oxygenated subsurface waters at the surface.
- Upwelling can also occur when a tropical cyclone transits an area. The churning of a cyclone eventually draws up denser, cooler and nutrient rich water from the deep ocean. Also this causes the cyclone to weaken.
- Artificial upwelling simulated by devices that convert wave energy or ocean thermal energy by pumping water to the surface. Such devices have been shown to produce plankton blooms.

1.2 Variations in Upwelling

Upwelling intensity depends on wind strength, stratification, surface currents and bathymetry. In some areas, upwelling is a seasonal event leading to periodic bursts of productivity. Wind - induced upwelling is associated with temperature gradient between land and the sea. In temperate latitudes, this gradient is highly

variable with respect to seasons, creating periods of strong upwelling in the spring and summer to weak or no upwelling in the winter. For example, off the coast of Oregon, there are four or five strong upwelling events separated by periods of very little to no upwelling during the next six months. In contrast, tropical waters have more consistency in temperature gradient, creating constant upwelling throughout the year. The Peruvian upwelling, for instance, occurs most of the year, resulting in one of the world's potential sites of sardines and anchovies (⁵Bakun 1973).

In anomalous years, when the trade winds weaken or reverse along the central Pacific, the water that is upwelled is much warmer and low in nutrients, resulting in a sharp reduction in the biomass and phytoplankton productivity. This event is known as the El Nino-Southern Oscillation (ENSO) event. The Peruvian upwelling system, particularly vulnerable to ENSO events, is found to exhibit wide interannual variability in productivity.

Changes in bathymetry can affect the strength of an upwelling. For example, a submarine ridge that extends out from the coast will produce more favorable upwelling conditions than neighboring regions. Upwelling typically begins at such ridges and remains strongest at the ridge even after developing in other locations.

Coastal upwelling is found to influence weather and cli-

mate of a region. Along the northern and central California coast, upwelling was found to lower SST and increases the frequency of summer fogs. The relatively cold surface waters chill the overlying humid marine air to saturation so that thick fog develops. Besides, upwelling of cold water inhibits formation of tropical cyclones (e.g., hurricanes), because tropical cyclones derive their energy from warm surface waters. During El Nino and La Nina, changes in SST patterns associated with warm and cold-water upwelling off the northwest coast of South America and along the equator in the tropical Pacific affect the inter-annual distribution of precipitation around the globe.

1.3 Chemical and Biological Response to Upwelling

The physical process involving the offshore transports of the coastal waters and upliftment of cold subsurface waters change the water properties considerably. The water devoid of any nutrients is replaced by nutrient rich waters. Nitrate, phosphate and silicate shows quick response to the process, with a hike in their concentration at the surface waters, like nitrate levels increasing up to $10\mu M$, phosphate up to $1.5\mu M$, and silicate up to $2.5\mu M$. This increase in the nutrients triggers the primary production in the

surface waters and may cause the blooming of certain algae. This enhanced phytoplankton growth leads to a higher secondary production (mesozooplankton) which is subsequently transferred to the tertiary production (pelagic fishery). Another peculiarity of the upwelling areas is that they are the spawning grounds for many pelagic fishes (Oil Sardine, Mackerel and Anchovies). The spawning of sardine is closely related to the occurrence of upwelling and is found that, they shift their spawning location according to the shift in upwelling area (⁴Bakun and Parish, 1982).

1.4 Description of the Study Region

The SEAS is a small portion of NIO (Fig. 1.3), which is distinguished by two features. The northern boundary is closed at 25°N, making it essentially a tropical ocean undergoing strong seasonality due to the occurrence of southwest and northeast monsoon. The NIO can be roughly divided into three major areas, 1) the equatorial belt stretching between 10°N and 10°S with the Somalia basin on its west 2) the Bay of Bengal and 3) the Arabian Sea. NIO has two sources of high saline water, the Persian Gulf and the Red Sea. The NIO does not extend to the Arctic waters in the north because of its blocking by the Asia continent and does not get ventilated to the NH. The AS has a negative water balance where evaporation exceeds precipitation and runoff, which makes

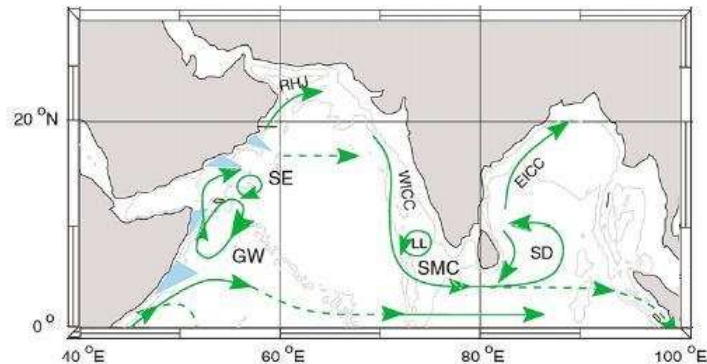


Figure 1.3: Surface circulation in the NIO

it a unique system with asymmetric circulation. In the equatorial belt, surface circulation is completely different from that prevailing further below 10°S , and reverses itself semiannually. The deep waters to this area come from the Antarctic and Atlantic oceans. Hence, the thermohaline circulation in the north is weak in association with the deep vertical convection.

The continental shelf, as marked by the 200 *m* contour, is approximately 120 *km* wide off the southern tip of India, that narrows down to about 60 *km* off 11°N and widens to about 350 *km* off Gulf of Cambay. The shelf remains about 200 *km* wide to the north up to Karachi, west of which the shelf narrows to less than 50 *km*. The shelf is narrow all along the Arabian coast and is less than 50 *km* wide at the entrance of the Red Sea. The chain of coral islands present in the region have significant influence on

the AS dynamics and productivity.

There is a chain of lagoons and backwaters along the southwest coast line. The Coastal Rivers/lakes/inlets, especially those which are falling in the SEAS are short in length and have limited catchment areas. Also, most of them are non-perennial. Some of the major lakes/rivers/barmouth emptying in to the SEAS are Ashtamudy bar mouth (8.8°N), Kayamkulam bar mouth (9.1°N), Vembanad bar mouth (10°N), Azhicode or Kodungallure bar mouth (10.2°N), Chettuva Barmouth (10.5°N), Ponnani barmouth (10.8°N), Beypore Harbour (11.12°N), Azheekkal Harbour (11.9°N), Nethravathi or Payaswini river (12.8°N), Tadri river (14.5°N), Karwar Kalinadi (14.8°N), Zuari estuarine mouth (15.4°N) and Mandovi estuarine mouth (15.5°N).

The AS is approximately a triangular basin with the largest zonal extent of about 3000km and a slightly smaller meridional extent. The smaller size of the AS implies that, its coastal regime, stretched along two sides of the triangulate basin occupies upto 25% of total area and hence, the interaction between the coastal and oceanic regimes is quite important. The important upwelling zones in the NIO are the Somali, the Oman systems, in addition to the SEAS upwelling system of which, the processes associated with each one are more complicated and ecologically significant.

By its geographical position, the AS can be considered as

a tropical oceanic system. Physical processes in the upper 1000 *m* are seasonal and the upper 100 *m* are largely wind driven, whereas vertical mixing is influenced by the changes in density. Coastal currents become more significant during monsoons. Hydrography and circulation of the AS is governed by the monsoon winds, characterized by southwesterly winds during SM and northeasterly winds during WM. The other two seasons, FIM and SIM are fairly inactive with weak and unorganized wind and current patterns. The signatures of SM winds are strongly felt in the physical and the consequent biogeochemical processes occurring in the NIO. Strong winds blowing parallel to the coast force the surface waters to move offshore to be replaced by the subsurface nutrient rich waters favoring high biological productivity. The enhanced growth of phytoplankton supports greater zooplankton abundance, which can boost up the fish stocks (¹²⁷Wiggert et al., 2005).

Unlike the wind of most upwelling zones along the eastern ocean boundaries, the SM winds blow almost directly onshore, causing an equator ward component of windstress. This induces an offshore component of surface Ekman transport throughout the year. However this is not adequate enough to explain the well-defined seasonality in the upwelling, as evidenced through several in situ observations. Based on the above facts, it can be assumed that upwelling along the west coast of India is initiated by the

basin wide wind forcing rather than local wind forcing.

1.5 Earlier Studies

Till the 19th century, presence of cold water along the western boundaries of Peru, California and South Africa were generally believed to be due to advection of cold water from higher latitudes. Later, ²²De Tesson (1844), identified the cold water off Peru as due to upwelling. ¹²⁸Witte (1880) gave theoretical explanation to the process that upwelling can occur either due to earth's rotation on periodontal currents or by off shore wind driving the water away from the coast. Later, after the experience in Challenger Expedition ² Bachan (1895), explained that offshore winds that derive surface water offshore induce upwelling. ¹¹⁹Thorade (1905), and ⁵⁴Mc Ewan (1912) explained upwelling as a direct effect of prevailing winds that blow parallel to the coast with coast on the left side of the wind direction. ¹¹⁶Sverdrup et al., (1942) noticed that upwelling occurs in the regions of diverging currents.

According to ³¹Hidakka (1954), most intense upwelling occurs when the wind makes an angle of 21.5° with the coast line in an offshore direction. ¹³²Yoshida (1967) studied upwelling with a comprehensive approach, using a quasi-steady model. Accordingly, if resonance occurs between pole ward directed internal

Kelvin waves and the forcing disturbance, the internal waves attain appreciable amplitude and can produce localised upwelling without any apparent wind. Other theoretical studies based on models include, Kindle and O'Brien (1974), ²⁵ Gill and Clark (1974) and ¹³¹Wyrтки (1981). In addition, ¹²⁶Weisberg (1991) brought out the role of undercurrents in equatorial upwelling.

Theoretical studies to explain the process of upwelling quantitatively has been started with the introduction of Ekman theory ²³(Ekman, 1905). Subsequently, ¹¹⁴Sverdrup(1938), ¹¹⁵Sverdrup and Fleming (1941) and ¹³²Yoshida (1967) worked in the same line and later the theory has modified to Ekman-Sverdrup model. Many applied mathematical and numerical models for explaining upwelling has come out. ³⁰Haugen et al., 2002 applied MICOM for the first time in the SEAS to study the seasonal circulation and coastal upwelling. Other study based on model is three dimensional sigma coordinate primitive equation POM (⁸²Rao et al., 2008).

In the NIO, the shifting over of the SM winds from NEM winds causes reversal of surface current system (¹³⁰Wyrтки, 1973; ¹¹⁸Tchernia, 1980) and the development of strong upwelling system along Somalia (¹⁷Bruce, 1974; ¹⁶Brown et al., 1980; ¹²⁰Tsai et al., 1992), Arabia (⁹⁰Sastry and D'Souza, 1972; ¹⁷Bruce 1974; ¹⁰⁷Smith and Bottero, 1977) as well as north of the Findlater Jet

(¹⁰⁷Smith and Bottero, 1977; ⁴⁶Luther et al., 1990; ⁹Bauer et al., 1991; ¹⁵Brock and MacClain 1992). The nutrient enrichment and the associated peaks in biological production in the region is recorded by ⁸⁴Ryther and Menzel, (1965); ⁸⁵Ryther et al., (1966); ⁷⁷Qasim, (1977) and ¹²Berger et al., (1991).

Upwelling off the SEAS, as indicated by rapid upward movement of isotherms, surface cooling, and the associated fall in coastal sea level, occurs during the SM months from May to September. Historically several studies have been reported in the literature to describe and explain the observed upwelling in the SEAS. Of these studies, important contributions are from ⁷⁸ Banse, 1959, 1968; ⁹⁶⁹⁷⁹⁸ Sharma, 1966, 1968, 1978; ¹⁰⁰Shetye, 1984; ⁵¹ McCreary and Chao, 1985; ³⁴ Johannessen et al., 1987; ¹⁰¹ Shetye et al., 1990; and ⁹⁵ Shankar et al., 2005.

All these studies based on relatively sparse and limited hydrographic data sets had reported the onset of upwelling in the deeper depths as early as February/March, that gradually reaches the near-surface layers by May and continues until September in association with southward flowing surface coastal currents [⁹⁷ Sharma, 1968; ¹⁰⁰ Shetye, 1984; ³⁴ Johannessen et al., 1987] Other studies in the region reporting upwelling were from ³³Jayaraman (1957), ⁷⁹Ramamithram and Rao (1973), ⁸⁰ Rao et al., (1974) and ⁴⁰Lathipha and Murthy (1978). ¹²³Varadachari

and Sharma (1967) reported large divergent zones in Kochi-Karwar area during SM, which leads to intense upwelling in the area. ³⁸Kumar and Mohankumar (1996) and ³⁹Kumar and Mathew (1996), explained the flow and thermocline structure during pre-upwelling and the seasonal variability in hydrographic condition along the shelf waters of the SEAS. Later on, ⁵⁰Maheswaran et al., (1999) explained the initial phase of the process of upwelling and the associated hydrography with in situ evidences during the months of May-June.

SEAS is biologically one of the most productive regions of the world oceans contributing substantially to fishery resources due to the well known upwelling process during SM (⁴⁷ ⁴⁸ ⁴⁹ Madhupratap et al., 1994, 1996, 2001). ⁵⁹Murthy (1987) investigated the characteristics of neritic waters including DO and zooplankton bio volume and found, biological production is first enhances in the southern part than in the north.

Enormous studies have been conducted explaining the chemical and biological response of upwelling in the SEAS as well as in different part of the world (⁶²Nair, R.V., 1959; ⁷Banase, 1959; ¹¹³Subramanyan and Sharma, 1965; ⁵⁸Murty, A.V.S., and M.S., Edelman, 1971; ⁹²Shah, 1973; ⁴Bakun and Parrish, 1982; ¹⁵Brock et al., 1992; ⁷⁵Prasannakumar et al., 2001; ¹²⁷Wiggert et al., 2005; ⁸⁸Santos et al., 2007; ³⁷ Krishnakumar et al., 2008;

³⁶ Krishnakumar and Bhat, 2008; ²⁸Habeeb et al., 2008 and ⁸⁷Sanjeevan et al., 2009). Upwelling and its impact on the survival of fish egg/larvae, migratory pattern and the recruitment-upwelling intensity relation are all key subjects relating upwelling and the biological implications (⁴Bakun and Parrish, 1982; Balan, 1984; ²¹Cury and Roy, 1989; ⁷⁰Pauly and Tsukuyama, 1987; ⁴²Longhurst and Wooster, 1990). Other relevant topic related to the shelf upwelling is the increased occurrence of hypoxic or anoxic bottom waters associated with the process, which of course, have significant role in modifying the biogeochemistry of the ecosystem (⁶³Naqvi et al., 1990; ⁶⁴Naqvi and Noronha, 1991; ⁶⁵Naqvi et al., 1998; ⁶⁶Naqvi and Jayakumar, 2000; ⁷⁸Rabalais et al., 2001).

To address the dynamics of the process of upwelling, the alongshore wind stress and wind stress curl have been identified as the most important local forcings responsible for the occurrence of upwelling through Ekman dynamics during the SM [¹⁰⁵Shetye et al., 1985; ¹⁰²Shetye and Shenoi, 1988]. The upwelling first appears in the southern latitudes along the southwest coast of India and progressively advances poleward in association with the northward propagating upwelling coastal Kelvin waves during the premonsoon season resulting in maximum upwelling off Kochi [⁵²McCreary et al., 1993; ⁹³Shankar and Shetye, 1997]. The

multilayer numerical models driven by climatological winds that simulated the ocean circulation in the north Indian Ocean have demonstrated the importance of remote forcing from the equator through propagating Kelvin and Rossby waves [²⁰Clarke, 1983; ⁷³Potemra et al., 1991; ¹³³Yu et al., 1991; ⁵² ⁵³McCreary et al., 1993, 1996; ¹⁸Bruce et al., 1994; ⁹³Shankar and Shetye, 1997; ²⁹Han and Webster, 2002].

Though upwelling signals are observed in sea level from February (⁹⁹Shenoi et al., 2005) onwards, the chemical and biological indications of upwelling in the surface–subsurface waters are observed only in association with the commencement of the SM (June). With the onset in May end, weak-to-moderate upwelling occurs off Cape and spreads northwards along the coast as the monsoon advances, reaching up to the Goa coast during peak monsoon season (July–August).

The classical explanation of coastal upwelling describes wind-induced divergence caused by Ekman transport (¹¹⁶Sverdrup et al., 1942). ³⁴ Johanessen et al., (1987) noted that the wind is an important driving force from February onwards and upwelling is associated not only with local wind but also with larger-scale monsoonal (SW) conditions, which drive the anticyclonic Arabian Sea monsoon gyre. Studies by ¹⁰⁵ Shetye et al. (1985); ⁵⁷ Muralaiah and Prasannakumar (1996); ⁶¹ Naidu et al., (1999),

and ^{43,44}Luis and Kawamura (2002a, 2002b) explain the phenomena as offshore divergence of the alongshore wind stress component. However, using a numerical model, ⁵²McCreary et al., (1993) found a large decrease in the shoaling and decrease in the upper-layer thickness off the west coast of India when switching off the Bay of Bengal winds, which was also observed by ¹⁸Bruce et al., (1994) and ⁹³ Shanker and Shetye (1997).

According to ³Bakun et al., (1998) and ¹⁰⁹Smitha et al., (2008), the strong westerly monsoon winds at the southern extremity of the Indian subcontinent are tangential to the landmass and drive a very strong offshore Ekman transport. This strong upwelling signal should tend to propagate northwards along the Indian coast via the coastally trapped wave mechanism. The offshore extend of upwelling or upwelling front are studied by ¹Antony et al., (2002) and ⁸⁶Sanil Kumar et al., (2003) and showed that fronts occur quite near to the coast (average 110 *km* from the shore) with strong temperature gradient and with currents weaker towards the coastal belt.

Various model studies conducted along this region have clearly shown that the winds over the equatorial IO play an important role in modulating the circulation features of the NIO ⁷³ Potemra et al., 1991; ¹³³Yu et al., 1991; ^{52,53}McCreary et al., 1993 & 1996; ⁹⁴Shankar et al., 2002]. Wind jets in the equa-

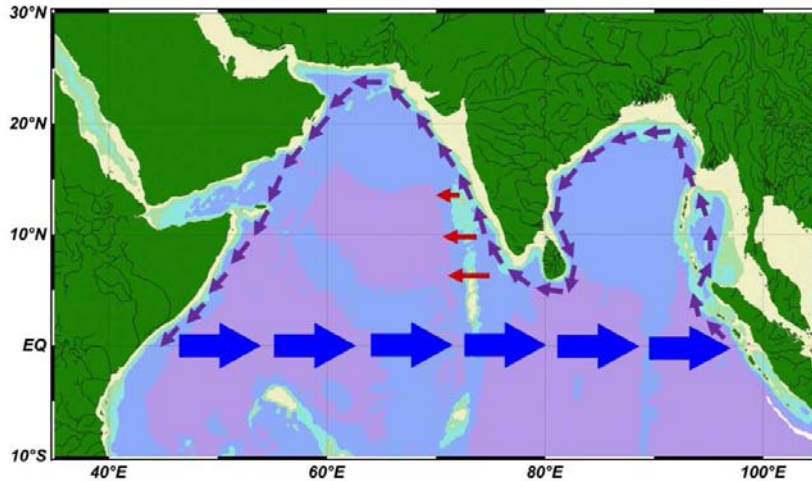


Figure 1.4: Trajectory of the Kelvin wave (blue thick arrow), Coastal Kelvin wave (violet thin arrow) and westward propagating Rossby waves (red arrows) along the west coast of India.

torial Indian Ocean between 5°S to 5°N excite equatorial Kelvin waves (Fig. 1.4) which on reflection from the eastern boundary of the Bay of Bengal, propagates along the perimeter of this basin as coastal Kelvin wave and radiate westward propagating Rossby waves. The coastal Kelvin waves propagate along the periphery of the Bay of Bengal, bend around Sri Lankan coast and enter the west coast of India after about one month with a phase speed of 2.7 m/s [^{52, 53} McCreary et al., 1993 & 1996; ¹⁹ Chelton et al., 1998, ⁹⁴ Shankar et al., 2002]. The coastally trapped planetary wave up-slope the subsurface isotherms and the Ekman transport due to the northerly wind transport the water offshore. The upwelling

Kelvin waves radiate upwelling Rossby waves which propagate off shore and promote cyclonic circulation in the Lakshadweep Sea during summer.

The zonal wind stress climatology is relatively stronger over the east central equator and shows strong intraseasonal variability with pronounced peaks during the monsoon transitions resulting in Spring and Fall Wyrтки Jets. These westerly wind bursts produce downwelling Kelvin waves that propagate along the equator [⁹¹ Sengupta et al., 2007]. When these westerly wind bursts weaken or replaced by easterlies during winter, the upwelling Kelvin waves get triggered and propagate along the equator. In addition, the surface wind stress curl climatology along the equator is negative during April–November and positive during December–March that triggers eastward propagating downwelling and upwelling Kelvin waves.

The Kelvin waves also trigger Rossby waves that propagate westward both along the equator and off the equator. ⁹⁴ Shankar et al. [2002] have carried out a detailed study highlighting the relative importance of various processes both local and remote that modulate the sea level and circulation in the north Indian Ocean. Their study reveals that the equatorial zonal winds and the along-shore winds off the Myanmar coast have shown a relatively weaker role in modulating the upwelling and downwelling cycles observed

along the southwest coast of India. Whereas, the local alongshore winds together with the remote forcing along the southern coast of Sri Lanka may play an important role in modulating the observed interannual variability in the processes of upwelling in the SEAS (²⁶Gopalakrishna et al., 2008).

1.6 Objectives of the Present Study

Although most of the coastal upwelling in the AS is wind driven uniform systems, mesoscale studies along the southwest coast of India shows high spatial and temporal variability in the forcing mechanism and intensity. As the wind in most upwelling zones in the eastern ocean boundaries there generally exists an equator ward component of wind stress and therefore an offshore component of surface Ekman transport is expected throughout the year. But as the studies supported with in situ evidences indicates that the process is purely seasonal and recurring, the explanation purely based on local wind forcing only is not sufficient to support the observations. So, this can be stated that upwelling along the SEAS is an effect of basin wide wind forcing rather than local wind forcing. Present study on the upwelling of the SEAS, in an integrated approach covering the latitudinal and seasonal variations (based on SST, wind forcing, and Surface Chlorophyll distribution), forcing mechanisms (Local wind and remote forcing)

and the factors influencing (ASHSW, Bay of Bengal water, Runoff, geomorphology and coastal orientation) the system.

The specific objectives are;

- To understand the upwelling pattern in the SEAS, and delineation of different upwelling zones according to the forcing mechanism and intensity.
- To give theoretical formulation for the process and derivation of upwelling indices.
- To understand the spatial and temporal variation.
- To study the chemical and biological response to the varying wind field and the time lag between the physical forcing and biological production.
- To estimate the total PP associated with the coastal upwelling ecosystem of the SEAS and its variability during different years.

Chapter 2

Upwelling Mechanism

“Refining is inevitable in science when you have made measurements of phenomena for a long period of time.”

– Charles Richter.

2.1 Introduction

UPWELLING off southwest coast of India, as indicated by rapid upward movement of isotherms, surface cooling and the associated fall in coastal sea level, occurs during the SM months from May to September. Though upwelling signals are observed in sea level from February (⁹⁹Shenoi et al., 2005) onwards the chemical and biological indications of upwelling in the surface or subsurface waters is observed only in association with the commencement of the summer monsoon. With the onset of the southwest monsoon in May, weak to moderate upwelling occurs off Cape

coast and spreads northward along the coast as the monsoon advances, reaching up to the Goa coast during peak monsoon (July-August). Though several attempts have been made to explain the phenomenon, a clear picture on the formation and spread of the upwelling process off Indian coast is still not available. The classical explanation of coastal upwelling describes wind-induced divergence caused by Ekman Transport (¹¹⁶Sverdrup et al., 1942 and ³⁴Johanssen et al., 1987) noted that wind is an important driving force from February onwards and upwelling is not only associated with local wind but also with more large scale monsoonal (SM) conditions which drive the anticyclonic Arabian sea monsoon gyre. Studies by ¹⁰⁵Shetye et al., 1985; ⁵⁷Muraleedharan and Prasannakumar, (1996); ⁶¹Naidu et al., (1999) and ^{43, 44}Luis and Kawamura, (2002a) & (2002b), explain the phenomena as offshore divergence of the alongshore wind stress component. However, using a numerical model, ⁵²McCreary et al., (1993) identified the role of remote winds at BoB on triggering the system, which was also observed by ¹⁸Bruce et al., (1994) and ⁹³Shanker and Shetye (1997). According to ³Bakun et al., (1998), the strong westerly monsoon winds at the southern extremity of the Indian subcontinent are tangential to the landmass and drive a very strong offshore Ekman transport. This strong upwelling signal should tend to propagate northward along the Indian coast via the coastally

trapped wave mechanism.

In this chapter, the role of tangential winds off the Cape coast, long-shore component of the wind stress along the southwest coast, the influence of remote forcing in the form of the coastally trapped Kelvin waves and the ASHSW in the formation and northward extension of the upwelling process in the SEAS are explained. Comparisons are made on the basis of upwelling indices derived from SST and wind (Fig. 2.1), vertical velocities from wind and isothermal shift, surface salinity distribution and the monthly composite images of surface Chlorophyll distribution.

2.2 Materials and Methods

2.2.1 Upwelling Index (UI) from SST

Monthly averages of SST for eleven years (from January 1990 to December 2000) from Reynolds reconstructed SST field are examined in $1^{\circ} \times 1^{\circ}$ latitude-longitude grids for the area $4^{\circ} 30' N$ to $14^{\circ} 30' N$ latitude and $70^{\circ} 30' E$ to $78^{\circ} 30' E$ longitude in the Arabian Sea (Fig. 2.1). Before conducting the analysis, interannual variations in SST in the eleven year data were verified to detect any significant influence of Indian Ocean Dipole events ⁸¹ (Rao et al., 2002) during 1994 and 1997 and El Nino and La Nina during 1997 and 1998 respectively. Considerable variations ($\sim 0.5^{\circ}C$) in

SST were observed during 1997 and 1998 (the warm phase and cold phase respectively). However, the eleven year averaged data is not expected to have any bias in the analysis, since the anomalies are almost equal and opposite and will thus balance between them. Following the approach of ¹²⁹Wooster et al., (1976), ⁷⁶Prell and Streeter, (1982) and ⁶¹Naidu et al., (1999) the Local Temperature Anomaly (LTA) is calculated as coastal upwelling Indices by comparing the coastal and offshore SST. Since the influence of upwelling is known to extend 200-400 *km* from the coast in the southwest coast (¹Antony et al., 2002), the offshore stations are chosen off 3° to the coastal stations. This is cross checked with thermal fronts observed during two FORV Sagar Sampada cruises (SS 217 during September 2003 and SS 237 during August 2005) and found matching except off Goa (15°N) where it is almost four times lesser than that recorded by ¹Antony et.al., (2002). The LTA is calculated as;

Along the SW Coast,

$$LTA_{wc} = T_{lon-3} - T_{lon}$$

Off Cape,

$$LTA_{kk} = T_{lat-3} - T_{lat}$$

Where,

T_{lat} and T_{lon} represent the coastal stations between latitudes 8.5°N to 14.5°N and longitude 76.5°E to 78.5°E;

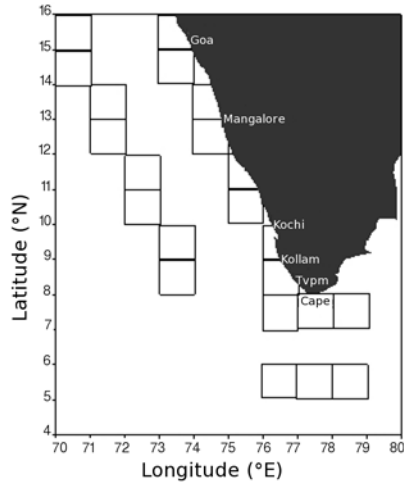


Figure 2.1: Location map and the $1^\circ \times 1^\circ$ squares used to derive upwelling indices.

T_{lon-3} and T_{lat-3} represents SST at 333 km away from the coast.

LTA_{WC} and LTA_{kk} respectively refer to Local Temperature Anomaly along the southwest coast and Cape coast.

The positive LTA values suggest coastal upwelling process.

2.2.2 Upwelling Index (UI) from Wind

A unique wind-forcing pattern occurs over the Indian Ocean, unlike the pattern over the other oceans. The winds blow strongly during May-September, the southwest monsoon, forming the Find later jet over the Arabian Sea with maximum speeds of

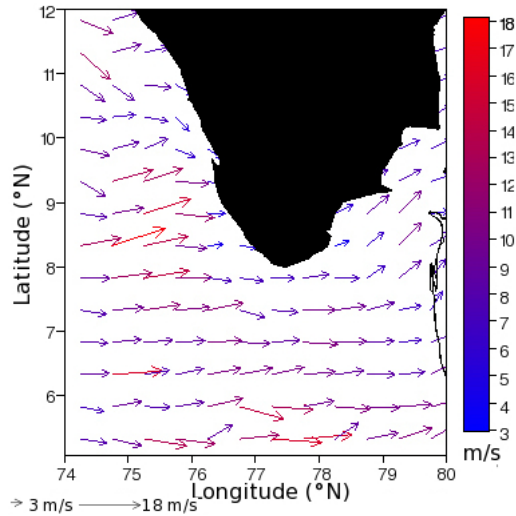


Figure 2.2: Wind pattern during July 2005 (from Quikscat Scatterometer) showing the tangential winds at the southern tip.

about 16 m/s . The winds during the season are generally southwest over most part of the Arabian Sea and they become northerly along the west coast of India. However, off the southern tip of peninsular India, they are from the west, stronger and are tangential to the coast (Fig. 2.2). During the WM (November-February) the winds are from northeast and have maximum magnitude of about 6 m/s . During the transition months, the SIM (March-May) and FIM (October), the winds are very weak.

To evaluate the theoretical model's suggestions that a northerly wind along the west coast of the Indian continent drives an offshore Ekman drift together with a surface flow parallel to

the coast; Ekman transport (M_x in $kg/m/s$) is calculated in $1^\circ \times 1^\circ$ latitude-longitude grids for the west coast and the Cape coast (Fig. 2.1). Monthly averaged wind data (both U and V components) from Comprehensive Ocean Atmosphere Data Sets (COADS Enhanced) for eleven years (in $1^\circ \times 1^\circ$ latitude-longitude grids) from January 1990 to December 2000 are used to understand the role of local wind stress on the coastal upwelling processes. According to the classical square law formula ⁵ (Bakun, 1973), the alongshore component of the wind stress off Cape and southwest coast is computed as,

$$\tau = \rho_a C_d C_d |U| U \text{ off Cape}$$

and

$$\tau = \rho_a C_d |V| V \text{ off southwest coast;}$$

$\rho_a = 1.29 kg/m^3$ is density of air

C_d is the non-dimensional drag coefficient, which is a function of both wind speed and stability. In general, C_d increases with wind speed and stability of overlying atmosphere;

$$1000C_d = 0.29 + 3.1/U_{10} + 7.7/U_{10}^2 \quad (3 < U_{10} < 6m/s)$$

and

$$1000Cd = 0.60 + 0.07 * U_{10} \quad (6 < U_{10} < 26m/s)$$

Where U_{10} is wind speed at 10 m above the sea level.

U and V are the estimated wind vectors near the sea surface with magnitude $|U|$ and $|V|$. Along the west coast of India, the alongshore components are obtained with reference to the inclination of the coastline by adding the coastal inclination to the wind direction. Whereas along Cape, as the winds are tangential to the coast (Fig. 2.2), no inclination is considered in computing the along shore wind stress component.

Under Ekman's assumptions of steady state motion, uniform wind and infinite homogeneous ocean, the mass transport per unit width of ocean surface is directed 90 degrees to the right (in the NH) of the wind direction. This is related to the magnitude of the wind stress by $M = \tau/f$, where $f = 2\omega \sin\phi$ is Coriolis force due to Earth's rotation at latitude ϕ , ω =angular Velocity of Earth's rotation and is equal to 7.292×10^{-5} radians/sec.

2.2.3 In Situ Observations

Temperature profiles from CTD Profiler (SeaBird Electronics 911 series) and wind data from AWS collected onboard FORV Sagar Sampada in four cruises (FORV 234, 235, 236 & 237) during May-September 2005 are used to explain the vertical structure and to compute upwelling velocity during the study period.

Spatial variation in upwelling along the Coastal region is established from vertical velocity computed from isothermal shift and wind at the six selected transects Cape (8°N), Tvpm (8.5°N), Kollam (9°N), Kochi (10°N), Mangalore (13°N) and Goa (15°N). Vertical velocity in m/day is calculated from the shift in 24°C isotherm between May 2005 and July 2005 for the southern transects up to Kochi. Data collected during May - June 2005 and August - September 2005 is used for Mangalore and Goa transects. Significance of taking average wind velocity during the two observations has been verified by analysing the day-to-day variations in the wind field and correspondingly the changes in the thermal structure. For this time-series observations conducted along Kollam (9°N lat) and Tvpm (8.5°N lat) transects during 24th June to 6th July 2006 were analysed and observed daily undulations in the thermal section as shallowing and deepening of isotherms according to the variations in wind. Vertical velocity of the wind driven upwelling is estimated following ⁸⁹ Sarhan et al., (2000).

$$Velocity = \tau / \rho w f L$$

where τ is wind stress. ρW is the density of seawater, 1025 kg/m^3 , f is Coriolis force and L is the cross-shore length scale of upwelling.

Surface Salinity values derived from CTD-SeaBird 911 (calibrated against salinity derived from water samples collected simultane-

ously with a rosette sampler and analysed with guideline 8400 Autosal) collected onboard FORV Sagar Sampada during May, June and September (during 1997-2003) in different cruises (SS142, SS173, SS203 and SS217) were made use to understand the surface salinity distribution during different monsoon months.

2.2.4 Observations from Satellite

Climatology of the monthly (June-September) composite maps of Chlorophyll *a*, Ocean Colour Level 3-binned product, for four years (2003-2006) derived from MODIS AQUA at 9 km spatial resolution from Goddard Space Flight Centre (GSFC) NASA are used to describe the surface productivity patterns in the area.

2.3 Results and Discussion

2.3.1 Upwelling Off Southern Tip (Cape)

Seasonal variations in LTA from the eleven year average data gives positive LTA values $>0.25^{\circ}C$ for the Cape (Fig. 2.3a), except for the SIM. Peak values are recorded during July and August with considerable horizontal gradient in temperature ($LTA = 0.85^{\circ}C$). After August, LTA decreases gradually reaching near to zero values by February. Ekman mass transport from the mean monthly climatology for the eleven year indicates strengthening of offshore

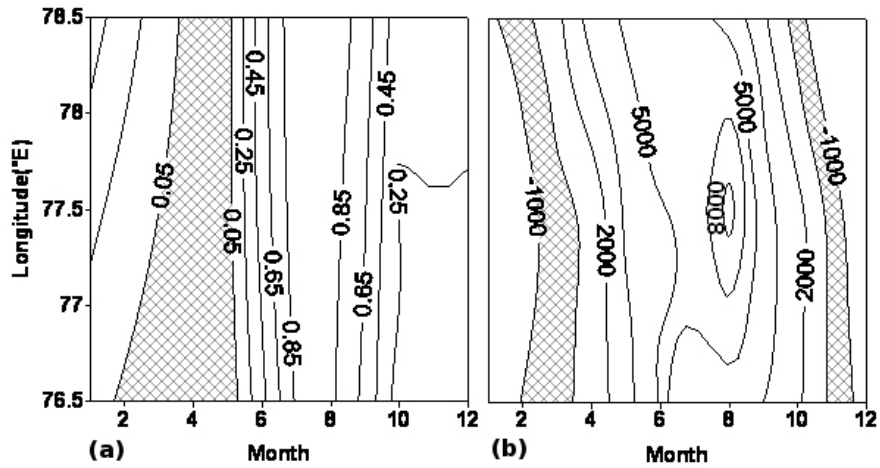


Figure 2.3: Variation of (a) LTA and (b) Ekman mass transport ($kg/m/s$) as a function of time (month) and space (longitude) at Cape. Shaded part indicates negative values.

mass transport off Cape from May to October, with a maximum (8000 kg/m/s) in August (Fig. 2.3b) corresponding to the strong westerly winds that are tangential to the coast during the SM.

The influence of wind in driving the upwelling process off the Cape coast is ascertained by comparing the observed vertical shift of the 24°C isotherm with the vertical velocity estimated from wind. The upslope of the 24°C isotherm at the rate of 1.17 m/day is less than the estimated vertical Ekman velocity of 1.62 m/day . The latter highlights the influence of tangential wind stress.

2.3.2 Upwelling Off Southwest Coast

Along the southwest coast of India LTA values are positive

during May to October up to 13.5°N latitude (Fig. 2.4a) with the rest of the area north of 13.5°N recording negative values which indicates the absence of upwelling features in the surface temperature distribution of the area. Fig. 2.4a also depicts local variation in upwelling during June-August with LTA higher than 0.7°C between 9°N to 10°N (between Kollam and Kochi). LTAs weaken northwards reaching almost zero values at 13.5°N latitude.

However, Ekman mass transport derived from the long-shore component of the wind stress gives weak positive values throughout the year between 8.5°N and 14.5°N latitude (Fig. 2.4b). The mass transport is strong at south during June-July (4000 $kg/m/s$) and reduces progressively northwards, which is consistent to the observations of ¹⁰⁴Shetye et al., (1991), ⁶⁸ Pankajakshan et al., (1997) and ³Bakun et al., (1998) on the upwelling patterns off the southwest coast.

With a view to understand the observed anomaly between the LTA and the Ekman transport, comparison was made between the vertical shifts in the 24°C isotherm to the vertical Ekman transport from wind stress across selected transects of the west coast namely Tvpm (8.5°N), Kollam (9°N), Kochi (10°N) for the period from 14th of May 2005 to 5th of July 2005 and Mangalore (13°N) and Goa (15°N) for the period 4th June 2005 to 3rd September 2005. Along the transect off Tvpm the upslope of 24°C

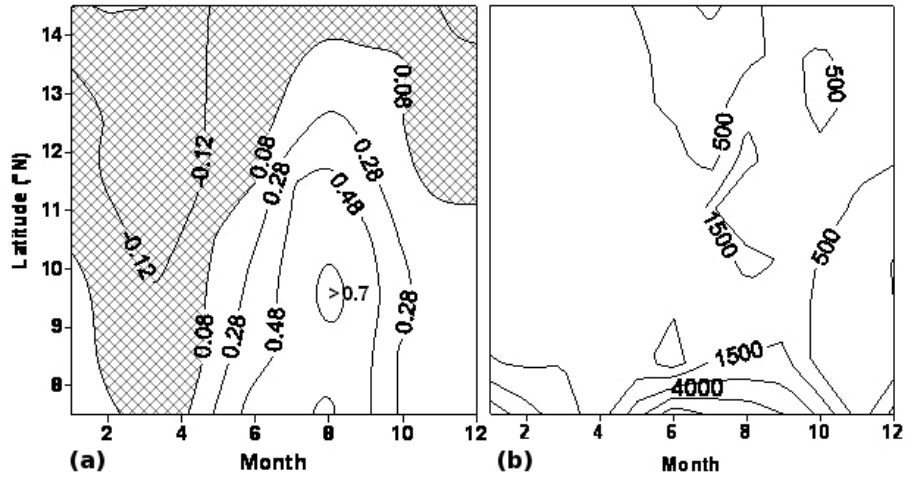


Figure 2.4: Variation of (a) LTA and (b) Ekman mass transport ($\text{kg}/\text{m}/\text{s}$) as a function of time (month) and space (latitude) along the south-west coast of India. Shaded part indicates negative values

isotherm occurs at the rate of $0.857 \text{ m}/\text{day}$ which is closer to the vertical Ekman transport ($0.745 \text{ m}/\text{day}$) from the wind. The best-fit regression equation of LTA and Ekman transport ($LTA = 0.2164 + 0.0002x$) is applied on the wind stress off Tvpm and found that the estimated LTA (0.552°C) corresponds approximately to the observed LTA (0.561°C). The above observations indicate that upwelling along the Cape-Kollam coast (8°N to 9°N lat) is driven predominantly by the alongshore component of the wind stress.

North of Kollam (9°N), weak Ekman transport is persistent throughout the year (Fig. 2.4b) with peak values of $1500 \text{ kg}/\text{m}/\text{s}$ during June-July up to 13°N lat, further north of which it falls

to around 500 kg/m/s. However, LTA from the in-situ SST observations are positive only up to 13.5°N (0.175°C for July), north of which the values are negative. The general trend is that the LTA does progressively increase towards south (with peak value of 0.721°C at 9.5°N in August) and decreases progressively towards north (-0.084°C at 14.5°N in June). All along the coast, LTA are high during July and August, which corresponds to the peak southwest monsoon period. The role of wind stress in maintaining the LTA was tested by applying the regression equation ($LTA = 0.2164 + 0.0002x$) for Tvpm (8.5°N) to the local wind stress for each degree latitude north of 8.5°N. For the area 9°N to 13°N the derived LTA are significantly lower than the observed LTA and then could explain only part of the upwelling process is due to windstress and further implies the role of remote forcing in the sustenance of observed LTA. This is further tested by comparing the vertical shift of the 24°C isotherm off Kollam and Kochi for the period May to July with the vertical Ekman Transport from wind stress. Both at Kollam and Kochi the isothermal shift was at the rate of 1.1m/day whereas the estimated vertical transport was only 0.38m/day for Kollam and 0.55m/day for Kochi. These observations suggest that the upwelling process along the area 9°N to 13°N is influenced by the combined effect of local winds and remote forcing.

North of 13°N, LTA progressively decreased reaching negative values at 14°N. The observed LTAs are lower than LTA derived from wind stress by applying the regression equation ($LTA = 0.2164 + 0.0002x$) for T_{ypm} on the local wind stress. The seasonal averages of the observed and derived LTA are 0.086°C and 0.363°C for 13°N-14°N and 0.052°C and 0.288°C for 14-15°N. Similarly the observed rate of the vertical transport at 13°N (0.35 *m/day*) and 15°N (0.067 *m/day*) are lower than the values derived from wind stress (0.365*m/day* for 13°N and 0.24*m/day* for 15°N). From this it is expected that the process of upwelling along this coastal strip is suppressed somehow, despite having winds favourable for upwelling.

2.3.3 Surface Salinity Distribution

Surface salinity plots (Fig. 2.5) for May, June and September reveal the formation and fate of the upwelled waters along the coast. During May, the southwest monsoon winds are weak and upwelling is confined to a narrow zone between 9°N-10°N. During June, the southwest monsoon winds are stronger and the upwelling process extends along the coast from 9° to 13°N. The upwelled waters of the area are characterised (in temperature, salinity and density values) by the presence of the BoB waters on the surface. These waters are transported offshore to a distance of

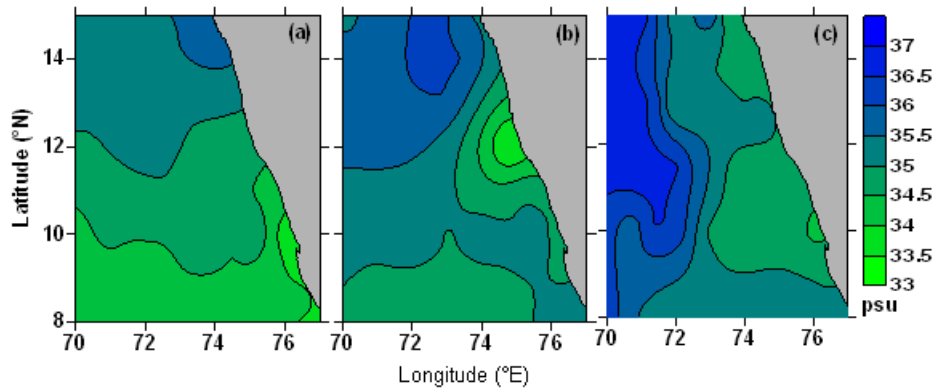


Figure 2.5: Sea surface salinity for (a) May, (b) June, and (c) September show the southwards propagation of the ASHSW.

approximately 200km by the combined effect of Ekman transport and Rossby waves radiated from coastally trapped Kelvin waves (⁹³Shanker and Shetye, 1997; ⁹⁹Shenoi et al., 2005). Further north, the upwelling is weak and confined close to the coast possibly due to the suppressive effect (cold dense upwelled waters are pushed to the coast by warm high saline waters while its propagation to the southeast) of the southward extending ASHSW (⁵⁷Muraleedharan and Prasannakumar, 1996).

On the basis of water mass studies ¹¹¹Stramma et al (1996) had indicated that water at the shelf edge was a mixture of low salinity water advected out of the BoB around Srilanka and higher salinity Arabian Sea water. ⁹³Shanker and Shetye (1997) examined the dynamics of the coastal circulation of the

region using a one and a half layer dynamically reduced gravity model and observed that the upwelling Rossby waves radiated by the upwelling coastally trapped Kelvin waves with a peak in July propagating poleward along the Indian west coast are instrumental in generating the fall in sea level during active monsoon. ⁷⁴Prasannakumar and Prasad (1999) while describing the ASHSW had noted that as the SM winds become progressively well established during June to September, the open ocean circulation reverses its direction with a zonal current towards east that become stronger, and that under the influence of the SM circulation the high salinity core is pushed southeastward and slowly spreads towards south along the west coast of India. The salinity plots for May, June and September are consistent to the above observations.

Inferences from upwelling indices, vertical velocities and surface salinity pattern strongly indicate absence of remote forcing in the region between 8°N to 9°N and this makes the conclusion that the Kelvin waves reach the west coast of India, get coastally trapped at about 9°N and propagate pole ward as the coastally trapped waves thereby demarcating a narrow strip of the coast between Cape and Kollam (8°N to 9°N) as the “Shadow Zone” (Fig. 2.6). This could be explained in terms of the 2000m isobath (Fig. 2.6), which may act like a cliff in the path of the wave deviating it to

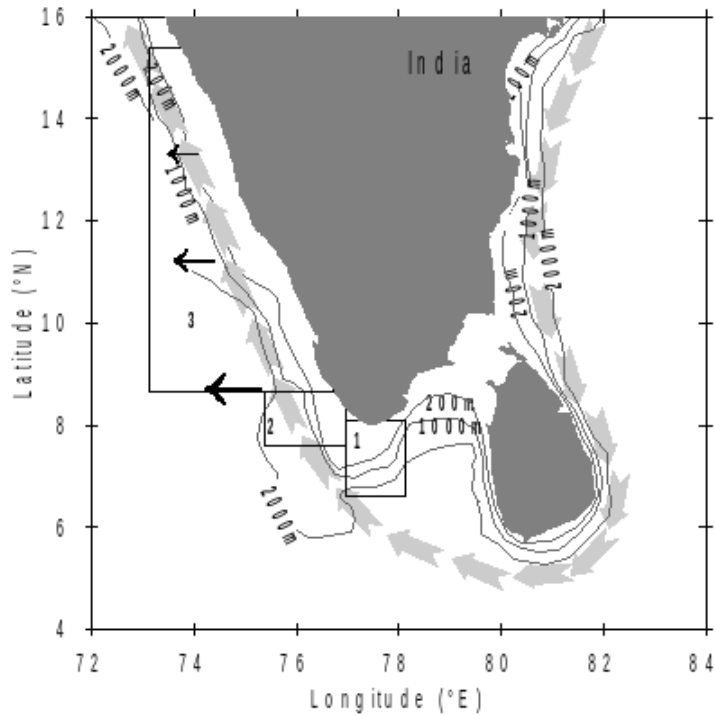


Figure 2.6: Schematic representation of different upwelling zones classified according to the formation mechanism, as well as intensity. Arrows along the coast represent coastal Kelvin waves. Westwards-directed black arrows depict Rossby waves, the phase velocity of which decreases moving from the equator; upwelling at area 1 is strongly wind driven; area 2 is a shadow zone with weak wind-driven upwelling; upwelling at area 3 is the result of remote forcing, as well as wind stress.

its optimal energy path. Upwelling process along the shadow zone is thus purely driven by the long-shore component of the wind stress as indicated by the rate of the vertical Ekman pumping. The absences of the BoB water on the surface layer of the shadow zone further substantiate the above view.

Upwelling along the area 9°N to 13°N is under the combined influence of wind stress, and the upwelling mode of the Kelvin and Rossby waves (⁹³Shanker and Shetye, 1997). As a result, moderate to intense upwelling occurs along the coastal belt from 9° to 13°N. The vertical velocity/isothermal shift in the area 9° to 11°N far exceeds the vertical shift computed from wind stress. The upwelled waters have distinct signatures of the BoB waters and are transported to about 200 *km* offshore by the Rossby waves. North of 13°N, the intensity and extend of upwelling weakens due to the suppressive effect of the ASHSW and the weakening of the Rossby waves (¹⁴Brandt et al., 2002 and ¹⁰³Shetye, 2005). However with the advancement of monsoon, the wind become stronger and pushes out the ASHSW to the offshore resulting in weak upwelling confined close to the coast. At the extreme north (14°N to 15°N) upwelled waters are confined very close to the coast and are thus not reflected in the LTA estimates, perhaps due to the high resolution (1°X1°) of the data. This explains the occurrence of negative LTA at the extreme north of the study area. Longitu-

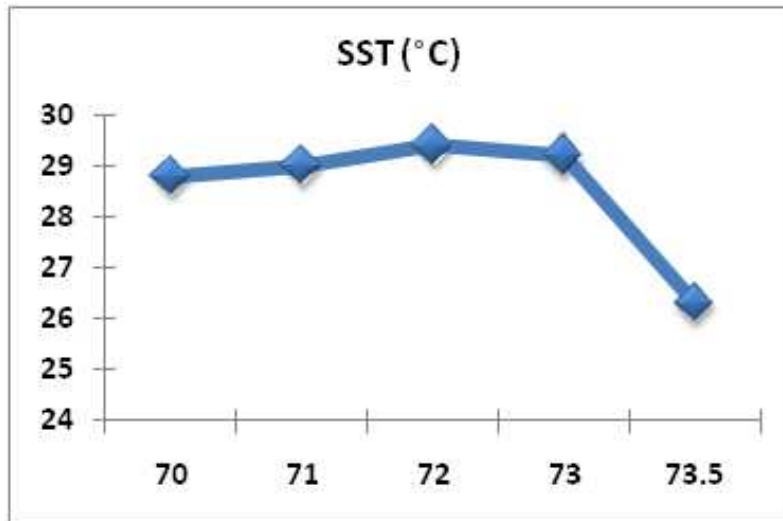


Figure 2.7: SST ($^{\circ}C$) variation along the $15^{\circ}N$ transect during September 2003, showing the limited offshore extension of upwelling.

dinal variations in SST off the Goa coast ($15^{\circ}N$) clearly show that upwelling is confined very close to the coast (Fig. 2.7).

2.3.4 Surface Chlorophyll *a* Distribution

Observations on the upwelling patterns of the southwest coast are further verified using the four year (2003-2006) climatology monthly composite images of surface Chlorophyll *a* distribution along the study area for the southwest monsoon (Fig. 2.8). During July surface Chlorophyll *a* maxima are seen as isolated patches south of Cape and west off Tvpm ($8.5^{\circ}N$). A narrow stretch of low primary productivity demarcates the shadow zone between $8^{\circ}N$

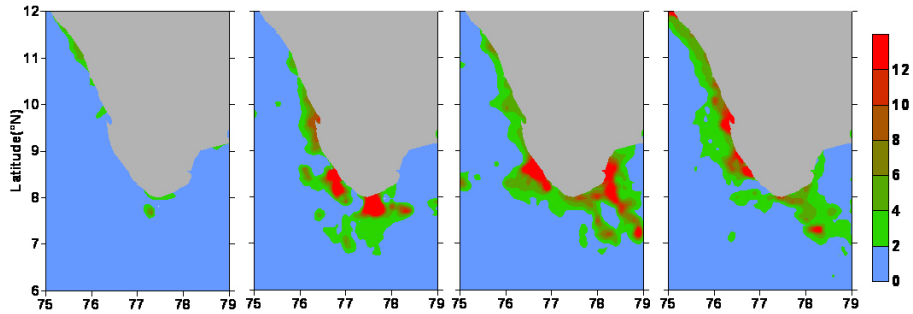


Figure 2.8: Four-year climatology (2003–2006) of monthly composite surface Chlorophyll from MODIS AQUA for June–September.

to 8.5°N . With the advancement of the southwest monsoon the Chlorophyll a patches extend northwards along the west coast corresponding to the geomorphology of the coast and the northward propagation of the monsoon. The offshore extent of the surface Chlorophyll a spread is maximum between 8.5°N and 9°N , which is south of the peak upwelling area (9°N to 13°N) as inferred from the surface salinity distribution (Fig. 2.5b).

The discrepancy should be due to the lag phase between the availability of nutrients and the actual primary production. The WICC transports the surface waters of the west coast southward and at the extreme tip of peninsular India; the surface Chlorophyll patch is transported equator ward by the combined action of the offshore Ekman transport and the WICC. The formation and the fate of the Chlorophyll a maxima south of Cape coast and al-

ong the west coast of India are consistent to the observations on the upwelling patterns for the coast.

2.4 Conclusion

Upwelling along the southwest coast and southern tip (off the Cape) are localised phenomenon under the influence of varying forcing mechanism. Along Cape, upwelling is strong and is influenced by the SM winds that are tangential to the coast. Chlorophyll *a* maxima are recorded in June when the southwest monsoon winds are strongest at this point. Surface Chlorophyll *a* is transported equator ward due to the combined effect of off shore Ekman mass transport and WICC. Along the west coast, the area between 8°N and 9°N represent the shadow zone, where the role of remote forcing is weak and the upwelling occurs exclusively by Ekman transport brought out by the long-shore component of the wind stress. The area north of this (9°N to 13°N) show moderate to intense upwelling under the combined influence of the wind stress and remote forcing in the form of coastally trapped Kelvin waves and the offshore radiating Rossby waves. Within this area the offshore propagation of the upwelled waters is maximum at the southern part and progressively weaken northwards perhaps due to the weakening of the offshore propagating Rossby waves.

Further north (13°N to 15°N), the process of upwelling is weak and confined very close to the coast, despite winds favourable for upwelling. This may be due to the presence of the southward flowing tongue of the ASHSW, which suppress the upwelling along the coast. During July and August the southwest monsoon winds are strong over the area, which may push the ASHSW slightly offshore leading to weak upwelling confined close to the coast.

Chapter 3

Theoretical Formulation of the Process of Upwelling

“It is a capital mistake to theorise before one has data.”

– Sir Arthur Conan Doyle.

3.1 Introduction

UPWELLING, the seasonal process occurring every year in the SEAS, has a strong significance in the biogeochemistry and fishery of the region. It is identified that 30-50% of the total pelagic fishery of India, is contributed in connection with the process of coastal upwelling. The area is observed suitable for spawning for number of pelagic fishes like Oil sardine, Indian mackerel and Anchovies etc. Also the survival of fish eggs/larvae and recruitment to fishery is highly influenced by the environmental parameters of this region during the season. A number of studies have been con-

ducted in different upwelling systems of the global ocean relating the intensity of the process upwelling and the recruitment index of related fishery. Studies by ⁴Bakun and Parrish (1982) and ²¹Cury and Roy (1989) introduced Optimum Environment Window (OEW) concept explaining the effects of environmental variation on the survival of larval pelagic fishes. According to them, there is an optimal limit of upwelling for sustained fishery, especially in wind driven systems. Turbulence and offshore transport is identified as the two factors which adversely influence the survival of eggs/larvae of fishes. As per ²¹Cury and Roy (1989), for Ekman type upwelling, the annual recruitment increases with upwelling intensity until wind speed reaches a value of roughly 5-6 m/s and decreases for higher values. And for a non Ekman type upwelling the relationship between recruitment and upwelling intensity is linear. This emphasizes the necessity of proper indexing or quantification of the process of coastal upwelling of the SEAS, to understand the dynamics and the associated biogeochemistry of this ecosystem. Upwelling indices are mainly based on wind-stress and offshore mass transport, ie, $M_x = \tau_y / f$, where M_x is the cross shore mass transport and τ_y is the stress due to along shore component of the wind. Here it is assumed that the offshore transport and upliftment of isotherms are purely due to the alongshore wind stress. In systems other than Ekman driven, this index does

not explain the process as is the case with the SEAS upwelling system.

Another accepted indexing for coastal upwelling is the LTA or the difference in SST between the offshore (the area beyond the outward limit of the upwelled water) and coastal locations. That is, $LTA = SST_{offshore} - SST_{coastal}$. Though this is an estimate based on the responding variable prevailing over the area it can be biased or erroneous due to the influence of freshwater runoffs, coastal currents and intrusion of other water-masses in to the region. Studies giving explanations to the process based on LTAs are plenty (¹²⁹Wooster et al., 1976, ⁷⁶Prell and Streeter, 1982 and ⁶¹Naidu et al., 1999).

Considering SEAS upwelling system, the process is too complex, and is not a uniform wind-driven upwelling but more localised with latitudinal variability in forcing mechanisms as well as intensity. As discussed in chapter two, the process is due to tangential wind stress off Cape (8°N) coast and along shore wind stress acts along Cape (8°N)-Kollam (9°N) strip which is termed as shadow zone, due to weak forcing in the area. The area north of Kollam is observed to be influenced by both alongshore wind stress and remote forcing like coastal Kelvin waves and offshore propagating Rossby waves and this extends up to Mangalore (13°N). Further north up to Goa (15.5°N) alongshore wind stress domi-

nates over remote forcing, may be due to the weakening of offshore propagating Rossby as they get decay as going away from the equator (⁹³Shanker and Shetye., 1997, ⁴⁵Luis and Kawamura, 2004, ¹⁰³Shetye, 2005). With this background information, an attempt has been made to estimate a new relationship for each region individually considering all the factors which are influencing the system adversely or favourably.

3.2 Data and Methodology

3.2.1 Upwelling Index from SST and Wind

The data and methodology as explained in chapter 2 is adopted for the present analysis to estimate UIs from SST and wind for the monsoon months (June-September) for the years 1993 to 2000.

3.2.2 SSHA from Satellite Altimetry

The joint US/French TOPEX/Poseidon (T/P) mission, launched in the summer of 1992, consists of a satellite dedicated to obtain the global measurements of SSH using radar altimetry. Altimeters on the ERS and T/P satellites measure SSH deviations from its long term mean at their nadir. There is a tradeoff between spatial and temporal resolution. Merged SSH dataset that takes advantage of both T/P's high temporal and ERS satellite's high spatial

resolutions, available from 1993 to 2000 on a $0.25^{\circ} \times 0.25^{\circ}$ grid resolution. Monthly means of SSHA in 1° latitudinal interval for the coastal region is used for the present analysis. Data for the coastal region between 7°N to 15°N is considered for the SM months (June - September).

3.2.3 Bottom Topography

Improved bathymetric datasets (ETOPO2v2) for the shallow water regions in the Indian Ocean from ¹⁰⁶Sindhu et al., 2007 is used to understand the bottom topography of the study region. For ETOPO2v2 the improved shelf bathymetry for the Indian Ocean region (20°E to 112°E and 38°S to 32°N) is derived by digitizing the depth contours and sounding depths less than 200 m from the hydrographic charts published by the National Hydrographic Office, India. The digitized data are then gridded and used to modify the existing ETOPO5 and ETOPO2 datasets for depths less than 200 m. In combining the digitized data with the original ETOPO dataset, appropriate blending technique is applied near the 200 m contour to ensure smooth merging of the datasets. For a better understanding of the process of coastal upwelling of the SEAS related with bottom topography, the region between 6°N - 16°N and 70°E - 80°E is selected as shown in Fig.3.1.

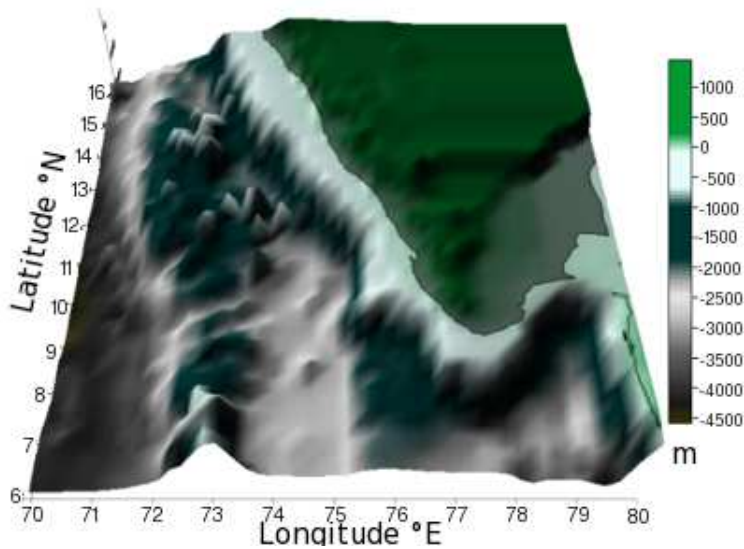


Figure 3.1: Bottom topography for the SEAS from etopo2v2

3.3 Theoretical Formulation

Based upon the results presented in chapter 2 and Fig. 3.2, the SEAS's coastal region can be divided into four different systems. (1) Off Cape, the process is strong and wind-driven (2) along the shadow zone, it is weak and is due to the along shore wind stress (3) Between Kollam and Mangalore, remote forcing dominate over wind stress and (4) Mangalore-Goa, alongshore wind stress dominates and the offshore extend is less due to the weak westward propagating Rossby waves as well as the suppressive action of the ASHSW.

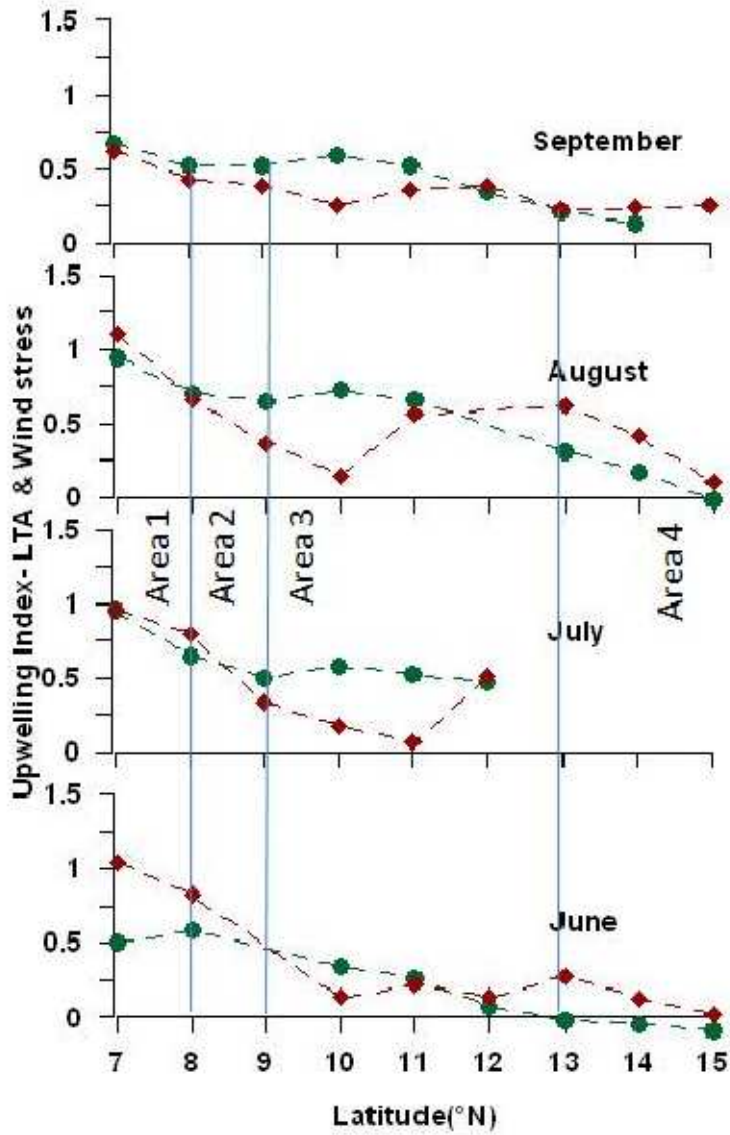


Figure 3.2: Eleven year Average UI derived from Wind stress (Red line) and SST (Green line)

3.3.1 Southern Tip (Cape)

At the southern tip of India (8°N, 77°30'), moderate to strong upwelling is getting initiated from May last week onwards and continue to observe with its peak in July-Aug months till it's cessation in September (¹¹⁰ Smitha, et al., 2007). Ekman transport and Ekman drift (Fig. 3.3a&b) derived using $V = \tau/\rho(A|f|)^{1/2}$ (⁹⁴ Shankar et al., 2002) from QuickScat Scatterometer wind averaged for 7 days at the southern tip showed strong southeastward drift of the surface current. The drift is south-southeastward in all the three months, which was stronger during July (18-40 *cm/sec*), in harmony with the southwest monsoon winds and weak during May and September (10-20 *cm/sec*). Surface drift velocities agree with the in situ observations during May 19th, July 5th and September 26th of the year 2005. This area is identified as highly turbulent with drastic offshore transport as evidenced from the currents which is greater than 40*cm/s*. Thus the upwelled water has got less residence time along the Cape due to drastic offshore transport. Major forcing mechanism in this area is tangential wind stress during SM. The analysis on offshore mass transport, LTA, vertical velocity due to Ekman transport and the isothermal shift between two consecutive samplings along this area showed that the upwelling is purely wind driven (¹⁰⁹ Smitha et al., 2008).

Since there are no major rivers emptying in this region

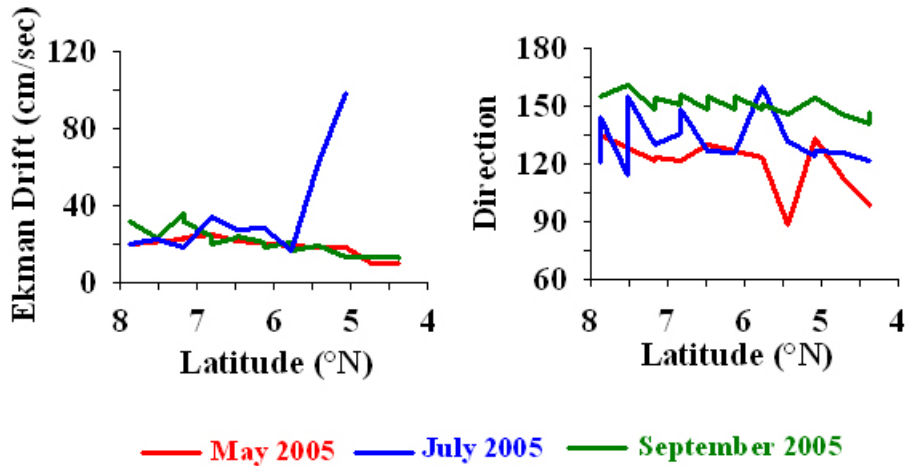


Figure 3.3: Latitudinal variation of Ekman drift (cm/sec) and direction for differnt SM months (red line represents obser- vation during June, blue for July and green for Sep- tember)

with considerable discharge, the chance of influence due to fresh- water runoff can be ruled out. The indexing of the process or estimation of the relation has been done by taking LTA as the re- sponse variable. At the southern tip, UI and LTA is a function of τ_x . To establish the relation between these two variables the x component of wind stress and the LTA for eight years have been subjected to regression analysis, and the relation obtained as fol- lows:

$$UI = LTA = 1.038\tau_x - 0.04$$

Where UI or LTA in $^{\circ}C$ and τ_x is the x-component of wind stress in $dynes/cm^2$ Other possible factor which influences LTA

is precipitation. In addition, mixing of the WICC with the upwelled water also can influence LTA and hydrography of this region. Whereas the ADCP derived near surface current pattern (⁶⁷Padmakumar et al., 2010) and the Ekman current (Fig.3.3b) in the off shore waters south to 8°N does not show any tendency of east ward flow, but is directed southwards. These rules out the possibility of any influence other than the freshwater factor due to precipitation, which is termed as K_{rf} . So the above equation can be modified as

$$UI = LTA = 1.038\tau_x - 0.04 + K_{rf}$$

3.3.2 Cape-Kollam Stretch (Shadow Zone)

Inferences from upwelling indices, vertical velocities, and the surface salinity pattern strongly indicate the absence of remote forcing in the region between 8°N and 9° N. This leads to the conclusion that the Kelvin waves reach the west coast of India, become coastally trapped at about 9°N and propagate poleward as the coastally trapped waves, thereby demarcating a narrow strip of the coast between Cape and Kollam (8° N to 9° N) as the shadow zone. This could be explained in terms of the 2000 m isobaths (Fig. 3.1), which is acting as a cliff like feature in the path of the Kelvin wave, deflecting it to its optimal energy path. The upwelling process along the shadow zone is thus purely driven by the along-

shore component of the wind stress, as indicated by the rate of the vertical Ekman pumping. In this area the LTA is a function of alongshore wind stress and the runoff through the Kallada river.

$$\text{ie., } UI = LTA \propto (\tau_y + K_{rf})$$

Where, the constant equating the relation is a measure of free flow path of the wind component. So the relation is

$$UI = LTA = \begin{cases} 11.75\tau_y - 0.03 + K_{rf} & \text{for } \tau < 0.2 \text{ dynes/cm}^2 \\ 0.0002\tau_y + 0.2164 + K_{rf} & \text{for } \tau > 0.2 \text{ dynes/cm}^2 \end{cases}$$

3.3.3 Kollam- Mangalore Stretch

In this region the upwelling is induced due to the combined influence of wind stress as well as remote forcing from BoB in the form of coastal Kelvin waves and westward propagating Rossby waves. The offshore extend of upwelling is more along the southern part of this region as evidenced by the surface salinity pattern (Chapter 2) and the suppressive forcing due to ASHSW is minimal in this area. Major freshwater sources like, Ashtamudi lake, Kayamkulam lake, vembanad lake system, Azheekkal, Chettuva Barmouth, Ponnani-Beypur estuarine system, Kadalundi river, Azhicode bar mouth, Chandragiri/Payaswini river debouching in to the region modifying the factor K_{rf} . In this context, the UI in the area is a function of τ_y , K_{rf} , and SSHA where SSHA account the role of planetary waves.

$$UI = LTA = \begin{cases} 0.4\tau_y - 0.045SSHA + K_{rf} + 1.5 & \text{when } H \geq H_{KT} \\ 0.0002\tau_y + 0.2164 + K_{rf} & \text{when } H < H_{KT} \end{cases}$$

where H is the depth and H_{KT} is the Kelvin threshold depth

3.3.4 Mangalore-Goa Stretch

Upwelling in this stretch is exerted due to combined influence of along shore windstress and remote forcing. Unlike the Kollam-Mangalore sector, this area is dominated by wind stress over planetary waves (Fig. 3.2). The Rossby waves get weaker in this region as reported by ⁹³Shanker and Shetye 1997 and ¹⁰³Shetye, 2005. The shoreward pushing of the ASHSW carried by the WICC, confines the influence of upwelling in a narrow coastal belt (chapter 2). Also major river runoffs from Nethravathi, Tadri, Karwar-Kalinadi, Zuari and Mandovi estuarine mouths are expected to influence and modify the index. In this context, the relation obtained through regression analysis with the eight years of data for the area is

$$UI = LTA = \begin{cases} 1.77\tau_y + 0.04SSHA + 1.2 + K_{rf} & \text{when } H \geq H_{KT} \\ 1.77\tau_y + 1.2 + K_{rf} & \text{when } H < H_{KT} \end{cases}$$

where K_{rf} accounts the variability in LTA due to freshwater discharge.

3.4 Validity and limitations of the Theory

Separate relation has been derived to explain the intensity of upwelling in each of the four sub regions classified according to the variability in forcing mechanism and intensity of upwelling. The validity of the relation has been checked with satellite observations for the period 2002-2009. Monthly composite of SST from MODIS AQUA (night measurements), wind fields from QuikSCAT Scatterometer and SSHA for the SM months (June-September) from the Jason altimetry were used to check the reliability of the theory in each sub region. Estimated indices were subjected to regression analysis against the satellite observations and found to be fit with an R^2 of 0.64.

A major limitation to point out in the present analysis is the use of SSHA data to account the role of planetary waves. Perhaps, best representation may be achieved from the equatorial winds and alongshore wind stress of WBoB which actually defines the inter annual variability in the amplitude and phase velocity of the planetary wave (¹⁹Chelton et al., 1998, ²⁶Gopalakrishna et al., 2008). These wind fields and the tangential wind forcing at the southern tip of Sri Lanka, together determines the remote forcing of SEAS, and an index based on these can perhaps forecast the upwelling system. Secondly, the parameters to explain the role of

bottom topography and coastal orientation are not taken into account. Another drawback is the non-availability of freshwater data for each river mouths in the study region. Hardly any studies have been conducted explaining the relation between extend of offshore propagation and the inductive forcing of upwelling. Whereas, it is of great concern in explaining the survival and migration pattern of the fish egg/larvae and the OEW concept explaining the adult recruitment - upwelling relation of the pelagic fishery.

Chapter4

Differential Response of the Upwelling on Biological Production

“Extra-ordinary claims require extra-ordinary evidences.”

– Carl Sagan.

4.1 Introduction

UPWELLING induced changes in the biogeochemistry of the South Eastern Arabian Sea (SEAS) has a major role in the explosive increase in the fishery potential of the area during SM. Great attention has been received by the region on this unique behavior, and general mechanisms to explain the oceanic processes associated with varying seasons are explained in several studies. In situ evidences for the coastal upwelling process in the near-shore region (8°N to 13°N) in a finer resolution ($\frac{1}{2}^{\circ}$ interval) is explained in the chapter. Earlier studies in the region explain the process as wind driven divergence caused by Ekman transport (the

classical explanation of coastal upwelling by ¹¹⁶Sverdrup et al., 1942). ³⁴Johannessen et al., 1981 had further explained its association with more large scale monsoonal conditions which drives the anticyclonic Arabian Sea monsoon gyre. Subsequent studies by Shetye et al., 1985; ⁵⁷Muraleedharan and Prasannakumar 1996; and ⁶¹Naidu et al., 1999 explain the process is offshore divergence of the alongshore windstress component. Studies by ⁵²McCreary 1993; ¹⁸Bruce et al., 1994 and ⁹³Shanker and Shetye, 1997; explained the process as due to the combined influence of remote forcing and local wind forcing. According to the study by ³⁰Haugen et al., 2002, using a high resolution model, Miami Isopycnic Coordinate Ocean Model (MICOM) the upwelling intensifies with the southwest monsoon and is strongest off Kochi (10°N) and Kollam (09°N). Recent study by Smitha et al., 2008 explained upwelling off the southern tip (Cape) and south west coast of India as highly localized features with different forcing mechanisms, and cannot be treated as a uniform wind driven system. In addition, the area between 8°N and 9°N lat represents shadow zone where the role of remote forcing is nominal and upwelling occurs exclusively by Ekman transport due to long-shore wind stress.

Coastal upwelling and the ensuing productivity sustains fishery for a number of commercially important fishes. Offshore transportation of nutrient rich productive waters is not as pro-

nounced along the region, as off Somali coast, where the upwelling is intense. Scene of high productivity especially primary along the southwest coast of India is confined to a narrow strip (70 km) hugging the coast. Whereas zooplankton biomass is highest in near shore waters and fairly dense population is observed up to a few hundred kilometers offshore. In the tertiary level, fishes especially sardines and Mackerels take advantages of this situation that their occurrence and spawning coincides with the productive conditions during southwest monsoon period (⁴⁷ Madhuprathap et al., 1994). The southwest coast of India is rich in primary (660 mgC/m²/day) and secondary (10-57 mgC/m²/day) production, and contributes nearly 50% of the total Indian Marine fish landings (¹²⁵ Vivekanadan et al., 2003; ¹⁰⁸ Smith and Madhuprathap, 2005).

The present chapter explains the following themes along the SEAS:

1. Oceanic response to the SM winds causing coastal upwelling. Spatial variation in the process and the chemical and biological responses are considered. Also the role of remote forcing is explained on the basis of SSHA data.
2. Upwelling front or offshore extend of upwelling is delineated, in terms of temperature, Chlorophyll *a* (Satellite derived), SSHA and the RRD.

3. The influence of day-to-day variations of wind in the physical, chemical and biological parameters and the time lag between physical forcing to biological production.
4. The differential response of the process of upwelling along two adjacent transects.

4.2 Data and Methods

4.2.1 In Situ Observations

In situ data collected onboard FORV Sagar Sampada during Cruise 227 (SS227) during 17th to 31st July 2004 and Cruise 246 (SS246) during 25th June to 6th July 2006 are used for the present study. The area covered by SS227 stretched between 8°30' to 13°00'N latitude (Fig. 4.1a) along the continental shelf in eleven transects comprising 6 stations at 20, 50, 75, 100, 150 and 200 m depths in half-degree latitude intervals. Whereas, during SS246, emphasis has been given for the temporal variation in the process, taking repeated observations, limiting the observations to two transects (Fig. 4.1b) off Kollam (9°N) and off Tvpm (8.5°N). By considering the difference in the forcing mechanisms and intensity of upwelling in this area the particular transects has been selected as per the study conducted by ¹⁰⁹Smitha et al., (2008). In that study, it has been identified that, upwelling along 9°-13° N is due

to the combined influence of wind and remote forcing whereas it is purely wind driven between 8°N and 9°N. Zonal transects were designed for sampling off Tvpm fixing 50 *m* station for time series observations of the physico-chemical and biological parameters. Six stations were sampled at 20, 50, 75, 100, 150 and 200 *m* depths including the Time Series Station (TSS) at 50 *m* (alternate days) to monitor the day to day variation of upwelling. Whole experiments were repeated along transect off Kollam, so as to affirm the results as well as to study the spatial variations recorded by ¹⁰⁹Smitha et al., 2008. Sampling were scheduled in such a way that primary productivity measurements are carried out in the early morning (06 00 *Hrs*) at TSS.

Continuous monitoring of the surface meteorological parameters like Air temperature, Atmospheric pressure, Wind speed and direction were made in 10 *minutes* interval during SS227 using IDAS and in one *minute* interval during SS246 using onboard AWS during the entire period of observation. CTD (SBE Model 911 series, Sea-Bird Inc.) was operated in all the stations to collect temperature, salinity, Dissolved Oxygen and density (sigma-t) data in 1 *m* bin depth intervals. At standard depths, the CTD salinity values were calibrated and corrected with the values derived from onboard Autosal (Guidline 8400).

Samples for dissolved oxygen were immediately fixed with

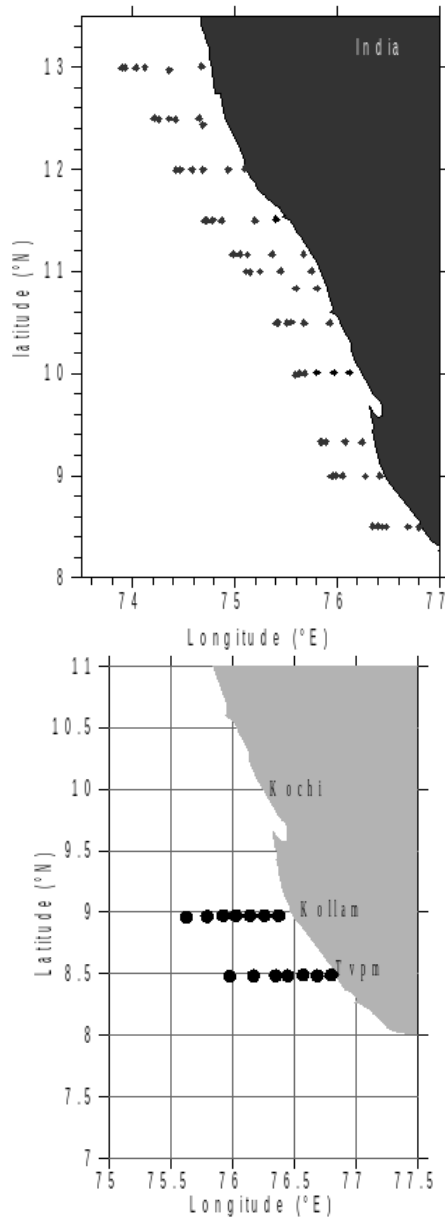


Figure 4.1: Station location during SS227 and SS246

Winkler A and Winkler B reagents (²⁷Grasshoff et al., 1983) and subsequently analyzed onboard by titration method (Dosimat model 665) after calibration. Nutrients (Nitrate and Phosphate) were analyzed by using the onboard segmented flow Analyser (SKALAR SAN plus Model) after calibration using appropriate standards and following standard procedures (²⁷Grasshoff et al., 1983).

For Chlorophyll estimation, one-Liter water sample was filtered through GF/F (0.7 μ m) filter papers, whilst the pigment was extracted in 90% acetone, and then analysed spectrophotometrically ¹¹²(Strickland and Parsons, 1972). PP measurements were carried out at selected stations during SS227 and at 50m depth station off Tvpm and Kollam during SS246. For the PP studies, ¹⁴C technique referred by ¹²²UNESCO, (1994) was followed.

Frontal scale due to the presence of shelf, determines the Rossby Radius of Deformation (RRD). According to ¹Antony et al., 2002 RRD can be worked out in *km* by:

$$\frac{(\sqrt{g'D'})}{f} \text{ Where } g' = g \frac{(r_2 - r_1)}{r}$$

r_2, r_1 are densities of the upper and lower layer

r is the mean density f is the Coriolis parameter ;

g is 9.8m/s², acceleration due to gravity

and

D' is the depth of the upper layer of the ocean.

Stability of the water column was computed for the TSS off Kollam and Tvpm in terms of Brunt Vaisala frequency (N^2) which is a measure of vertical homogeneity of the water column. The frequency with which a parcel or particle of fluid displaced a small vertical distance from its equilibrium position in a stable environment will oscillate, a measure (in inverse time units) of the stratification or resistance to turbulence. It will oscillate in simple harmonic motion with an angular frequency defined by:

$$N^2 = gE = \frac{-1}{\rho} \left[\frac{\delta\rho(s,t,p)}{\delta z} \right] - \frac{g}{C^2} \text{ (radians/sec)}^2$$

Where,

g is the gravitational acceleration,

t is the potential temperature (⁷² Pond and Pickard, 1993).

In practice, the equivalent formula:

$$N^2 = \left(\frac{-g}{\rho}\right)\left(\frac{\delta\sigma_t}{\delta z}\right)$$

is often used, following ¹²¹Turner, 1973 and ⁶⁰Narasimha Rao, 2002. High values of N are usually found in the main pycnocline zone, that is where the vertical density gradient is maximum. When N^2 is positive, the medium is stable and when negative, the medium is unstable.

4.2.2 Satellite Observations

Weekly averaged QuikSCAT Scatterometer wind field (QuikSCAT Level 2B Ocean Wind Vectors in 25 km Swath), produced by

the NASA Physical Oceanography Distributed Active Archive Center, at Jet Propulsion Laboratory, California Institute of California (JPL / PO.DAAC) is used to understand the role of windstress on the process of upwelling. The TOPEX/Poseidon and Jason SSHA product is generated from the Merged Geophysical Data Record. The SSHA represents the difference between the estimate of the sea surface height and a mean sea surface (the geoid). The sea surface height used was corrected for atmospheric effects (ionosphere, wet and dry troposphere), effects due to surface conditions (electromagnetic bias), and other contributions (ocean tides, and inverse barometer). Monthly composite maps of the Chlorophyll *a*, Ocean Colour Level 3-binned product for July 2004 derived from MODIS AQUA at 9 *km* spatial resolution from Goddard Space Flight Centre (GSFC) National Aeronautics and Space Administration (NASA) are used to depict the Chlorophyll *a* patterns in the area.

4.3 Results and Discussion

4.3.1 Spatial Variation

4.3.1.1 Physical Forcing and Hydrography During SM 2004

The synthesised data were subjected to critical evaluation of various environmental and oceanographic changes during the

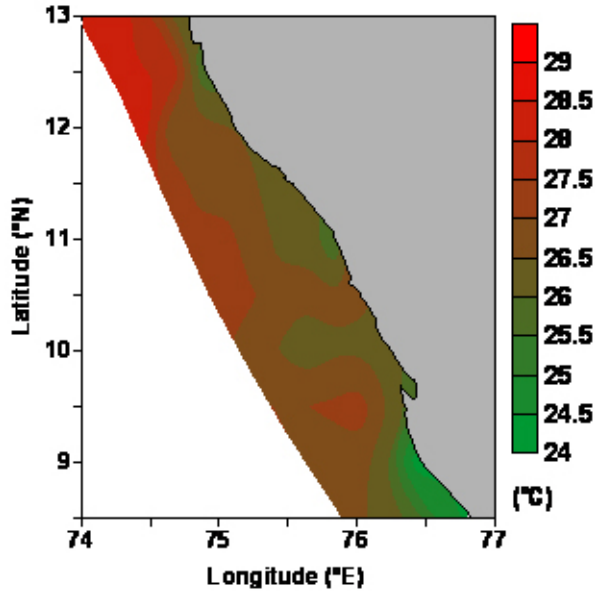


Figure 4.2: SST distribution

14 day cruise SS227. Air temperature recorded values between 23.62°C and 28.85°C with wide variations in atmospheric pressure, between 1005 to 1011 *mb* during the observation. Upwelling favorable northerly winds with magnitude 2-18 *m/sec* were predominant over the region during the entire cruise. Wind pattern was uneven, with strong winds (>12 *m/sec*) off Kochi and Ponnani transects, whereas at north (13°N) and south (8.5°N) transects it was less than 7.5 *m/sec*.

Response of the Ekman mass transport was evidenced in the SST pattern (Fig. 4.2). Irrespective of the wind pattern, intense upwelling in terms of presence of cold waters (24°C) in the surface

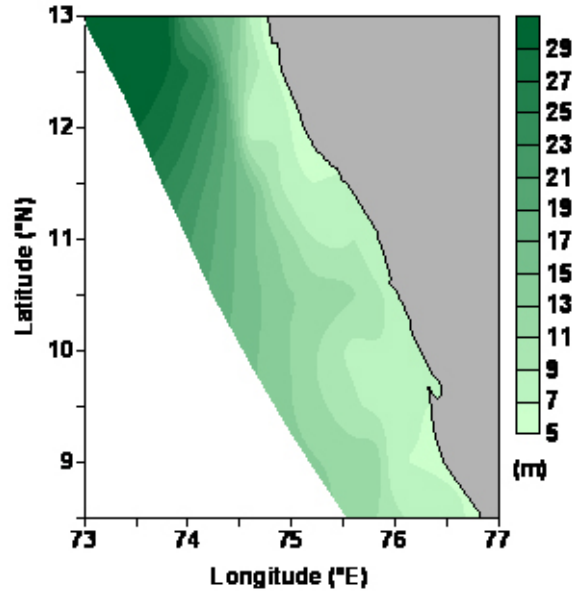


Figure 4.3: Variation in the Mixed Layer Depth

were observed in the southern latitudes ($8.5^{\circ}N$ to $9.5^{\circ}N$), whereas offshore extension of low SST waters were more off Kochi and its southern part as indicated in the distribution pattern of the $26^{\circ}C$ isotherm. Mixed layer depth (Fig. 4.3) calculated using the density criteria (⁴¹ Levitus, 1982) was very thin (5-9m) along the coastal belt with strong horizontal gradient to offshore ($0.22m/km$) in the northern transect.

Surface salinity (Fig. 4.4) distribution indicates the heavy discharge of fresh water along the coast especially from Ponnani and Beypore estuaries at $11.5^{\circ}N$ latitude. Low saline plume of 31.4 was found to propagate offshore and then to southward to mix

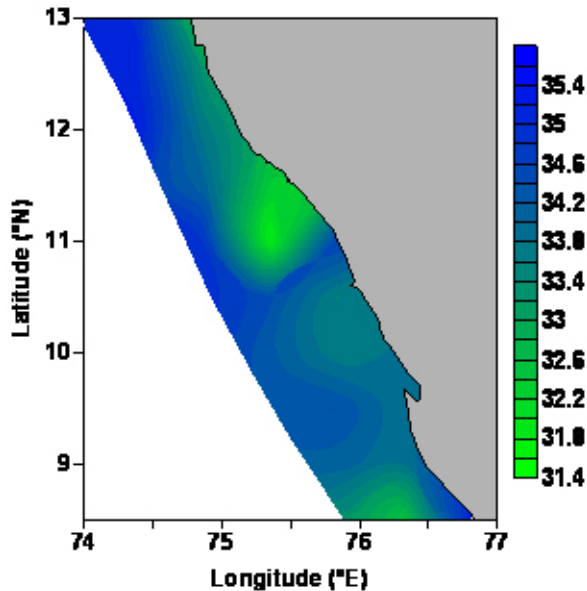


Figure 4.4: Distribution of Surface Salinity

up with high saline Arabian Sea water from northern Arabian sea (35.5). These low saline water occupies the region dominantly and was observed very near to the coast with in 30 km at 13°N. Southward extension of the high saline water along the continental shelf was observed up to 9°N. Limited offshore extension of upwelled waters is observed in the northern stations, where the influence of Arabian Sea High Saline water (salinity > 35.5) is present; suggesting the suppressive action of the latter on upwelling.

4.3.1.2 Dissolved Inorganic Nutrients

The upwelled water, deficit in oxygen (0.8 to 2.5 μM) but

replete in nutrients (up to $12\mu M$) was found to spread over the entire shelf and prevailed just below the thin surface layer (10 m). Major external inputs of nutrients like NO_3 and PO_4 to the coastal oceanic zone are by coastal upwelling and through fresh water discharge. During the particular collection (SS 227), the peak values in NO_3 ($12\mu M$), (Fig. 4.5) may be from the riverine inputs, as identified from the salinity and density pattern. Distribution of NO_3 suggests the minimum offshore extension in northern latitudes. Surface PO_4 distribution (Fig. 4.6) also exhibited more or less similar trend, with a maxima ($2.5\mu M$) along the coastal stretch $9.5^\circ N$ to $12.5^\circ N$ latitudes. Both NO_3 and PO_4 were observed to be gradually decreasing to offshore with varying extent. Low values of surface dissolved oxygen (0.8 to 2.5 ml/l) were observed along the coastal belt (Fig. 4.7) and the gradual increases towards the offshore up to 5.8 ml/l illustrate the presence of upwelled subsurface waters along the entire coast. Minimum value of 0.78 ml/l was observed off Kochi, where maximum intensity and offshore extension of upwelling was marked.

4.3.1.3 Biological Responses

The study region is characterized by regular seasonal oscillations in biological responses, so is an ideal area for exploring the possibilities to integrate the related ocean dynamics. During

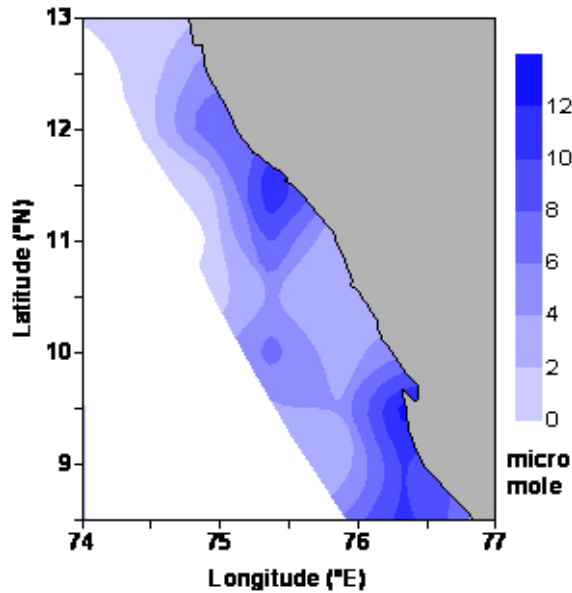


Figure 4.5: Distribution of Nitrate (NO_3 in μM) at 10 m.

the season, coastal upwelling in the area results in high biological productivity making it one of the most productive areas in the world (²⁴Gardner et.al., 1999, ⁷⁴Prasannakumar et al., 2001 and ¹²⁷Wiggert et al., 2005). The enhanced Chlorophyll *a* production (Fig. 4.8) was observed in pockets between 8.5°-10.5°N latitude and 11.5°-12.5°N latitude with surface values $11.21mg/m^3$ and $5mg/m^3$ respectively. Both of these high productive pockets dovetail with the heavy runoff from Vembanad and Beypore estuaries which is evident in the nutrient pattern with high concentration of nitrate and phosphate in the region. The rate of primary productivity distribution pattern (Fig. 4.9) was more or less same that

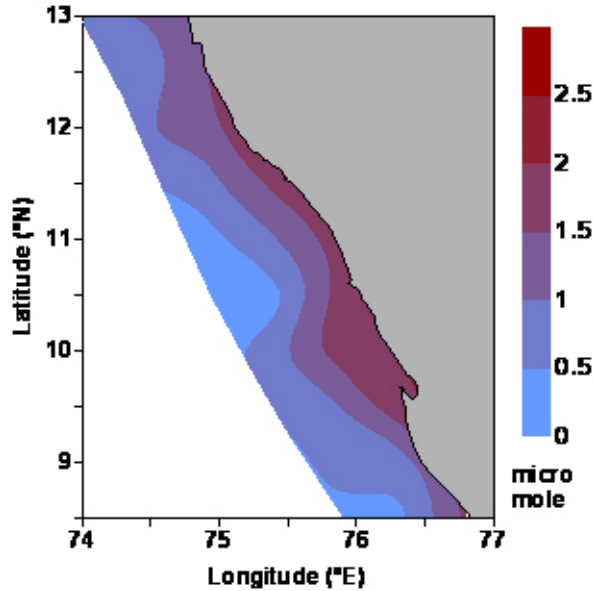


Figure 4.6: phosphate (PO_4 in μM) at 10 m

of Chlorophyll *a* with a southward shift to 8.5°-9.5° N in the location of the high productive pocket of 210-290 $mgC/m^3/day$. As Chlorophyll *a* is the measure of the standing stock of phytoplankton community and PP is the rate of carbon uptake per day, it is expected to show a linear relation. The lack association between locations of highest Chlorophyll *a* and PP during the present observation might be due to the influence by any of the local climatic parameters like solar radiation, cloud cover, rainfall and temperature etc. or the difference in phytoplankton species composition.

The influence of the physical forcing on the chemical and biological parameters are analysed to explain meridional variations

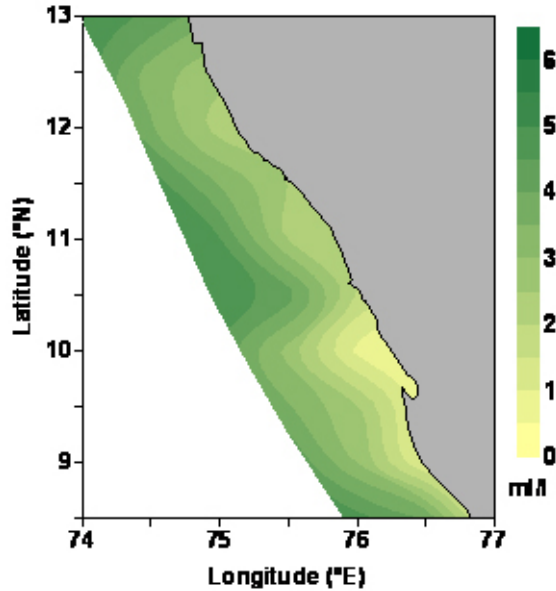


Figure 4.7: *DO(ml/l) at 10 m*

in 20m and 200 m isobaths (Fig. 4.10). Low SST of 24.2°C along the 20m contour indicates maximum upwelling in the south and the intensity decreased to north where the SST was maximum (27.8°C). Similar trend was observed offshore along the 200 m contour line, with a higher value of 26°C at south and 28.2°C at the northern latitudes. Cooler waters rich in nitrate content ($>2\mu M$) prevailed over the entire coast with pockets of high values of 11.8 μM , 8 μM and 10 μM along 9°N, 11.5°N and 12.5°N respectively. This high values extend to the offshore only in the southern transects up to 10.5°N indicating the limited offshore transport due to upwelling at north.

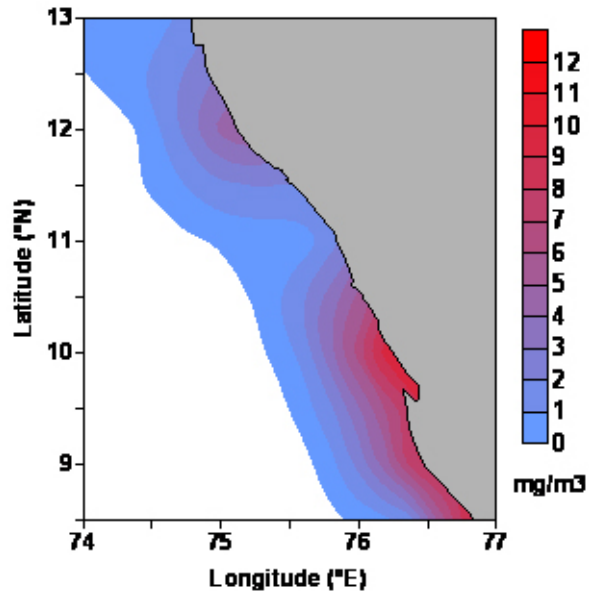


Figure 4.8: Distribution of Surface Chlorophyll (mg/m^3)

Regarding phosphate distribution, the value is always greater than $1.5\mu\text{M}$ along the near shore transects, and comparatively less value ($0.4\mu\text{M}$ to a maximum of $1.2\mu\text{M}$ off 10°N) along the offshore transect. As Nutrients and surface DO are expected to be negatively correlated in the upwelling regions, the present observation along both coastal and offshore waters corroborates this relation well. Also the latitudinal variation of nutrients and DO was well matching with SST at the southern latitudes indicating the case of intense upwelling. Along the off shore stations, the value of DO was approximately 4ml/l except off Kochi (10°N) indicating the presence of upwelled subsurface waters in the shelf

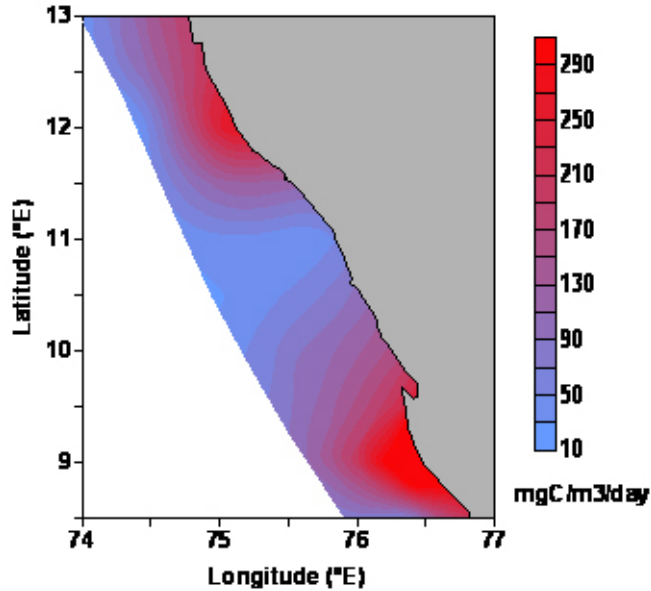


Figure 4.9: Surface PP $mgC/m^3/day$

edge.

In general the entire study region was dominant in cold and less oxygenated nutrient waters with high Chlorophyll *a*. High Chlorophyll *a* value of $11.8mg/m^3$ was observed at $10.5^{\circ}N$ at $20m$ depth station, and a low value of $1.6mg/m^3$ was recorded at $200m$ depth station. Rate of primary production at the surface was high as $500mgC/m^3/day$ along the $20m$ depth stations.

The central portion of the study area is less in productivity up to $11.5^{\circ}N$, sandwiching high primary production area of the northern and southern part with values $300mgC/m^3/day$ and $500mgC/m^3/day$ respectively. Along offshore maximum value recorded

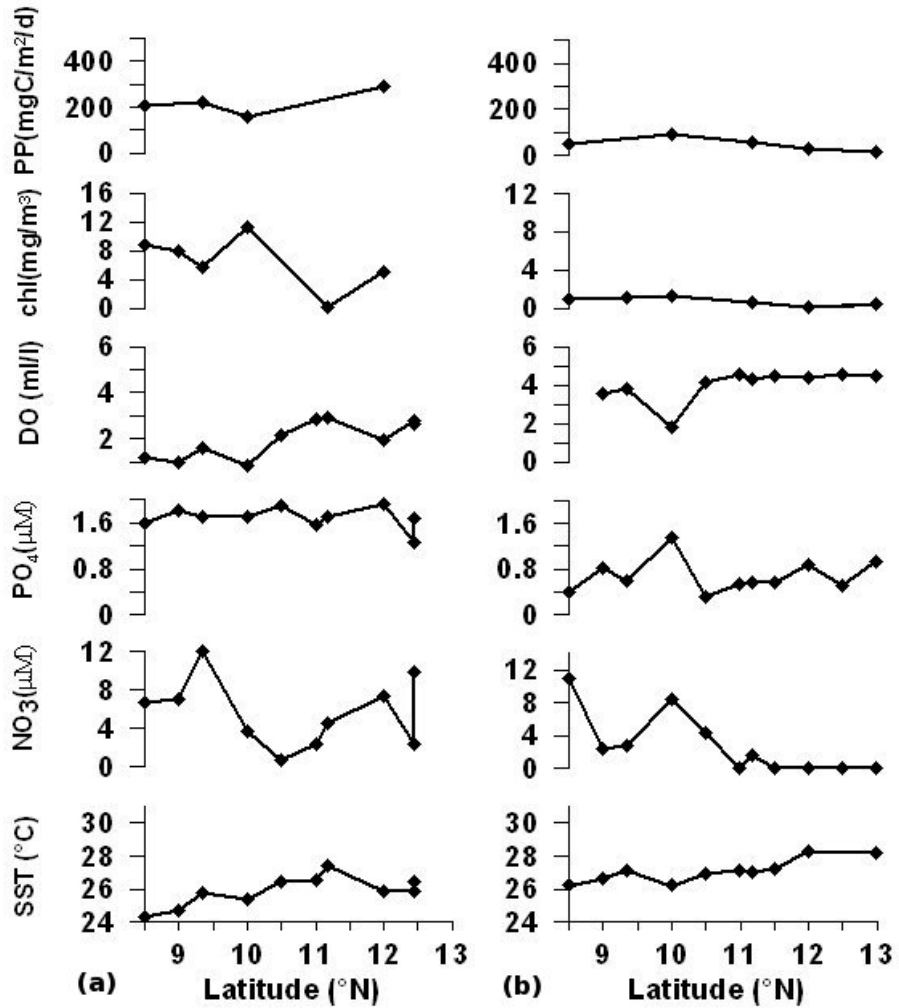


Figure 4.10: Latitudinal variations of different parameters 20 *m* (a) and 200 *m* (b) isobath.

was $130 \text{ mgC}/\text{m}^3/\text{day}$ off 9°N latitude which gradually decreased ($20 \text{ mgC}/\text{m}^3/\text{day}$) towards north.

4.3.1.4 Sea Surface Height Anomaly During the Season

Wind jet in the equatorial Indian Ocean between 5°S and 5°N , excites equatorial Kelvin waves, which on reflection from the eastern boundary of the Bay of Bengal radiates westward propagating Rossby waves and propagate along the perimeter of the BoB as coastal Kelvin waves (¹⁰³Shetye, 2005). A comprehensive numerical investigation using a two-and-half layer thermodynamic model provided considerable insights in the locally and remote forced dynamics of the region (⁵²McCreary et al., 1993). Studies by ⁵²McCreary et al., 1993 ; ⁹³Shankar & Shetye 1997 and ⁴⁵Luis & Kawamura, 2004, pointed out that the BoB set up coastal Kelvin waves, and on reaching southeast coast of India, bends around Sri Lanka and propagate pole ward along the west coast of India forcing changes in WICC.

Later on, ¹⁰⁹Smitha et al., 2008 explained the presence of a shadow zone of weak wind driven upwelling along the west coast of India between 8°N to 9°N . To ascertain this, the path of propagation of the particular wave is explained with the ten day average SSHA during May to September 2004 in the selected near coastal grids (Fig. 4.11b) along the east and west India coast (Fig. 4.11a).

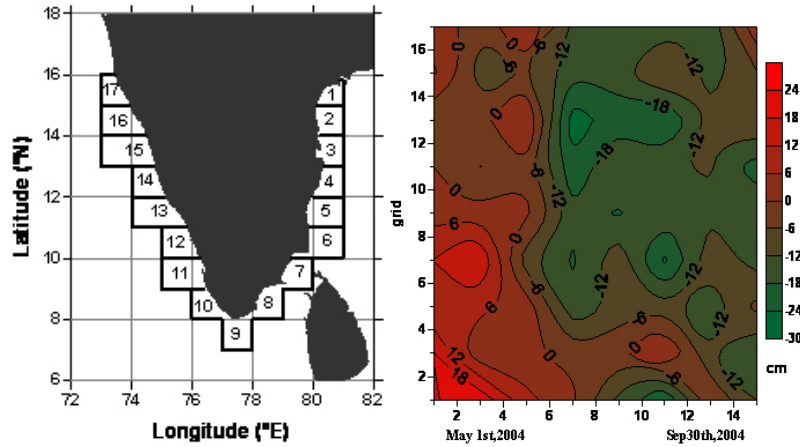


Figure 4.11: Ten day average SSH (*cm*) during May to September 2004 along the selected grids shown in the left

Though negative SSH anomaly indicating low in sea level was observed along the entire coastal area during the season, it was low down to -18 cm along the 9°N-14.5°N, the Kollam-Karwar sector, and further to -24 cm along 10°N to 13°N, the Kochi-Mangalore sector, supporting the result that the wave gets coastally trapped at around 9°N latitude.

Present analysis for the period of May-September 2004 shows lowering of sea level from the first week of May along the Kollam-Mangalore zone but active upwelling is observed to commence during the end of June, with peak off Kochi-Mangalore area during July. This process is observed to be sustaining till August end along the entire southwest coast up to Goa.

4.3.1.5 Upwelling Front

Upwelling front is the region of maximum thermal gradient associated with the offshore movement of the Ekman layer and its location in the shelf follows the strengthening and weakening of the upwelling circulation. The offshore limit of the coastal ocean variability due to upwelling during July 2004 is analysed in this section using SS227 data.

The offshore extension of 26°C isotherm is considered to study the extent of the coastal variability in temperature. Analysis suggests that maximum extension occurs off Kochi at 154 *km* and off Thiruvananthapuram at 150 *km* and decreases to north where it reached to the minimum of about 11 *km* off Kasaragod and 22 *km* off Mangalore (Table 4.1). Along other part of the study region, the recorded values for the offshore extension are 110 *km* off Purrakkad and Kollam; 77 *km* at Valapad, Thikkodi and Kannur and 66 *km* off Ponnani.

Though the upwelling in the study area is partly exerted by local alongshore wind, the intensity of upwelling does not match with the wind pattern during the study period. Surface values of salinity, density, DO , NO_3 and PO_4 were also taken into account for the frontal identification. It shows that SST is the most significant factor as the others are influenced by the fresh water discharge. The in-situ Chlorophyll *a*, also exhibit the same pat-

Transect	Latitude	Distance (km)
Tvpm	8.5	150
Kollam	9	110
Purakkad	9.5	110
Kochi	10	154
Valappad	10.5	77
Ponnani	11	66
Thikkodi	11.5	77
Kannur	12	77
Kasaragod	12.5	11
Mangalore	13	22

Table 4.1: Offshore spreading of $26^{\circ}C$ isotherm along different transects

tern of distribution as NO_3 and PO_4 with limited offshore extend comparing to that of the $26^{\circ}C$ isotherm. Concurrently, we analysed monthly composite of surface Chlorophyll *a* for July 2004 from MODIS AQUA (Fig. 4.12) for this region. Though the values are comparable with in situ data, the monthly composite from ocean color satellite evidenced more extended offshore propagation, especially off Kochi (200 km). However, only one patch of high concentration was observed in the satellite data in place of the two observed in the in-situ records (Kochi and Kannur). Comparison of the in situ and satellite information implies the northward progress of upwelling along with stronger off shore propagation in accordance with the season.

RRD values calculated for the ten transects are given in

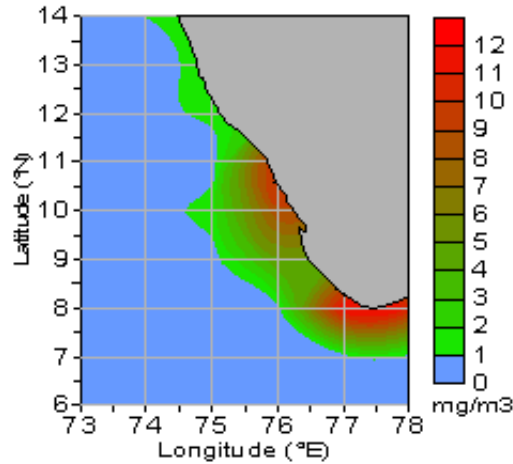


Figure 4.12: Monthly composite of surface Chlorophyll from MODIS Aqua for July 2004

table 4.2. As per the theory, the offshore decay scale of upwelling response is given by the RRD. The results suggest that Rossby radius is more at north and is 348 km at 12°N , 338 km at 13°N and 277 km at 12.5°N . The least recorded value of RRD is 117 km at 10.5°N .

The RRD derived and the upwelling fronts estimated from SST and Chlorophyll *a* showed a contrasting trend towards north. To affirm with, one more parameter the SSHA for the period is also taken into consideration. It is established that cooling of the coastal waters is associated with upwelling of the isotherms and therefore must introduce change in the surface elevation. The presence of coastally trapped Kelvin waves in the upwelling mode

Transect	latitude	$D'(m)$	$f \times 10^{-5}$	g'	$\sqrt{g'D'}$	R in km
Tvpm	8.5	38	2.155652	0.49315	4.3289	201
Kollam	9	20	2.28144	0.78199	3.9547	173
Purakkad	9.33	38	2.364366	0.914259	5.8942	249
Kochi	10	18	2.532485	1.294905	4.8279	191
Valappad	10.5	15	2.657723	0.644891	3.1102	117
Ponnani	11	35	2.782758	1.058959	6.0879	219
Thikkodi	11.5	38	2.907582	1.081593	6.4109	220
Kannur	12	100	3.032184	1.111955	10.5449	348
Kasaragod	12.5	68	3.156555	1.125757	8.7494	277
Mangalore	13	100	3.280686	1.228749	11.0849	338

Table 4.2: Calculated Rossby Radius of deformation (RRD).

also cause low in sea level along its path. So sea level can be treated as an index for upwelling. Ten day cycles of SSHA (merged satellite product) for 20th – 30th July for the purpose of tracking the coastal upwelling and thereby fronts due to sea level variation is presented in Fig. 4.13.

The figure shows that during the observation period the sea level remained low along the coastal belt which agrees with the recent studies conducted in this area (¹⁰⁹Smitha et al., 2008 and ²⁸Habeeb R et al., 2008). Accordingly, offshore propagation of Rossby waves and the offshore extension of upwelling are maximum in the southern part comparing to north. Again, shoreward pushing of the zero level surface observed between 11.5°N and 12.5°N latitudes coincide with high saline water observed in the

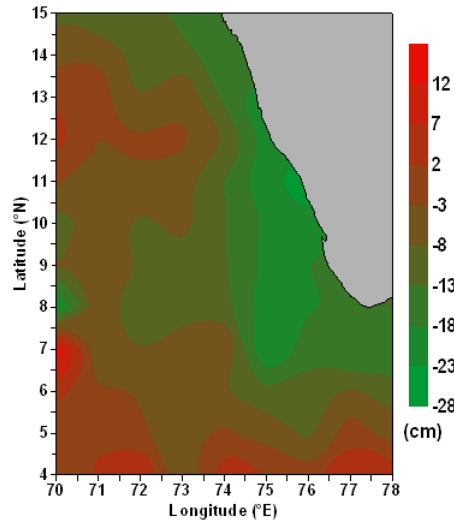


Figure 4.13: 10 day composite of SSH for the period 20th – 30th July 2004

SSS distribution. The limited offshore extension in the northern part can be suggested as the shoreward pulling of warm saline ASHSW. Presence of ASHSW causes density gradient, which is strong enough to prohibit the offshore movement of the upwelled water. And this density difference defines the maximum baroclinic RRD in the region.

Vertical distribution of temperature in each transects depicts maximum upsloping in the northern transects at Kannur, Kasaragod and Mangalore (D' in Table 4.2). This again leads to confusion regarding the intensity of upwelling along the region. However, the depth at which upsloping starts may not be directly related to the strength of upwelling. In order to explain this anal-

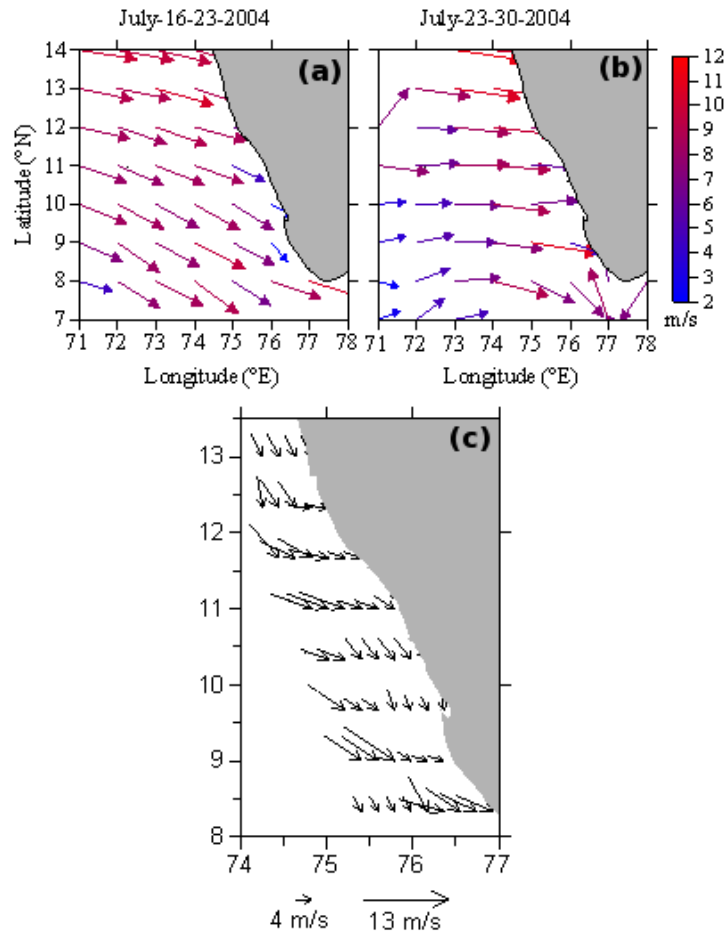


Figure 4.14: Weekly scatterometer data from QuikSCAT July 16th -23rd (a) and July 23rd to 30th (b). In situ data on wind along the cruise track of SS272 (c).

ysis was done on weekly wind from Scatterometer of QuikSCAT to understand the role of local wind in inducing intense upwelling at north. Scatterometer showed westerly to northwesterly winds throughout the region with magnitude between $2m/s$ and $12m/s$. Fig. 4.14a and Fig. 4.14b shows during July 16th to 23rd and July 23rd to 30th indicate strong winds at north ($12^{\circ}N$ to $14^{\circ}N$) compared to south. And the in situ wind pattern (Fig. 4.14c) derived out of the IDAS onboard, indicate a persistent NNW near coastal winds along the cruise track. This explains why the maximum up-sloping of isotherms is observed towards north and suggests the existence of lag phase between atmospheric, physical, chemical and biological responses. From these observations it can be concluded that RRD is not a measure of the actual length scale of the fronts as shown by ¹Antony et al., 2002, whereas it is influenced by the vertical density gradient of the water column. And this affirms the adverse impact of the coastal current on the offshore transport of upwelled waters.

4.3.2 Temporal Variation

Temporal variation in the process of upwelling was investigated using the day time series observations along Kollam and Tvpm during the SS246 cruise. Summer monsoon is characterized by variable winds with moderate to strong magnitude. Being the cool phase of the seasons, air temperature varied between

25.1°C and 25.3°C during the twelve day time series observations off Tvpm. Concomitant variation was observed with atmospheric pressure which shifted between 1006.5 *mb* and 1009 *mb*. The region was subjected to northerly and northwesterly winds, with magnitude ranging from 3 to 12 *m/sec*. Spatial average of the wind stress along the transect varied from 0.3 to 1 *dynes/cm²* (Fig. 4.15) during the cruise. Average SSTs recorded are 23.7 °C and 28 °C in the coastal and offshore waters respectively. MLD was shallow at 13*m* near the coast and at 32*m* in the off shore stations indicating active upwelling. Whereas, at the Time Series Station (TSS) off Tvpm at 50 *m* depth, day to day variations was observed between 24.02°C and 25.15°C in SST and 13 *m* and 27 *m* in MLD. Time series observations on vertical thermal structure indicated short period undulations in the isothermal shift in accordance with the change in the wind pattern. (Fig. 4.16) Coastal upwelling turns the surface waters to become cold, nutrient rich, less oxygenated condition. The SST showed two comparatively strong upwelling phases (days 3 and 9) and 3 relaxed phases (days 1, 5 & 11), with associated indication in the distribution of nutrients and DO.

Significant correlation obtained between wind and SST in this region with *R* value 0.82 affirms that the process is wind induced. The daily rainfall did data not show any relation to upwelling off Tvpm. SSS also not showed any variation during the

observation period leaving most of the values in a narrow range of 34.82 to 35.02. SST, SSS and the *sigma-t* values rules out any indication of land drainage of waters in transect.

Daily variations in chemical parameters like NO_3 , PO_4 and DO were looked into and the observations indicated clear evidence of environmental and physical forcing on nutrient distribution. Surface NO_3 recorded abnormally high at the TSS with a range of $6.5\mu M$ to $13.8\mu M$, where the maximum was associated with the first peak of upwelling on the 3rd day of observation. Consistent variation was observed in PO_4 distribution where the values varied between $1\mu M$ and $1.6\mu M$. NO_3 and PO_4 peaks corresponded to the peak upwelling, as indicated by low SST's which suggest that high nutrient availability is due to upwelling and not due to terrigenous discharges. DO values substantiate the observation on upwelling, except on the 7th day. DO was 2 ml/l during the first phase of peak upwelling and it increased to 3.1 ml/l in the relaxed state on the 7th day of observation. Again during the second upwelling phase (9th day) it decreased to 1.6 ml/l. Chlorophyll a and PP values ranged between $1.34\text{ mg}/\text{m}^3$ - $6.68\text{ mg}/\text{m}^3$ and $9.25\text{ mgC}/\text{m}^3/\text{d}$ - $287.7\text{ mgC}/\text{m}^3/\text{d}$, with an enhanced production in the 7th day of observation. It is suggested that this may be due to the peak upwelling in the 3rd day. It shows the existence of a lag phase of 4 days between nutrient enrichment and the respond-

ing biological production. Hence the increase in *DO* on the 7th day (3.1 *ml/l*) is preferably due to an active photosynthesis. Since the peak production occurs during the relaxation phase following the peak upwelling, the possibility of offshore advection of the nutrient rich upwelled water is assumed to be inconsiderable. During the second phase of upwelling (9th day) the nutrients (NO_3 -8 μM ; PO_4 -1.3 μM) and *DO* (1.6 *ml/l*) substantiate the process of active upwelling.

4.3.2.1 Upwelling off Kollam and Tvpm - A comparison

Even though the transects off Kollam and Tvpm are closer (55 *km* apart) they exhibit considerable variation in atmospheric and oceanic characteristics, preferably due to the peculiarity in bottom topography and coastal orientation. Kollam has a shelf width of 120 *km* whereas it is 87*km* off Tvpm. The inclination of the coast line is 40° to true north at Kollam and 30° at Tvpm. Moreover, Kallada river mouth with an annual discharge of 1595 Mm^3 is situated just 7 *km* south of transect, and the presence of which may be sufficient enough to trigger local influences in the upper ocean properties.

Atmospheric pressure and temperature showed considerable variation during the daily observations (Fig. 4.17). Pressure varied between 1006 *mb* and 1011*mb* and air temperature between

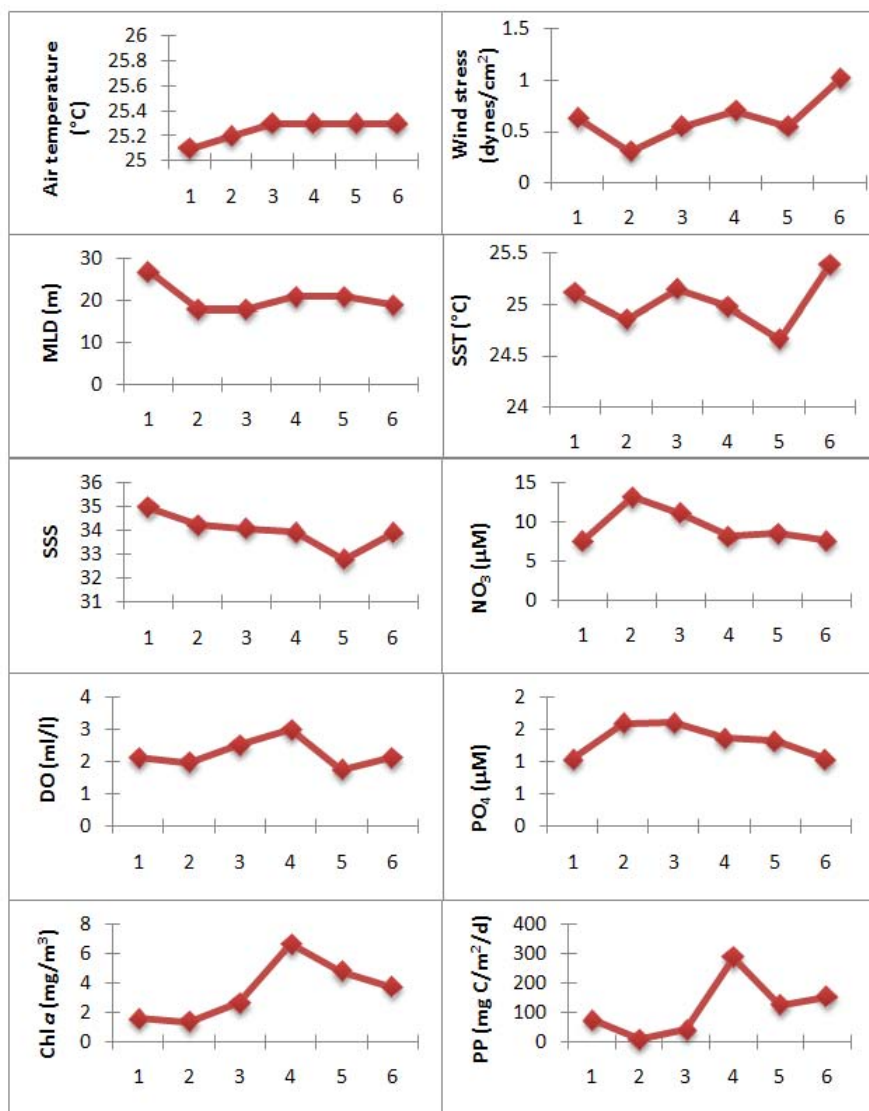


Figure 4.15: Variation in different parameters off Tvpm (during 25th June to 5th July 2006)..

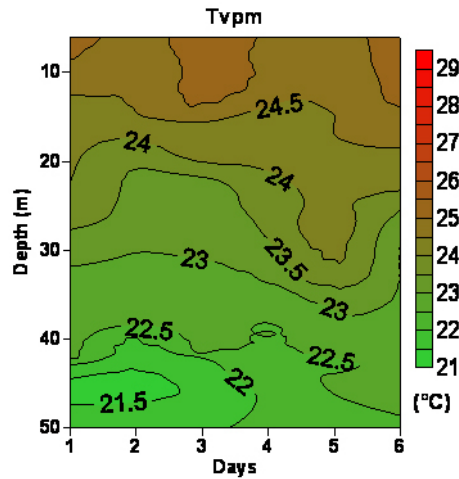


Figure 4.16: Variations in temperature in the TSS off Tvpm during the 12th day study period

25.7 °C and 27.4 °C. Comparatively, weak stress was experienced due to weak northerly and northwesterly winds (0.2 *dynes/cm*² to 0.6 *dynes/cm*²). Analysis between SST and wind stress gives weak regression coefficient of 0.04 indicating insignificant influence of local wind on the oceanic process. Regardless, LTA, the measure of upwelling intensity showed a higher value (4°C), than that off Tvpm (3°C). Moreover, MLD was shallow at 8 m-15 m and was not observed to be influenced by wind stress. Distribution of the bulk SST at 5m level shows upwelling peaks on 1st, 7th and 11th days of observations along with two relaxation phases on 3rd and 9th days corresponding to the peak and relaxation phases on 3rd and 9th and 1st, 5th and 11th days respectively off Tvpm. The low SSS

values of this region (32.00 to 34.00) with considerable daily variations, indicate the presence of fresh water discharge through the nearby Kallada river.

Distribution of Nitrate, Phosphate and *DO* are observed to be consistent with upwelling peaks and relaxation phases as evidenced in SST. During the first phase (1st day) of upwelling the observed values of NO_3 , PO_4 and *DO* are $8\mu M$, $1.5\mu mole$ and $2.2 ml/l$ respectively. During the second phase (7th day) it was $6\mu M$, $1.5\mu M$ & $2.1 ml/l$. In the third phase (11th day) the values were $5\mu M$, $1\mu M$ and $2.5 ml/l$ respectively. During the relaxation period, NO_3 was observed between 0 and $4\mu M$, PO_4 between 0.4 and $1\mu M$ and *DO* between 2.5 and $4.5 ml/l$. These variations in nutrients and *DO* is not agreeing with the daily SSS variations which suggest the least influence of fresh water discharge in the upper water column. Despite, it is found to be in direct relation with upwelling (SST). So it can be concluded that the influence of freshwater is limited to the skin surface is suppressing the indicators of upwelling at the surface.

Considering the biological productivity, analogous to the observations off Tvpm, a lag of four days was evidenced between nutrient enhancement and production. However, this relation was not found with PP during the period as observed at Tvpm. It is found that fluctuation in air temperature during the period is high

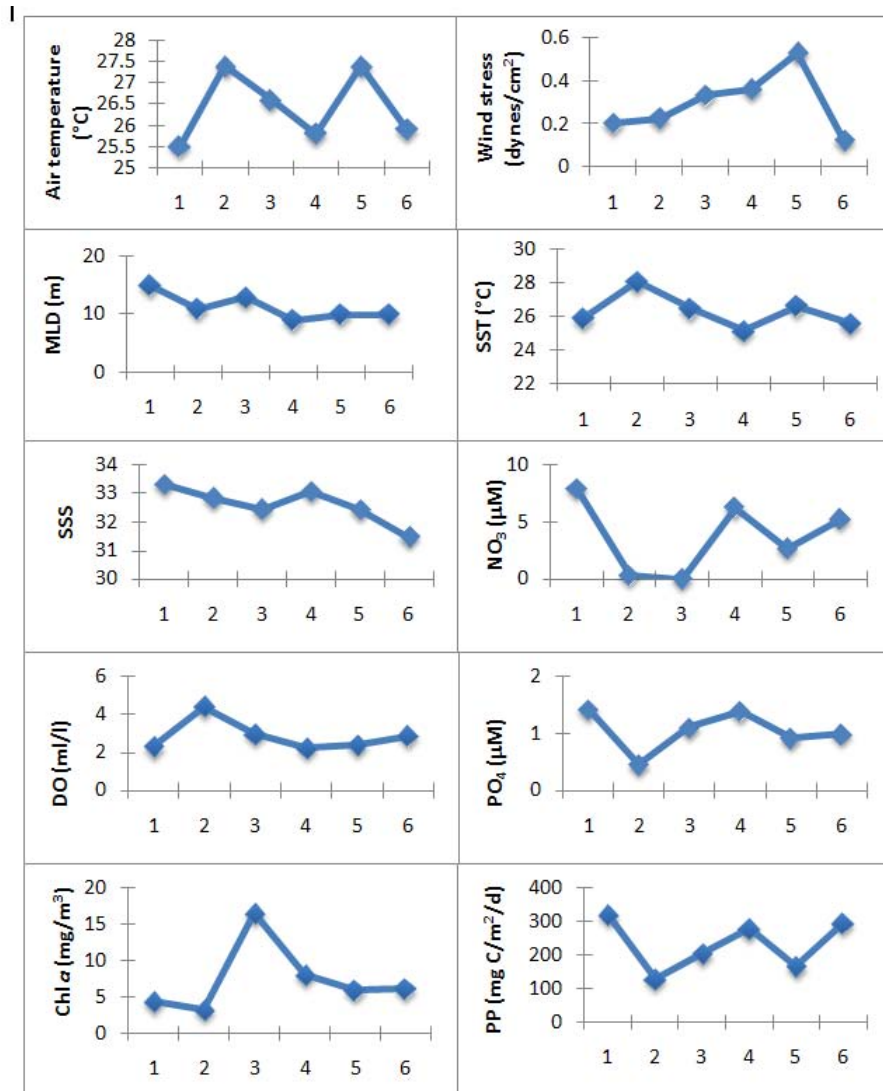


Figure 4.17: Variation in different parameters off Kollam (during 26th June to 6th July 2006)

(25.7 °C - 27.4 °C) due to extensive cloud cover (6-7 Octa -visual observation) without much precipitation. These automatically reduce sunlight for photosynthesis and thereby cause reduction in PP. These strongly suggest the influence of local climate variations on biological production.

Meteorological data indicates moderate to heavy rainfall over Kollam (614 mm) and Tvpm (344 mm) during the period of observation. SST, SSS, and rainfall in alternate days off Kollam and Tvpm recommend the relation between the parameters are linear off Kollam, but it is non linear off Tvpm. Kallada River (9° N) and Vamanapuram river (8.5°N) with discharge values of 1595 Mm^3 and 656 Mm^3 point out the riverine influence in the hydrography (SSS) of the corresponding transects. The downward transfer of momentum flux is restricted by the strong stratified layer that prevented the vertical wind mixing of the surface water column leading to shallow MLD off Kollam. Whereas, the deep mixed and isothermal layer and weak stratification off Tvpm can be best explained by strong wind stress.

The analysis of the stability (Brunt Vaisala frequency) of the water column indicate low frequency (0 to $3.2 \times 10^{-4}/s$) with maximum at thermocline, off Tvpm suggesting more or less homogenous water column and moderately high frequency (0 to $11.8 \times 10^{-4}/s$) off Kollam, indicating stratified water column off Kollam

preferably due to land runoff. It is observed that, irrespective of the complexity in the system off Kollam, the response due to physical forcing in terms of coastal upwelling is evident in the hydrographic and oceanographic characterization of the region.

From the observations it is obvious that there exist distinct physical processes defining the hydrography along the two transects. In brief, hydrography and oceanography of the sea off Kollam is supposed to be influenced by wind and remote forcing from the Bay of Bengal. Whereas off Tvpm, the observed hydrography was in well agreement with day to day change in the wind field and also the influence of fresh water discharge is minimal. Moreover, off Kollam the process is influenced by local climatic variations like rainfall and fresh water runoff through Kallada river.

4.4 Conclusion

Spatial and temporal variability in the coastal upwelling system of the SEAS is explained on the basis of in situ and satellite measurements. The impacts of the physical forcing on chemical and biological environment are well explained utilising the available information. Spatial variation in the processes of upwelling along the continental shelf and the role of remote forcing from Bay of Bengal in terms of the coastal Kelvin waves are explored in detail. In addition to the factors triggering upwelling - along

shore monsoon winds, coastal Kelvin waves, westward propagating Rossby components, there are significant influencing factors like coastal currents and river runoff that causes adverse impact on the system as evidenced off Mangalore and Kozhicode.

Coastal fronts were identified and estimated using different criteria such as SST, Chl *a*, SSHA and estimated RRD. All the inferences made out of this analysis strengthen the influence of ASHSW on the process in the northern latitudes of the study area. Strong upwelling does not imply more extended offshore transport in the northern transects as the presence of ASHSW causes density gradient strong enough to prohibit significant inter leaving across. But this density difference defines the maximum baroclinic RRD in this region.

Attempt has been made to portray temporal variation in upwelling along the south SEAS using in situ observations for 12 days. The process is found to be responding with wind stress and is episodic. There exists certain peak and relaxed phases in upwelling in both the transects during the observation. The hydrographic field responded to changes in wind field and the indication is seen in water column up to 40m depth along both the transects. And simultaneous changes were observed in SST, NO_3 , PO_4 and DO . A lag of four days was observed in primary production following upwelling of the cold, nutrient rich, less oxygenated

water to the surface. Since the peak production occurs during the relaxation phase following the peak upwelling, the possibility of offshore advection of the nutrient rich upwelled water is assumed to be inconsiderable.

In spite of the proximity of the two transects, the processes of upwelling are found to be different in terms of intensity and forcing mechanisms. In addition, influence of local climatic variations like rainfall, cloud cover and river discharge were also found to affect the process. Off Tvpm the process was chiefly wind driven and the indication of local climatic influence was not observed. Whereas, the situation changes off Kollam, where weak wind stress, high rainfall, and enormous river discharge and the associated meteorological parameters like cloud cover, air temperature also induced abrupt variations in the surface oceanic parameters. In spite of the weak windstress and the presence of comparatively warm, less dense and less saline fresh water, the intensity of upwelling was observed to be high off Kollam. Distribution of Nitrate, Phosphate and *DO* are observed to be consistent with upwelling peaks and relaxation phases as evidenced in SST. During the first phase (1st day) of upwelling, our earlier results suggesting the influence of remote forcing on upwelling between Kollam and Mangalore. Despite the suppressive forcing on upwelling is due to heavy discharge as evidenced from the stability

parameter Brunt Vaisala frequency. In conclusion, the spatial and temporal variability in coastal upwelling along the SEAS is well understood which can provide the physical basis for the biogeochemical behavior of the region that can be effectively utilised in ecosystem modeling.

Chapter 5

Primary Production Associated with Upwelling

“A theory has only the alternative of being right or wrong. A model has a third possibility; it may be right, but irrelevant.”

– Egan Manfred.

5.1 Introduction

UPWELLING and associated advection of nutrient-rich deep water to the surface and the subsequent stabilization of the nutrient-laden water in the euphotic zone by solar heating is the fundamental mechanism supporting the high biological productivity of most of the coastal ecosystems. A predictive understanding of marine ecosystems that is useful to man will be based on a hierarchy of generalizations. The fundamental generalizations relating phytoplankton growth to the nutrient content of seawater

have been established by ⁸³ Redfield (1934), ¹¹⁷ Sverdrup (1953), ⁷¹ Pauly and Christensen (1995) and ⁸⁸ Santos et al., (2007). They have established that broad scale variations in primary production both temporally and spatially are related to variations in the supply of inorganic nutrients and light.

The quantity of PP helps us not only to understand matter and energy bases of PP but also to assess and predict bio-resources, particularly fishery resources. Values of PP are also indicators of environmental quality and ecological contributions in sea water. Higher levels of primary production occur in shallow coastal waters within 200m depth contour. In addition certain offshore waters are influenced by diverging fronts and other hydrographic features which can bring nutrient rich subsurface water into the euphotic zone.

High PP in the SEAS is usually related to coastal upwelling activity that injects nutrients into the euphotic zone in response to prevailing longshore winds and remote forcing from BoB. The composition of these forcings changes zonally due to the factors like varying wind field, bottom topography and orientation of the coast line. The SEAS contributes about 30-50% of the total marine fish catch in India during the upwelling period. The area is colonized by planktonivorous small pelagic fishes like Oil sardines, Anchovies, Indian Mackerals etc. The population of these

species is characterized by significant interannual fluctuations in their abundance and have major place in the SEAS, where they are exploited commercially and play a role as forage fish for numerous predators such as large pelagic fishes, demersal fishes, seabirds, mammals etc. Earlier analysis of long term time series data Longhurst and Wooster (1990) on fish landings suggest the influence of environmental parameters on large scale fluctuations in the fisheries. Especially oil sardines fluctuate highly with the intensity of upwelling. According to ³Bakun and Roy (1998), ³⁶Krishnakumar et al., (2008), the spawning and recruitment strategies of clupeoids from the upwelling area were found to be adapted with the spatial and temporal pattern in the upwelling of the region. ⁴²Longhurst and Wooster (1990) have reported that the success in recruitment of oil sardine fishery is very much depended on the upwelling in the area.

Bakun and Parrish (1982) and Cury and Roy (1989) suggested the concept of Optimum Environmental Conditions or Optimal Environmental Window (OEW) with regard to nutrient enrichment (upwelling or mixing), concentration process (convergence or stratification) and retention process that maintain eggs and larvae in the suitable habitat were found to be crucial for the successful recruitment of clupeoids in the upwelling areas. Despite of their high rate of production, the adverse environmental conditions dur-

ing the upwelling season like, turbulence, offshore advection etc., can create havoc for their larval survival and subsequent recruitment success.

The phase level of the exploitable fishery potential in the SEAS is the upwelling associated primary production in the euphotic column. In order to understand the environmental variability and its influence due to change in environmental conditions, the upwelling intensity and the total PP associated are estimated for the region between 7°N to 16°N latitude and 71°N to 78°N longitude. For a better understanding of the biological response of the process of upwelling during different years the exercise has been done for a consecutive period of seven years (2003 -2009). The objectives of the analysis are to;

1. Study the inter-annual variability in the coastal upwelling of the SEAS with regard to LTA
2. Estimate the total PP associated with the upwelling and
3. Address the inter-annual variability in PP in relation to upwelling.

5.2 Data and Methodology

5.2.1 Upwelling Index from SST

Variation in SST is an accepted index for the process of coastal upwelling as it represents the responding variable of the process

irrespective of the forcing mechanism (¹²⁹Wooster et al., 1976, ⁷⁶Prell and Streeter, 1982 and ⁶¹Naidu et al., 1999). This is based on the fact that, the difference in SST of the inshore area (where the subsurface cold water replaces the offshore transport) and the SST of the offshore area directly measures the intensity of upwelling. Though different approaches are suggested by different authors, grids separated by 3° are considered for the LTA estimation in the present study. This interval is chosen based on the analysis of different parameters like SST, surface Chlorophyll *a*, SSHA, SSS and based on the understanding of the offshore extend of the process in different parts of the SEAS. Also, the region along the Cape and the region between Tyvm and Goa are treated separately. In the former case, the offshore transport is southward whereas in the latter it is westward. Thus along the SW Coast, $LTA_{wc} = T_{lon-3} - T_{lon}$ and Off Cape $LTA_{kk} = T_{lat-3} - T_{lat}$, where T_{lat} and T_{lon} represent SST at the coastal stations between latitudes 8.5°N to 14.5°N and longitude 76.5°E to 78.5°E. T_{lon-3} and T_{lat-3} represents SST at 333 *km* away from the coast. LTA_{wc} and LTA_{kk} refer to LTA along the southwest coast and along the Cape. The positive LTA values suggest the coastal upwelling process.

The data for the period 2003-2009 are considered for this analysis. Monthly 9X9 *km* resolution data are derived from MODIS AQUA and is processed using SeaWiFS Data Analysis System (Sea-

DAS), which is a comprehensive package for the processing, display, analysis, and quality control of ocean color data.

5.2.2 Model Description

5.2.2.1 Vertically Generalised Production Model (VGPM)

VGPM is a “Chlorophyll-based” model that estimates net primary production from Chlorophyll *a* using a temperature dependent description of Chlorophyll *a* specific photosynthetic efficiency (¹⁰ Behrenfeld and Falkowski, 1997a). For the VGPM, net primary production is a function of Chlorophyll *a*, available light, and the photosynthetic efficiency. Standard products are based on SeaWiFS/MODIS Chlorophyll *a*, MODIS AQUA SST data, and SeaWiFS PAR. The euphotic zone depths are estimated from a model developed by ⁵⁶ Morel and Berthon (1989) and based on the surface Chlorophyll *a* concentration.

$$PP_{eu} = 0.66125 P_{op}^B \frac{E_0}{E_0 + 4.1} C_{SAT} \times Z_{eu} \times D_{IRR}$$

The core equation describing the relationship between surface Chlorophyll *a* and depth integrated primary production is expressed as follows:

C_{SAT} is satellite surface Chlorophyll *a* concentration as derived from the measure-

ments of water leaving radiance (mg/m^3).
 VGPM calculations of net primary production were based on monthly average C_{SAT} .

D_{IRR} is daily photoperiod (in decimal hours) calculated for the middle of the month for each pixel based on the algorithm developed by ⁵⁵Meeus Jean (1991)

E_0 is Sea surface daily Photosynthetically Active Radiation (PAR) in $mol\ quanta/m^2/d$.

$$Z_{eu} = \begin{cases} 568.2(C_{TOT})^{-0.746} & \text{if } Z_{eu} < 102 \\ 200.0(C_{TOT})^{-0.293} & \text{if } Z_{eu} > 102 \end{cases}$$

Z_{eu} is the physical depth (m) of the euphotic zone defined as the penetration depth of 1% surface irradiance based on the Beer-Lambert law.

Z_{eu} is calculated from C_{SAT} following Morel and Berthon (1989). Where

$$C_{TOT} = \begin{cases} 38.0(C_{SAT})^{0.425} & \text{if } C_{SAT} < 1.0 \\ 40.2(C_{SAT})^{0.507} & \text{if } C_{SAT} \geq 1.0 \end{cases}$$

P_{Opt}^B is optimal rate of daily carbon fixation within a water column [$mgC(mgChl)^{-1}h^{-1}$] and can be modeled according to various

temperature dependent relationships.

$$P_{Opt}^B = \begin{cases} 1.13 & \text{if } T < -10 \\ 4.00 & \text{if } T > 28.5 \\ P_{opt}^{B'} & \text{otherwise} \end{cases}$$

$$P_{Opt}^{B'} = 1.2956 + 2.749 \times 10^{-1}T + 6.17 \times 10^{-2}T^2 - 2.05 \times 10^{-2}T^3 + 2.462 \times 10^{-3}T^4 - 1.348 \times 10^{-4}T^5 + 3.4132 \times 10^{-6}T^6 - 3.27 \times 10^{-8}T^7$$

The PP_{eu} is the daily carbon fixation integrated from the surface to Z_{eu} , (mgC/m^2)

5.2.2.2 Validation Against the In Situ Data

Chlorophyll a

Depth integrated monthly composite Chlorophyll *a* data for the SEAS during SM, are generated in 9X9 *km* spatial resolution using ocean color data. Daily photoperiod (in decimal hours) are calculated for the middle of the month for different latitudes from (⁵⁵Meeus Jean 1991) astronomical algorithms. Satellite derived Chlorophyll *a* data are then validated with corresponding in situ data on Chlorophyll *a* collected onboard FORV Sagar Sampada (45 stations) covering different phases of SM of the year 2009, following the methods described by ¹¹²Strickland and Parsons (1972). The relationship was weak ($Chl_{sat} = 0.511Chl_{insitu} - 0.099$)

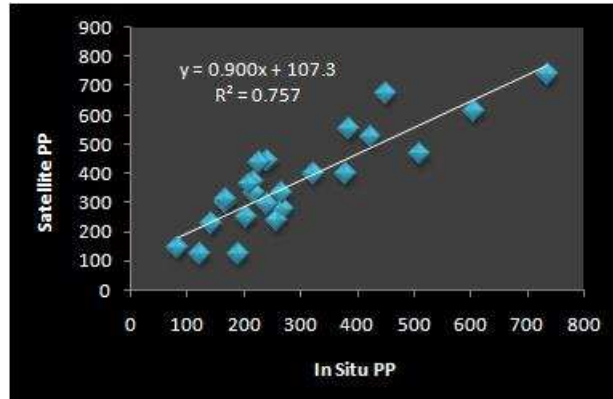


Figure 5.1: Relation between In-situ and satellite PP

with $R^2 = 0.507$ possibly due to the poor satellite coverage of the area due to cloud cover. SM data sets from SeaWiFS/MODIS AQUA are validated and corrected using the above formula. Calculated values of Chlorophyll a are then utilised in the further computations of PP.

Primary Productivity

Validation of VGPM based estimates of PP with in situ PP by ^{14}C technique (122 UNESCO, 1994) from 25 stations of FORV Sagar Sampada cruises 235 and 237 along the EAS during different phases of SM gave R^2 of 0.757 (Fig.5.1) indicating good relation between the two measurements. Thus the linear validation relation between the in situ as well as satellite PP is derived as $PP_{sat} = 0.9PP_{insitu} + 107.3$.

5.3 Results and Discussion

5.3.1 Upwelling- Inter Annual Variation

Inter annual variation in the process of coastal upwelling is of great concern since it contributes to variation in biological productivity. It is important in the estimation of fishery resources and thereby for an effective and sustainable management of the marine resources. The present analysis is based on the upwelling indices derived from SST, for the years 2003 to 2009 (Fig.5.2).

Considerable variability in both time and space is seen in the data with stronger upwelling in the southern regions. During the years 2005, 2006, 2008 and 2009 strong upwelling is recorded in the southernmost region of Cape, and is maximum during 2008 with LTA 3.3°C . In the remaining years, 2003, 2004 and 2007, the Cape-Kollam section showed intense upwelling suggesting a controversial result to the explanation of the shadow zone in the area.

This maximum intensity in the shadow zone can be due to the strong positive wind anomaly during the years where the average magnitude is greater than 7.2 m/s (³²Jayaram et al., 2010). Wind stress of weak alongshore and strong cross shore component as reported by him substantiate the strong upwelling off Cape during the years 2005 and 2006. It is noted that in all the years, the

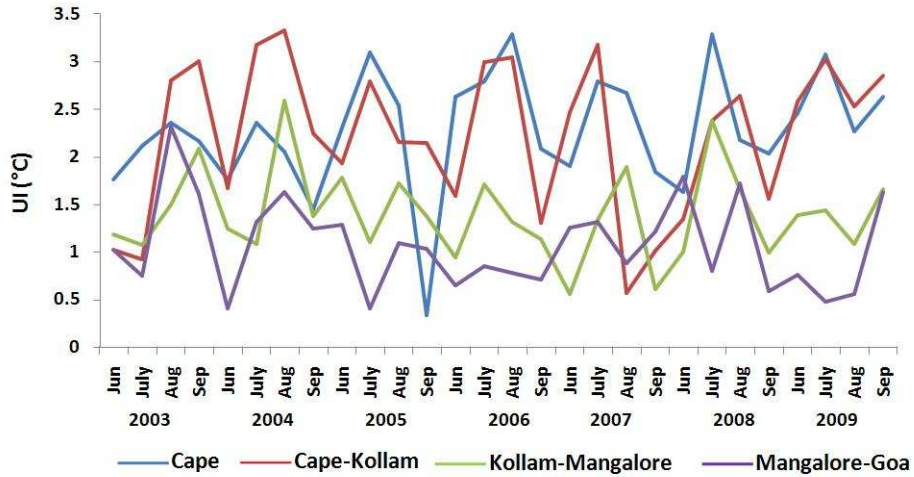


Figure 5.2: LTA (UI) for each sub region

initiation of the process of upwelling is along the Cape or within the Cape-Kollam sector (Fig. 5.2.).

The process is comparatively weak along the Kollam - Mangalore and Mangalore-Goa sectors and along the former it is observed to be starting in the end of June/July with certain lag. Whereas along the Mangalore-Goa sector, the process starts with the onset of SM in June, possibly due to the predominance of upwelling favorable winds. Considerable inter annual variability persists in these two regions, recording strong upwelling during 2003, 2004 and 2008. The process is weak along the Mangalore-Goa sector during 2006 ($LTA = 1^{\circ}C$), and a delayed strengthening was recorded during 2005 and 2009. Altogether, the process of upwe-

ling is weak along the northern sections compared to the southern tip as well as the Cape-Kollam sector. Also, the drastic decrease in the intensity of upwelling off Cape and off Cape-Kollam sector during September 2005 and August 2007 fails to explain the normal trend in the process along the region. The present analysis does not agree with ²⁸Habeeb et al., (2008) along the Tvpm-Goa sector pointing out that upwelling and the associated production is stronger/higher off Kochi. It is assumed that the region wise grouping in the present study have accommodated the strong upwelling of Kochi.

Ecosystem averaged upwelling measures are computed for this period and compared with the seven years climatological average. This is derived from the upwelling indices calculated separately for each latitudinal transects for the four SM months and averaged to a single entity to get a representative figure for the entire ecosystem. The average index for the ecosystem for a period of seven years is found to be 0.64°C (Table 5.1). Stronger upwelling is recorded in 2008 (0.68°C) followed by 0.67°C , 0.66°C and 0.65°C for the years 2004, 2005 and 2009 respectively, which are above the normal value of 0.64°C . Whereas an index value of 0.59°C , 0.62°C , and 0.58°C represents the weak upwelling years of 2003, 2006 and 2007. The weak upwelling recorded during 2003 can be due to the weak SM wind as reported by ¹²⁴Vinayachandran

UI (°C)	Year
0.638697	2003-09
0.588034	2003
0.672623	2004
0.656084	2005
0.621705	2006
0.580636	2007
0.676318	2008
0.652535	2009

Table 5.1: Upwelling Indices (*LTA*)-Average for the SEAS

(2004) particularly in the onset phase. In contrary, ²⁶ Gopalakrishna et al., (2008) reported that the upwelling during 2005 is the strongest and prolonged one for the period of his study (2002-2006). This contradiction may be due to the restriction of his study region to Kochi transect, with which the whole ecosystem of SEAS cannot be represented.

5.3.2 Primary Production - Inter Annual Variation

The monthly average PP per day associated with the SEAS upwelling (VGPM derived using satellite data) for the years 2003 to 2009 for each sub regions and the total PP for the whole ecosystem in million ton Carbon (*MtC*) are presented in Table 5.2. Considerable inter annual variation is noticed in all the four regions and preliminary analysis indicate the existence of one-to-one relation

Year	Average PP ($mgC/m^2/d$) for each sub-region				Total PP for SEAS (in MtC)
	Cape	Cape-Kollam	Kollam -Mangalore	Mangalore - Goa	
2003	770.0362	697.4611	562.2705	293.3817	24.7889
2004	1047.6487	793.1900	930.4409	743.4196	39.7621
2005	926.1104	764.9099	573.4576	488.8318	28.4935
2006	679.68041	709.3896	666.3459	702.0741	29.9739
2007	555.38213	578.3454	635.5901	734.2543	27.9148
2008	567.11746	720.8984	419.6536	358.0042	20.5434
2009	772.84656	761.8810	569.5924	336.3700	25.6365

Table 5.2: Year wise/sub region wise and total PP for the SEAS

between PP and the ecosystem averaged upwelling indices. Maximum PP estimate of 39.76 MtC is recorded in 2004, associated with the second strongest upwelling period. During other years, the values fall in the range of 24.78 MtC (2003) to 29.97 MtC (2006), with two abnormal values of 39.76 MtC (2004) and 20.54 MtC (2008). The unexpected low PP value associated with the strong upwelling year of 2008 is due to the non-availability of data during June, August and September and so is not considered in the present analysis.

Interannual variation is prominent in the region wise average PP per day (Table 5.2) recording high values off Cape, followed by Cape-Kollam region. Maximum value recorded off Cape is 1047.65 $mgC/m^2/d$, during 2004, followed by 926.11 $mgC/m^2/d$, in

2005 and $772.85 \text{ mgC/m}^2/\text{d}$, during 2009. The minimum PP measure of $555.38 \text{ mgC/m}^2/\text{d}$, recorded during 2007 is associated with the weak upwelling. Along Cape-Kollam sector, maximum PP is $793.19 \text{ mgC/m}^2/\text{d}$, recorded in 2004, followed by $764.91 \text{ mgC/m}^2/\text{d}$, in 2005 and $761.88 \text{ mgC/m}^2/\text{d}$, during 2009. The value of $578.34 \text{ mgC/m}^2/\text{d}$, recorded during 2007 is the lowest in the section. The pattern is different along the Kollam-Mangalore sector except that, the year of maximum production was same as that of the other regions (2004 with PP values $930.44 \text{ mgC/m}^2/\text{d}$). In this region the second highest PP of $666.35 \text{ mgC/m}^2/\text{d}$, is recorded during the year 2006 followed by $635.59 \text{ mgC/m}^2/\text{d}$, during 2007, which coincides with the below normal upwelling years. High PP of $743.42 \text{ mgC/m}^2/\text{d}$, during 2004 is observed along the Mangalore - Goa sector followed by $734.25 \text{ mgC/m}^2/\text{d}$, in 2007 and $702.07 \text{ mgC/m}^2/\text{d}$, during 2006. Also, this region recorded minimum production of $293.38 \text{ mgC/m}^2/\text{d}$, during 2003.

Region-wise month-wise PP averaged for 2003 to 2009 is shown in Table 5.3. The values varied in a small range between $600.37 \text{ mgC/m}^2/\text{d}$, and $808.94 \text{ mgC/m}^2/\text{d}$, except during the onset phase along the two northern sectors off Kollam - Mangalore ($367.02 \text{ mgC/m}^2/\text{d}$), and Mangalore - Goa ($594.65 \text{ mgC/m}^2/\text{d}$). This clearly indicates the northward progress of the process of upwelling with the advancement of the SM winds.

Sub-region	June	July	Aug	Sep	Avg PP
Cape	782.5242	801.7146	808.9438	792.1396	796.4781
Cape-Kollam	686.9667	687.2876	694.8191	694.0795	690.7926
Kollam-Mangalore	367.024	664.0175	679.3886	653.4826	592.3015
Mangalore - Goa	594.6447	636.3794	636.4887	600.3704	617.2899

Table 5.3: Region wise - month wise long term averaged PP ($mgC/m^2/d$)

Both along the Cape and Cape-Kollam sectors, enhanced PP are observed in the start of the SM month itself showing PP values of $782.52 \text{ mgC}/m^2/d$, and $686.97 \text{ mgC}/m^2/d$, respectively. The high values of PP recorded during July and August indicates that the upwelling is well established in all the sections by July. All the four sub-regions showed high rate of production during July-August and starts to decrease during September. The region off Cape is marked as the high productive zone with a seasonal average of $796.48 \text{ mgC}/m^2/d$, followed by Cape - Kollam ($690.79 \text{ mgC}/m^2/d$), Mangalore - Goa ($617.29 \text{ mgC}/m^2/d$), and Kollam - Mangalore ($592.30 \text{ mgC}/m^2/d$).

Further, detailed analysis of the monthly average PP for all the years between 2003 and 2009 (Fig.5.3) has been done separately for each sub-region. The interannual variation was evidenced in monthly pattern along different sub regions. The analysis was done subjected to the three phases of upwelling in different sub-regions considering June as the onset phase, July-August

as peak phase and September as the withdrawal phase.

Along the Cape, PP during the onset phase of June was considerably less in 2003 ($470 \text{ mgC}/\text{m}^2/\text{d}$) as compared to the remaining years. Along the Cape-Kollam section the values were in the range of $480\text{-}800 \text{ mgC}/\text{m}^2/\text{d}$, which is less as compared to Cape region. Along Kollam-Mangalore section the range was still less ($400 \text{ mgC}/\text{m}^2/\text{d}$ to $720 \text{ mgC}/\text{m}^2/\text{d}$) and the maximum value is recorded during 2004. In the northern most sectors along Mangalore - Goa it further decreased to the minimum range of $200 \text{ mgC}/\text{m}^2/\text{d}$ to $600 \text{ mgC}/\text{m}^2/\text{d}$ during 2003 and 2004 respectively.

The months of July and August were observed as the maximum production ($600 \text{ mgC}/\text{m}^2/\text{d}$ to $1000 \text{ mgC}/\text{m}^2/\text{d}$) period in all the sub regions except for the year 2003. Less production is marked during July 2003 (average for all the sub regions was $487 \text{ mgC}/\text{m}^2/\text{d}$), compared to other years. This can be due to the delayed SM winds during the onset 2003, as explained by ¹²⁴Vinayachandran (2004). Cape and the Cape-Kollam sections are the high production zone during all the years, except the weak upwelling year of 2007 where the high production is marked in the Mangalore-Goa stretch.

During September, the production showed a general decreasing trend except during 2006 and 2008 indicating the weakening of the process of upwelling has not taken place during these

years. The average PP for all the sub-regions during the month recorded between $350 \text{ mgC}/\text{m}^2/\text{d}$ to $800 \text{ mgC}/\text{m}^2/\text{d}$. And the highest value of $1100 \text{ mgC}/\text{m}^2/\text{d}$ is recorded along the Cape during 2004. As observed in the other months, maximum production observed during September is along the Cape followed by Cape-Kollam sector, except the year 2007.

In brief, there exists a one-to-one relation with the intensity of upwelling and the total PP associated with it. The northward progression of the process of upwelling with the advancement of SM wind is evidenced in the PP pattern also. The southern sections (Cape and Cape-Kollam region) are shown as high productive regions among the four except during 2007, the weak upwelling year where the northern transects showed high PP values.

The relation between the UI and the corresponding PP for each latitudinal transects and for the SM months (June-September) were made to regression analysis, and the relation is found to be relevant with $R^2 = 0.575$ (Fig.5.3) for an optimum values of UI and PP and the relation is $PP = 179.2UI + 287.4$. In detail, the relation does not hold well for anomalous PP values and for very strong LTA values which may be associated with algal blooms or the strong offshore transport.

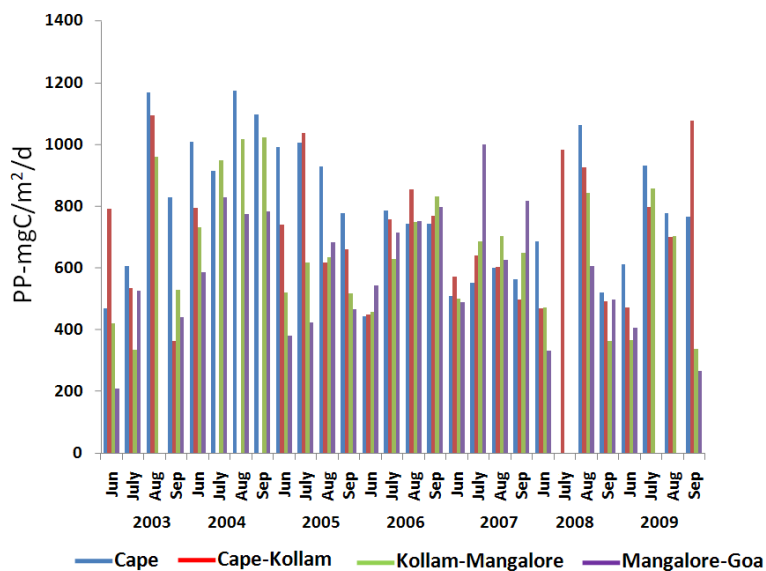


Figure 5.3: Distribution of monthly averaged PP in $mgC/m^2/d$ for SM months in each sector during 2003-2009

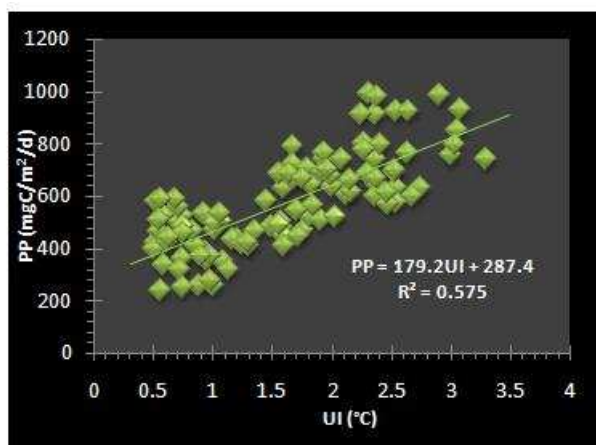


Figure 5.4: Relation between UI and PP for 2003-2009.

5.4 Conclusion

Many studies have come out with emphasize on the physical processes and associated chemical and biological implications. This study attempts an integrated approach relating the physical forcing and biological responses associated with the SEAS. It is shown that there exists a one-to-one relation with the intensity of upwelling and the total PP associated with it. The northward progression of the process of upwelling with the advancement of SM wind is evidenced in the PP pattern also. The Cape and Cape-Kollam sub-regions are shown as high productive areas among the four sub-regions considered. In addition, an attempt to derive theoretical basis of the relation between the response variable LTA and the biological production PP has been done by analysing seven years of satellite/model data on UI and PP. Thus it can be estimated that for an optimal upwelling period, the PP associated with it can be formulated as $PP = 179.2UI + 287.4$. The estimation was done after validation/correction of satellite Chlorophyll a and the modeled PP data against the in situ data collected. Furthermore, the study explored the extensive possibilities of satellite measurements on ocean color (Chlorophyll a) and PP, as the in situ PP data available are of low resolution with regard to space and time. It recommends the reliability and usability of satellite/modeled PP data in the region.

Chapter 6

Summary and Conclusion

“One can only see what remains to be done...”

– Marie Curie

UPWELLING regions represent a small portion of the global ocean surface but accounts for a disproportionately large fraction of the oceanic primary production as well as fishery. Upwelling associated biogeochemistry has received great attention due to its influence on the biological production including the potential fishery of that area. The interannual variability of the process can further, influence the fishery and thereby, affect the economy of countries which rely on fishery. So understanding and quantifying the upwelling is of great importance for marine resources management. While, direct measurement of this process is extremely difficult, proxies like mass transport, Local Temperature Anomaly (*LTA*), isothermal shift are generally used to evaluate the intensity of the process of upwelling. Even though several studies

have come out from the South Eastern Arabian Sea explaining the physical process of upwelling, nutrient enrichment and enhanced biological production, studies explaining the transfer of energy between these components are lacking. The response of different sub-regions of the ecosystem giving emphasis to the meso-scale variations and the influence of local climate variables has received only little attention. In this context, the present study illustrates the spatial variability of the upwelling system in terms of forcing mechanism, intensity and the spatio-temporal variability in the physical, chemical and biological parameters. In addition, an attempt has been made to identify the lag phase of the biological response to the physical forcings. The total Primary Production associated with the upwelling ecosystem during different years is also derived.

The results presented in this study is mainly based on the data collected onboard FORV Sagar Sampada during the different active monsoon periods. In situ data on different physical, chemical and biological parameters collected during SS227 and SS246 were used to explain the spatial and temporal variation. In addition, the data collected during the cruises SS142, SS173, SS203, SS217, SS235, SS236, SS237 and SS238 from selected stations/transects were also considered to substantiate the results. Besides, climatological as well as satellite data were used to

explain the results in a better resolution (both in space and time). The parameters include wind speed, direction, SST, SSS, DO, nutrients, Chlorophyll a and primary productivity. The study was conducted as a part of the Marine Living Resources Programme (MLRP) funded by the Ministry of Earth Sciences (MoES) and implemented by the Centre for Marine Living Resources and Ecology (CMLRE) in association with the National Institute of Oceanography (NIO), Regional Centre, Kochi.

The study explains the process of coastal upwelling in the SEAS with an integrated approach involving in-situ, satellite, climatological data and model results on different physico-chemical and biological parameters. Understanding of the process of upwelling, its spatial variation in terms of forcing mechanism and intensity is well explained. It is identified that, the process of upwelling off the southern tip (off Cape) and the west coast of India is highly localised with different forcing mechanisms, and they cannot be treated as a uniform wind-driven upwelling system. Off Cape, upwelling is due to the south-westerly winds that are tangential to the coast, the area between 8°N and 9°N represents the shadow zone with negligible influence of the remote forcing, where the upwelling is forced by the longshore wind stress. Moderate to relatively intense upwelling was observed between Kollam and Mangalore (9° N to 13° N) due to the combined influence of the

longshore wind stress, coastally trapped Kelvin waves and the offshore propagating Rossby waves. North of the area (13°N to 15°N), upwelling was weak due to weak wind stress, where it was confined to the coastal belt, indicating the suppressive effect of the southward flowing Arabian Sea High Saline Water on the upwelling along this coastal stretch.

The results derived from the climatological data suggests the complexity of the system which necessitates a theoretical formulation to explain and quantify the process. With the three major components inducing or influencing the process, windstress ($U&V$ components), SST and SSHA derived at 1° latitude interval for eight years, a mutual relation has been derived to explain upwelling in terms of the responding variable LTA . In addition the factor k_{rf} was added to represent the influence of fresh water runoff in the area. The sub regions were treated separately as Cape, Cape-Kollam sector (shadow zone), Kollam-Mangalore sector and Mangalore-Goa sector.

The spatio-temporal variation in upwelling and its biological responses are explained on the basis of in situ and satellite measurements. In-situ observations during the peak upwelling month (July) indicated an intense upwelling in the southern parts up to Kochi (10°N), as evidenced from the distribution of SST, nutrients, Chlorophyll a , and primary production. It was observed

that, in addition to the inductive forces like alongshore windstress and coastal Kelvin waves, suppressive effect due to the coastal currents and river runoff also have major influence on the intensity of coastal upwelling in these regions. The coastal fronts estimated through SST, Chlorophyll *a* and SSHA data are in contradiction with that of the computed Rossby Radius of Deformation (RRD) suggesting that RRD is not a proper estimate of offshore extend of upwelling. RRD is probably influenced by the vertical density gradient of the water column. The analysis on the northern transects indicate an adverse impact on the offshore propagation of upwelled waters due to coastal currents. Variability of the upwelling signals, based on the time series observations at Tvpm and Kollam indicates that there exists a lag of four days to get their impacts on primary production following upwelling of the cold, nutrient rich, less oxygenated subsurface waters. The results also show the influence of local climatic variations (cloud cover and land runoffs) on the system.

The biological significance of the process of upwelling is evident in the spectacular fish production, along the southwest coast of India during summer monsoon. The control of physical forcing on the biological production (primary level) is of great significance, as it promotes very high abundance of pelagic fishery in the region. Based on the above, the energy flow depicting the various process

cascading down up to the level of biological production (how biology varies with varying SST) has been derived. Furthermore, the interannual variability in the process of upwelling in terms of the *UI (LTA)* is explained with seven years of data. The total PP associated with the upwelling ecosystem is estimated using satellite derived ocean color and modelled PP data. The results showed a one-to-one relation with the intensity of upwelling and the total PP associated with it. The northward progression of the process of upwelling with the advancement of summer monsoon wind is also evidenced in the *PP* pattern. Cape and Cape-Kollam sub-regions are found to be high productive areas among the four sub-regions studied. The present study validates the credibility of the satellite/model derived data on explaining the biological production.

6.1 Concluding Remarks

The present study has proposed to understand the South Eastern Arabian Sea upwelling system and categorise the major factors (forcing and responding variables) influencing the process. The result of this study can be used as a basic outline of the ecosystem model explaining the physical process of upwelling in a sub-regional scale and its influence on the chemical and biological parameters including the primary production which can be further utilised in estimating or predicting the pelagic fishery of the re-

gion. Thus the study is relevant in understanding and explaining the basic pathways between different compartments of the SEAS ecosystem and to contribute for the effective and sustainable management of the marine resources of the area.

A better understanding of the dynamics as well as the outward extend of the process could have been possible if the in situ data during monsoon months covering the onset, peak and withdrawing phases of upwelling along the entire ecosystem was available. Time series data for a period of one month is the minimum requirement for such studies to explore the response of each component under varying physical forcing (wind field), chemical (nutrients) and biological (on phytoplankton, microzooplankton and mesozooplankton) properties. Furthermore, information on fresh-water discharge along the southwest coast would have added more valuable results on this localised phenomenon.

6.2 Scope for Future Work

- The current measurement at fine resolution (vertical as well as horizontal) associated with upwelling can improve the knowledge base of shelf circulation associated with upwelling.
- The role of bottom topography which determines the spatial variation in the process is least exploited for the region. The

possibility of such study based on fine resolution multi layer coastal models to explain the coastal processes can be explored.

- The role of equatorial winds and West Bay of Bengal along-shore winds in driving the coastal Kelvin and Rossby waves along the SEAS can be attempted.
- The development of an ecosystem model for the SEAS upwelling system addressing all physico-chemical and biological parameters would be the most exciting study in future.

Bibliography

- [1] Antony, M.K., G. Narayana Swamy, and Y. K. Somayajulu, 2002. Offshore limit of coastal ocean variability identified from hydrography and altimeter data in the eastern Arabian Sea. *Continental Shelf Research*, 22, 2525-2536.
- [2] Bachan, A., 1895. Reports on oceanic circulation based on the observations made onboard H.M.S.Challenger and other observations. *Rep. Scient. Res. Voy. 'Challenger' physics and Chemistry*, part 8, Appendix, 33.
- [3] Bakun, A. and C., Roy and S., Lluch-Cota, 1998. Coastal upwelling and other processes regulating Ecosystem Productivity and Fish production in the Western Indian Ocean. *Large Marine Ecosystems of the Indian Ocean-Assessment, Sustainability and Management*. Edited by Kenneth Sherman, Ezekiel N.Okemwa and Micheni J.Ntiba, 103-141.
- [4] Bakun, A., and R.H., Parrish, 1982. Turbulence, transport and pelagic fish in the California and Peru Current systems. *Calif. Coop. Oceanic Fish. Invest. Rep.*23:99-112.
- [5] Bakun, A., 1973. *Coastal Upwelling Indices, West Coast of North America, 1946-71*. NOAA Technical Report NMFS SSRF-671., U.S. Department of commerce, National Oceanic and Atmospheric Administration., National Marine fisheries Service.

- [6] Balan, V., 1984. The Indian oil sardine: a review. *Mar. Fish. Inf. Serv. Tech. Ext. Ser.*, 60:1-10.
- [7] Banse, K., 1959. On upwelling and bottom trawling off the southwest coast of India, *J. Mar. Biol. Assoc. India*, 1, 33– 49.
- [8] Banse, K. 1968. Hydrography of the Arabian Sea shelf of India and Pakistan and effects on demersal fishes, *Deep- Sea Research.*, 15, 45– 79.
- [9] Bauer, S., Hitchcock, G.L., and Olson, D.B., 1991. Influence of monsoonally forced Ekman dynamics of upper layer depth and phytoplankton biomass distribution in the Arabian Sea. *Deep-Sea Research.*, 38, 531-553.
- [10] Behrenfeld, M. J., and P. G., Falkowski, 1997a. A consumer's guide to primary productivity models. *Limnol. Oceanogr.*, 42, 1479–1491.
- [11] Behrenfeld, M. J. and P. G. Falkowski, 1997b. Photosynthetic rates derived from satellite-based Chlorophyll concentration. *Limnol. Oceanogr.*, 42, 1–20.
- [12] Berger, W. H. and G., Wefer, 1991. Productivity of the Glacial Ocean: Discussion of the Iron Hypothesis. *Limnology and Oceanography* Vol. 36 (8), 1899-1918.
- [13] Boyce, D.G., M.R., Lewis, and B., Worm, 2010. Global phytoplankton decline over the past century. *Nature* /doi:10.1038, 466, 591-596.
- [14] Brandt, P., Stramma, L., Schott, F., Fischer, J., Dengler, M., Quadfasel, D., 2002. Annual Rossby waves in the Arabian Sea from TOPEX/POSEIDON altimeter and in situ data. *Deep-Sea Research II* 49, 1197-1210.
- [15] Brock, J.C., McClain, C.R., Anderson, D.M., Prell, W.L., Hay, W.W., 1992. Southwest monsoon circulation and environments of recent planktonic foraminifera in the northwestern Arabian Sea. *J. of Paleooceanography*, 7, 799-813.

- [16] Brown, O.B., Bruce, J.G., and Evans, R.H., 1980. Evolution of SST in the Saomali basin during the southwest monsoon of 1979. *Science*, 209, 595-597.
- [17] Bruce, J.G., 1974. Some details of upwelling off the Somali and Arabian coasts. *Journal of Marine Research*, 32, 419-432.
- [18] Bruce, J.G., D.R.Johnson, and J.C.Kindle., 1994. Evidence for eddy formation in the eastern Arabian Sea during the northeast monsoon. *Journal of Geophysical Research*, 99, 7651-7664.
- [19] Chelton, D. B., R. A. Deszoeke, and M. G. Schlax, 1998. Geographical variability of the first baroclinic Rossby radius of deformation, *J. Phys. Oceanogr.*, 28, 433 – 460.
- [20] Clarke, A. J., 1983. The reflection of equatorial waves from oceanic boundaries, *J. Phys. Oceanogr.*, 13, 1193– 1207.
- [21] Cury, P. and C. Roy, 1989. Optimal environmental window and pelagic fish recruitment success in upwelling areas. *Can. J. Fish. Aquat. Sci.* 46: 670-680.
- [22] *De Tesson, U., 1844. *Voyage Autour du Monde Sur In Fregate 'La Venus Pendant Iesannees' 1836 – 1836*, Paris, Vol 10.
- [23] *Ekman, V. Walfred. 1905. On the influence of the earth's rotation on ocean current. *Ark f.mat. Astr. Och. Fysik.k.sv. Vet.AK*; Stockholm, 1905-06.v.2. No.11.
- [24] Gardner, W.D., Gundersen, J.S., Richardson, M.J., Walsh, I.D., 1999. The role of seasonal and diel changes in mixed-layer depth on carbon and Chlorophyll distributions in the Arabian Sea. *Deep-Sea Res. II* 46, 1833–1858.
- [25] Gill, A.E. and A.J., Clarke, 1974. Wind – induced upwelling, coastal currents and sea level changes. *Deep- Sea Res.*, 21:325-346.
- [26] Gopalakrishna, V.V.; Rao, R.R.; Nisha, K.; Girishkumar, M.S.; Pankajakshan, T.; Ravichandran, M.; Johnson, Z.; Girish, K.; Aneeshkumar, N.; Srinath, M.; Rajesh, S.; Rajan, C.K. 2008. Observed anomalous upwelling in the Lakshadweep Sea during the

- summer monsoon season of 2005. *J. Geophys. Res. (C: Oceans)*. : 113(5); 2008; doi: 10.1029/2007JC004240, 12 pp.
- [27] Grasshoff, K., M. Erhardt, and K. Kremling. 1983. *Methods of seawater analysis*. Verlag Chemie,.
- [28] Habeebrehman, H., Prabhakaran, M.P., Jacob, J., Sabu, Pa., Jayalakshmi, K.J., Achuthankutty, C.T. and Revichandran, C., 2008. Variability in biological responses influenced by upwelling events in the Eastern Arabian Sea. *J. Mar. Syst.*: 74(1-2); 545-560.
- [29] Han, W., and P. J. Webster, 2002. Forcing mechanisms of sea level interannual variability in the Bay of Bengal, *J. Phys. Oceanogr.*, 32, 216– 239, doi:10.1175/1520-0485(2002)032.
- [30] Haugen, V.E, O.M. Johannessen and G. Evensen. 2002. Mesoscale modeling study of the oceanographic conditions off the southwest coast of India. *Proceedings of the Indian Academy of Sciences (Earth and Planetary Sciences)*, 111, 321-337.
- [31] *Hidakka, K., 1954. A contribution to the theory of upwelling and coastal currents. *Trans. Am. Geophys. Un.*, 35: 431- 444.
- [32] Jayaram, C., C., Neethu, K. A. Joseph, and A. N. Balchand,. 2010. Interannual Variability of Upwelling Indices in the Southeastern Arabian Sea: A Satellite Based Study. *Ocean Sci. J.*, 45(1):27-40. DOI 10.1007/s12601-010-0003-6.
- [33] *Jayaraman, R. and S.S., Gogate, 1957. Salinity and temperature variation in the surface water of the Arabian Sea off the Bombay and Sourashtra coasts. *Proc. Indian Acad. Sci.*, 45B: 151-164.
- [34] Johannessen, O. M., G. Subbaraju, and J. Blindheim, 1987. Seasonal variations of the oceanographic conditions off the southwest coast of India during 1971–1975, *Fisk Dir. Skr Hav Unders*, 18, 247– 261.
- [35] Kindle, J.C., J.J. O'Brien, 1974. On upwelling along a zonally oriented coast line. *J. phys. Oceanogr.*, 4: 125-130.
- [36] Krishnakumar P.K., and G.S. Bhat., 2008. Seasonal and inter-annual variations of oceanographic conditions off Mangalore coast

- (Karnatak, India) in the Malabar upwelling system during 1995-2004 and their influences on the fishery. *Fisheries Oceanography*, 17:1, 45-60, 2008.
- [37] Krishnakumar P.K., K.S., Muhamed, P.K., Ashokan, T.V., Sattianandan, P.U., Zacharia, K. P. Abdurahiman, Veena Shettigar, and R.N., Durgekar, 2008. How environmental parameters influenced fluctuations in oil sardine and mackerel fishery during 1926 -2005 along the south west coast of India? *Marine fisheries information service, T& E Ser.*, No.198.
- [38] Kumar, P.V.H., and N., Mohankumar, 1996. On the flow and thermocline structure off Cochin during pre-monsoon season. *Continental Shelf Research*, 16: 457-468.
- [39] Kumar, P.V.H., and B. Mathew, 1996. Seasonal variability of hydrographic conditions in the continental shelf of the west coast of India. *NPOL RR No. 1/96*.
- [40] Lathipha, P.N., and A.V.S., Murthy, 1978. Studies of upwelling along the west coast of India using geo-potential anomaly. *Indian J. of Mar. Sci.*, 7(4): 219-221.
- [41] Levitus, S., 1982. *Climatological atlas of the world ocean*. NOAA professional paper 13.
- [42] Longhurst, A. R., and Wooster, W.S., 1990. Abundance of Oil sardine (*Sardinella longiceps*) and Upwelling on the Southwest Coast of India. *Canadian Journal of Fisheries Aquatic Sciences*, 47, 2407-2419.
- [43] Luis, A.J., and H. Kawamura, 2002a. Dynamics of the mechanism of sea surface cooling near the Indian tip during winter monsoon. *Journal of Geophysical Research*, 107, 3187, doi:10.1029/2000JC000455.
- [44] Luis, A.J., and H. Kawamura, 2002b. A case study of SST cooling dynamics near the Indian tip during May 1997. *Journal of Geophysical Research*, 3171, doi:10.1029/2000JC000778.
- [45] Luis, A.J. and Kawamura, H., 2004. Air-Sea interaction, Coastal

- circulation and primary production in the Eastern Arabian Sea – A Review. *Journal of Oceanography*, Vol 60, 205- 218.
- [46] Luther, M. E., J. J. O'Brien, and W. L. Prell. 1990. Variability in upwelling fields in the northwestern Indian ocean. 1. Model experiments for the past 18,000 years. *Paleoceanography* 5: 433–445.
- [47] Madhupratap, M., S.R. Shetye, K.N.V. Nair and S.R. Sreekumaran Nair, 1994. Oil Sardine and Indian Mackerel: their fishery, problems and coastal Oceanography. *Current Science*, 66, 340-348.
- [48] Madhupratap, M., Prasanna Kumar, S., Bhattathiri, P.M.A., Kumar, M.D., Raghukumar, S., Nair, K.K.C., Ramaiah, N., 1996. Mechanism of biological response to winter cooling in the north-eastern Arabian Sea. *Nature* 384:549-552.
- [49] Madhuprathap, M., K. N. V. Nair, T. C. Gopalakrishnan, P. Haridas, K. K. C. Nair, P. Venugopal and M. Gauns, 2001. Arabian Sea oceanography and fisheries of the west coast of India. *Current Science*, VOL. 81, NO. 4.
- [50] Maheshwaran, P.A., G. Rajesh, C, Revichandran, and K.K.C.Nair, 1999. Upwelling and associated hydrography along the west coast of India during southwest monsoon. *PORSEC Proceedings*, Vol (2); 873-878.
- [51] McCreary, J.P. and S.Y. Chao, 1985. Three-dimensional shelf circulation along an eastern ocean boundary. *J. Mar. Res.*, 43, 13-36.
- [52] McCreary, J.P., P.K. Kundu and R.L. Molinari., 1993. A numerical investigation of dynamics, thermodynamics and mixed layer processes in the Indian Ocean, *Progress in Oceanography.*, vol.31, 181-244.
- [53] McCreary J. P., Han W, Shankar, D., and Shetye, S. R., 1996. Dynamics of the East India Coastal Current, 2. Numerical solutions; *J. Geophys. Res.* 101 13,993–14,010.
- [54] *McEwen, G. F. 1912. The distribution of ocean temperatures along the west coast of North America deduced from Ekman's theory

- of the upwelling of cold water from the adjacent ocean depths. *Int. Rev. Hydrobiol.* 5:243-286.
- [55] *Meeus, Jean. (1991) *Astronomical algorithms*. Richmond, Va.: Willmann-Bell. ISBN 0943396352.
- [56] Morel, A. and J. Berthon, 1989. Surface pigments, algal biomass profiles, and potential production of the euphotic layer: Relationships reinvestigated in view of remote-sensing applications. *Limnol Oceanogr.* 34: 1545 – 1562.
- [57] Muraleedharan, P.M. and S. Prasannakumar., 1996. Arabian Sea upwelling – A comparison between coastal and open ocean regions. *Current Science*, vol.71, No.10, 842-846.
- [58] Murty, A.V.S. and M.S. Edelman, 1971. On the relation between the intensity of the southwest monsoon and oil sardine fishery of India. *Indian J. Fish.*, 13 (1 & 2): 142-149.
- [59] Murthy, A.V.S., 1987. Characteristics of neritic waters along the west coast of India with respect to upwelling, dissolved oxygen and zooplankton biomass. *Indian J of Mar. Sci.*, 16(2); 129-131.
- [60] Narasimha Rao T. V., 2002. Spatial Distribution of Upwelling off the Central East Coast of India. *Estuarine, Coastal and Shelf Science*, 54, 141-156.
- [61] Naidu, D. P., M.R.Ramesh Kumar and Ramesh Babu, V., 1999. Time and space variations of monsoonal upwelling along the west and east coast of India. *Continental Shelf Research*, 19, 559-572.
- [62] Nair R.V., 1959. Notes on the spawning habits and early life-history of the oil sardine *Sardinella longiceps* Cuv. & Val. *Indian J. Fish.*: 6(2): 342-359.
- [63] Naqvi, S.W.A., R.J., Noronha, K., Somasundar, and R. Sengupta, 1990. Seasonal changes in the denitrification regime of the Arabian Sea. *Deep- Sea Research*, 37, 693-711.
- [64] Naqvi, S.W.A. and R.J., Noronha, 1991. Nitrous oxide in the Arabian Sea. *Deep- Sea Research*; 38: 871-890.

- [65] Naqvi, S.W.A., T. Yoshinari, D.A. Jayakumar, M.A., Altabet, P.V. Narvekar, A.H. Devol, J.A. Brandes, and L.A. Codispoti, 1998. Budgetary and biogeochemical implications of N₂O isotope signatures in the Arabian Sea. *Nature*, 394; 462-464.
- [66] Naqvi, S.W.A., and D. A. Jayakumar, 2000. Increased marine production of N₂O due to intensifying anoxia on the Indian continental shelf. *Nature*; vol. 408; 346-348.
- [67] Padmakumar, K. B., B.R. Smitha, C. T. Lathika, C. L. Fanimol, G. SreeRanjamma, N. R. Menon and V. N. Sanjeevan, 2010. Extensive blooms of *Trichodesmium erythraeum* in the South Eastern Arabian Sea during the onset phase of Summer Monsoon 2009. *Ocean Science Journal*, 45(3):151-157, DOI 10.1007/s12601-010-0013-4.
- [68] Pankajakshan, T., Jaydeep Patnaik and Aravind K. Gosh., 1997. An Atlas of Upwelling Indices along East and West Coast of India. Indian National Oceanographic Data Center, National Institute of Oceanography (CSIR), Goa.
- [69] *Pauly, D., and M., Soriano. 1987. Monthly spawning stock and egg roduction of peruvian anchoveta (*Engraulknngens*), 1953 to 1982. In:
- [70] D. Pauly and I. Tsukqama (eds.). The Periivian anchoveta. and its upwelling ecosystem: three decades of change. *ICURM Stud. Rev.*, 15: 167-178.
- [71] Pauly, D., and V. Christensen, 1995. Primary production required to sustain global fisheries. *Nature* (374): 255-257.
- [72] Pond, S., and G.L. Pickard, 1993. *Introductory Dynamic Oceanography*, Pergamon Press, New York, pp240.
- [73] Potemra, J.T., M.E. Luther, and J.J.O'Brien, 1991. The seasonal circulation of the upper ocean in the Bay of Bengal. *J. Geophysical Research*, 96, 12, 667-12, 683.
- [74] Prasannakumar, S. and T.G. Prasad., 1999. Formation and spreading of Arabian Sea High Saline Water Mass. *Journal of Geophysical Research* :104 (C1);1455-1464.

- [75] Prasannakumar, S., Madhupratap, M., Kumar, M.D., Muraleedharan, P.M., D'Souza, S.N., Gauns, M., Sarma, V.V.S.S., 2001. High biological productivity in the central Arabian Sea during the summer monsoon driven by Ekman pumping and lateral advection. *Curr. Sci.* 81, 1633–1638.
- [76] Prell, W.L. and H.F. Streeter, 1982. Temporal and spatial patterns of monsoonal upwelling along Arabia: A modern analogue for the interpretation of Quaternary SST anomalies. *Journal of Marine Research.* 40, 143-155.
- [77] Qasim, S.Z., 1977. Biological Productivity of the Indian Ocean. *Indian J. of Mar. Sci.*, 6, 122-137.
- [78] *Rabalais, N.N., Turner, R.E. and W.J. Weisman Jr., 2001. Hypoxia in the Gulf of Mexico. *J. of Environ. Qual.*; 30: 320-329.
- [79] Ramamirtham, C. P. and D.S. Rao, 1973. On upwelling along the west coast of India. *J. of Mar. Biol. Ass. India*, 15: 306-317.
- [80] Rao, L.V.G., K.P.T. Cherian, K.R. Varma and V.V.R. Varadachari, 1974. Hydrological features of the inner shelf waters along the west coast of India during winter, spring and summer. *Mahasagar*, 7 (1&2); 15-20.
- [81] Rao, S.A., V.V. Gopalakrishna, S.R. Shetye and T. Yamagata, 2002. Why were cool SST anomalies absent in the Bay of Bengal during the 1997 Indian Ocean Dipole Event? *Geophysical Research Letters*, volume 29, No.11, 10, 1029/2001 GLO14645.
- [82] Rao AD, M. Joshi, M. Ravichandran, 2008. Oceanic upwelling and downwelling in the waters off west coast of India. *Ocean Dyn* 58:213-226, doi:10.1007/s10236-008-0147-4.
- [83] Redfield, A. C. 1934. On the proportions of organic derivatives in sea water and their relation to the composition of plankton, p. 176-192. In James Johnstone Mem. Vol. Univ. Liverpool.
- [84] Ryther, J.H., and D. W. Menzel, 1965. On the production, composition and distribution of organic matter in the western Arabian Sea. *Deep- Sea Res.*, 12, 199-209.

- [85] Ryther, J.H., R.H., John, K. P., Allan, A., Bakun, and M., M., Jones. 1966. Primary Organic Production in Relation to the Chemistry and Hydrography of the Western Indian Ocean. *Limnology and Oceanography*, Vol. 11, No. 3 (Jul., 1966), pp. 371-380.
- [86] Sanilkumar, K.V., V.K. Unni and V.V. James, 2003. Upwelling characteristics of the southwest coast of India during 2003. *Proceedings, METOC-2004*.
- [87] Sanjeevan, V.N., P. Jasmine, B.R. Smitha, T. Ganesh, P. Sabu, and T. Shunmugaraj, 2009. Eastern Arabian Sea Marine Ecosystems. *Proceedings of the symposium on Marine ecosystems: Challenges and opportunities, MECOS2009, Kochi*. 1-2.
- [88] Santos, A.M.P., C. Alexandra, D.S. Antonina, T. Moita, P.B. Oliveira, A. peliz, and Pedro Re., 2007. Physical-biological interactions in the life history of small pelagic fish in the Western Iberia Upwelling Ecosystem. *Progress in Oceanography* Doi:10.1016/j.pocean. 2007.04.008.
- [89] Sarhan, T., J.G. Lafuente., Manuel Vargas., M.V. Juan and F. Plaza., 2000. Upwelling mechanism in the northwestern Alboran Sea. *Journal of Marine Systems*, 23, 317-331.
- [90] Sastry, J. S., D'Souza, R. S. (1972). Oceanography of the Arabian Sea during southwest monsoon season. Part 111. Salinity. *Indian J. Meteorol. Geophys.* 23: 479-490.
- [91] Sengupta, D, R. Senan, B.N. Goswami and J. Vialard, 2007. In-traseasonal variability of equatorial Indian Ocean zonal currents. *J. Clim.*, 20, 3036-3055.
- [92] Shah, N.M., 1973. Seasonal variation of phytoplankton pigments and some associated oceanographic parameters in the Laccadive Sea off Cochin. In B. Zeitzschel [ed.] *Biology of the Indian Ocean*. Chapman and Hall, Ltd, London. 175-185.
- [93] Shankar, D., and S.R. Shetye., 1997. On the dynamics of the Lakshadweep high and Low in the southeastern Arabian Sea. *Journal of Geophys. Res.*, 102, 12551-12562.

- [94] Shankar, D., P. N. Vinayachandran & A. S. Unnikrishnan, 2002. The monsoon currents in the North Indian Ocean. *Progress in Oceanography*, 52, 63–120.
- [95] Shankar, D., S. S. C. Shenoi, R. K. Nayak, P. N. Vinayachandran, G. Nampoothiri, A. M. Almeida, G. S. Michael, M. R. Rameshku-
mar, D. Sundar, and O. P. Sreejith, 2005. Hydrography of the eastern Arabian Sea during summer monsoon 2002, *J. Earth Syst. Sci.*, 114, 459– 474, doi:10.1007/BF02702023.
- [96] Sharma, G.S., 1966. Thermocline as an indicator of upwelling. *J. of Mar. Bio. Ass. India*. 8(1); 8-19.
- [97] Sharma, G.S., 1968. Seasonal variation of some hydrographic properties of the shelf waters off the west coast of India. *Bull. Nat. Inst. Sci. India*, 38: 263-276.
- [98] Sharma, G.S., 1978. Upwelling of the southwest coast of India. *Indian J. of Mar. Sci.* ; 7; 209-218.
- [99] Shenoi, S.C., D. Shanker, V.V. Gopalakrishna and F. Durand, 2005. Role of ocean in the genesis and annihilation of the core of the warm pool in the southeastern Arabian Sea. *Mausam*, 56, 1, 147-160.
- [100] Shetye, S.R., 1984. Seasonal variability of the temperature field off the south-west coast of India. *Journal of Earth System Science* , 93, 4, 399-411, DOI: 10.1007/BF02843257.
- [101] Shetye, S.R., Gouveia, A.D., Shenoi, S.S.C., Sundar, D., Michael, G.S., Almeida, A.M., Santanam, K., 1990. Hydrography and the circulation off the west coast of India during southwest monsoon 1987. *Journal of Marine Research*, 48:359-378.
- [102] Shetye, S.R. and Shenoi, S.S.C., 1988. Seasonal cycle of surface circulation in the coastal north Indian Ocean. *Proc. Ind. Acad. of Sci. (Earth and Planetary Sci.* 97:53-62.
- [103] Shetye, S.R., 2005. Dynamics of circulation of the waters around India: Recent Developments and key issues for the future. *Oceanology*, Edited by Harsh K. Gupta, Published by Universities Press (India) private Limited, 138-149.

- [104] Shetye, S.R., A.D., Gouveia S.S.C., Shenoi, G.S., Michael, D., Sundar, A.M., Almedia, and K. Santanam., 1991. The Coastal current off western India during the northeast monsoon. *Deep-Sea Research*, Vol. 38, No.12, 1517-1529.
- [105] Shetye, S.R., S.S.C. Shenoi, M.K. Antony, and V.K. Kumar, 1985. Monthly-mean wind stress along the coast of the North Indian Ocean. *Proceedings of the Indian Academy of Sciences (Earth and Planetary Sciences)*, 94, 129-137.
- [106] Sindhu B., I. Suresh, A. S. Unnikrishnan, N. V. Bhatkar and S. Neetu, 2007. Improved bathymetric datasets for the shallow water regions in the Indian Ocean. *Journal of Earth System Science*, Volume 116, 3, 261-274.
- [107] Smith, R.L. and J.S. Bottero, 1977. On upwelling in the Arabian Sea. In *A Voyage of Discovery*: 291-304.
- [108] Smith, S.L., and M. Madhuprathap, 2005. Mezozooplankton of the Arabian Sea: patterns influenced by seasons, upwelling and oxygen concentrations. *Progress in Oceanography*, 65, 214-239.
- [109] Smitha, B.R., V. N. Sanjeevan, K.G. Vimalkumar, and C. Revichandran, 2008. On the upwelling off the southern tip and along the west coast of India. *J. of Coastal Res.*, 24, 4C, 95-102.
- [110] Smitha, B.R., K.G. Vimalkumar, V.N. Sanjeevan and C. Revichandran, 2007. Coastal process at the southern tip of India during summer monsoon 2005. *Proceedings, METOC Kochi*.
- [111] Stramma, L., Fischer, J., and F. Schott, 1996. The flow field off southwest India at 8°N during the southwest monsoon of August 1993. *Journal of Marine Research*, 54, 55-72.
- [112] Strickland, J.D.H., T.R. Parsons, 1972. *A Practical Handbook of Sea Water Analysis*, second ed., vol. 167. *Bulletin Fisheries Research of Board Canada*, 310pp.
- [113] Subrahmanyam, R. and A.H. Viswanatha Sarma 1965. Studies on the phytoplankton of the west coast of India. Part IV. Magnitude of the standing crop for 1955-1962, with observations on

- nanoplankton and its significance to fisheries. *J. Mar. Biol. Ass. India*, 7(2) : 406-419.
- [114] Sverdrup, H. 1938. On the process of upwelling. *Journal of Marine Research*. 1: 155-164.
- [115] Sverdrup, H. U., and R. H. Fleming. 1941. The waters off the coast of southern California, March to July, 1937. *Bull. Scripps Inst. Oceanogr.* 4:261-378.
- [116] Sverdrup H, U., M. W. Johnson and R.H. Fleming., 1942. *The Oceans: their Physics, Chemistry and Biology*. Prentice-Hall, New York, 1087pp.
- [117] Sverdrup, H.U., 1953: On conditions for the vernal blooming of phytoplankton. *J. du Conseil*, 18, 287-295.
- [118] Tchernia, P., 1980. *Descriptive regional oceanography*, Pergamon, Oxford, 253 pp.
- [119] *Thorade, H., 1909. *Über die kalifornische Meeresströmung*. *Ann d. Hydrogr. U. Mar. Meteor*, Bd. 37; 17-34.
- [120] Tsai P.,T.,H., J.J.O'Brien and M.E.Luther, 1992. The 26-day oscillation in the satellite sea surface temperature measurements in the equatorial western Indian Ocean, *Journal of Geophysical Research*, 97, C6, 9605-9618.
- [121] Turner, J.S. 1973. *Buoyancy effects in fluids*, Cambridge University Press, 250.
- [122] *UNESCO, 1994. *Protocols for the Joint Global Ocean Flux Study (JGOFS). Core Measurements*, IOC Manuals and Guides, vol. 29. UNESCO, Paris, 170pp.
- [123] Varadachari, V.V.R. and G.S. Sharma, 1967. Circulation in the surface waters of the North Indian Ocean. *J. Indian Geophys Uni*: 4(2): 61-73.
- [124] Vinayachandran, P.N., 2004. Summer cooling of the Arabian Sea during contrasting monsoons. *Geo Phy. Res. Letters*, VOL. 31, L13306, doi:10.1029/2004GL019961.

- [125] Vivekanadan, E., M. Srinath, V.N. Pillai, S. Immanuel, and K.N. Kurup, 2003. Trophic model of the coastal fisheries ecosystem of the southwest coast of India. In: Assessment, Management and Future directions for coastal fisheries in Asian countries. G.Silvestre, L. Garces, C. Luna, M. Ahmed, R.A.V, Santos, L.Lachika-Alino, V. Christensen & D. Pauly (eds) Manila, Philippines: World fish Center Conference Proceedings 67, pp, 281-298.
- [126] Weisberg, R.H. and T.J. Weiyarate, 1991. On the annual cycle of equatorial upwelling in the central Atlantic oceans. *J. of Phys. Oceanogr.* 21: 68.
- [127] Wiggert, J.D., R.R. Hood, K. Banse, and J. C. Kindle, 2005. Monsoon-driven biogeochemical processes in the Arabian Sea. *Prog. Oceanogr.* 65, 176–213.
- [128] *Witte, E., 1880. 'Das Emporquellen Von Kaltem wasser an meridionalen Kustin , *Ann, Hydreogr, Berlin*, 8: 192-193.
- [129] Wooster, W.S.A., A. Bakun and D.R. McLain, 1976. The Seasonal upwelling cycle along the eastern boundary of the North Atlantic. *Journal of thMarine Research.* 34, 131-141.
- [130] Wyrtki, K., 1973. Physical Oceanography of the Indian Ocean. *Biology of the Indian Ocean* 3: 18-36.
- [131] Wyrtiki, K., 1981. An estimate of equatorial upwelling in the Pacific. *J. of Phy. Oceanogr.* 11: 1205.
- [132] Yoshida, K., 1967. Circulation in the eastern tropical ocean with special reference to upwelling and under currents. *Japan J. Geophys.*, 4:1-75.
- [133] *Yu, L., J.J.O'brien, and J. Yang, 1991. On the remote forcing of the circulation in the Bay of Bengal. *J. Geophys. Res.*, 96, 20449-20454.

*Original not referred.

Publications

- **Smitha, B.R.**; V.N. Sanjeevan, Vimal Kumar, K.G.; Revichandran, C. 2008. On the upwelling off the Southern Tip and along the west coast of India. J. Coast. Res.: 24(SI 3); 2008; 95-102.
- **Smitha, B.R.**, V.N.Sanjeevan, Vimal Kumar K.G and C.Revichandran., 2007. Coastal processes of the southern tip of India during summer monsoon 2005- - Proceedings, National symposium on Emerging Trends in Meteorology and Oceanography, METOC 2007, Kochi, 213-217.
- Padmakumar, K. B., **B.R. Smitha**, C. T. Lathika, C. L. Fanimol, G. SreeRenjamma, N. R. Menon and V. N. Sanjeevan, 2010. Extensive blooms of *Trichodesmium erythraeum* in the South Eastern Arabian Sea during the onset phase of Summer Monsoon 2009. Ocean Science Journal, 45(3):151-157, DOI 10.1007/s12601-010-0013-4.
- Lekshmi S., **Smitha B.R.**, C. Revichandran, Pankajakshan

- T., V.N.Sanjeevan, Abdul Rasheed and Aruna C., 2007. Observational evidence of upwelling off the Southwest coast of India during June-July 2006. Proceedings, National symposium on Emerging Trends in Meteorology and Oceanography, METOC'07, Kochi, 203-207.
- Sanjeevan, V.N., Jasmine, P., **Smitha, B.R.**, Ganesh, T., Sabu, P. and Shunmugaraj, T. 2009. Eastern Arabian Sea Marine Ecosystems. Proceedings of the symposium on Marine ecosystems: Challenges and Opportunities, MECOS-2009, Kochi. 1-2.
 - Vimalkumar, K.G., Dineshkumar, P.K., **Smitha, B.R.**, Habeebrehman, H., Josia Jacob, Muraleedharan, K.R., Sanjeevan, V.N., Achuthankutty, C.T., 2007. Environ. Monit. Assess. DOI10.1007/10661-007-9863.